WARRIP

WESTERN AUSTRALIAN ROAD RESEARCH AND INNOVATION PROGRAM

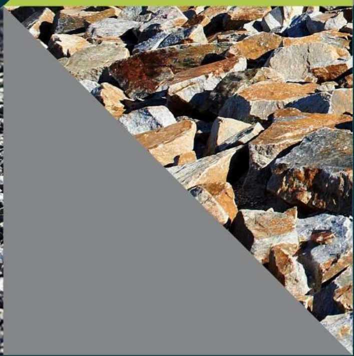

Ground Instrumentation for Traffic Speed Deflectometer (TSD)

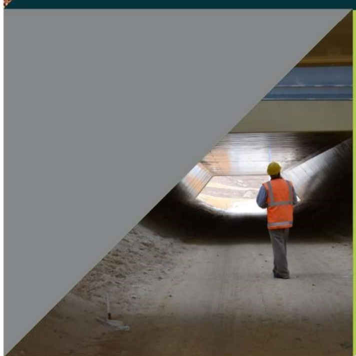

by Dr Jeffrey Lee, Dr Dominik Duschlbauer, Dr Gary Chai

AN INITIATIVE BY:

Ground Instrumentation for Traffic Speed Deflectometer (TSD)

for Main Roads Western Australia

Reviewed

Project Leader

Dr Jeffrey Lee

Quality Manager

Dr Gary Chai

PRP17037-02
June 2019

Australian Road Research Board
ABN 68 004 620 651

Victoria
500 Burwood Highway
Vermont South VIC 3133
Australia
P: +61 3 9881 1555
F: +61 3 9887 8104
info@arrb.com.au

Western Australia
191 Carr Place
Leederville WA 6007
Australia
P: +61 8 9227 3000
F: +61 8 9227 3030
arrb.wa@arrb.com.au

New South Wales
2-14 Mountain Street
Ultimo NSW 2007
Australia
P: +61 2 9282 4444
F: +61 2 9280 4430
arrb.nsw@arrb.com.au

Queensland
21 McLachlan St
Fortitude Valley QLD 4006
Australia
P: +61 7 3260 3500
F: +61 7 3862 4699
arrb.qld@arrb.com.au

South Australia
Level 11, 101 Grenfell St
Adelaide SA 5000
Australia
P: +61 8 8235 3300
F: +61 8 8223 7406
arrb.sa@arrb.com.au

VERSION CONTROL					
ARRB Project No	PRP17037		Client Project No	2018-002	
Path	t:\desiree hamann\190628_prp17037_tsd ground instrumentation_final.docx				
Author/Project Leader	Dr Jeffrey Lee	QM	Dr Gary Chai	Editor	Kieran Sharp

Task	Date	Technical/Quality Checks	Responsibility	By (Initials)
1	27 May 2019	Project Leader (PL) reviews completed draft report	Project Leader	JL
2	27 May 2019	Spell check	Author	JL
3	27 May 2019	All tables and figures/images checked for source and permission for use (where appropriate/applicable)	Author	JL
4	12 June 2019	Library references and superseded references checked. Library comments addressed	Library/Author	TM
5	5 June 2019	PL sends report to Support Unit	Author	JL
6	24 June 2019	Support Unit checks format	Support Unit	MK
7	28 May 2019	PL sends draft report to MRWA counterpart for comment	Project Leader	JL
8	5 June 2019	Support Unit sends report to the Quality Manager (QM)	Support Unit	JL
9	9 June 2019	QM reviews report for research rigour, technical accuracy and overall quality of the report	QM	GC
10	12 June 2019	QM sends report to Editor	QM	GC
11	18 June 2019	Editor edits report (degree of editing to reflect quality of report)	Editor	KS
12	18 June 2019	Editor returns report to QM	Editor	KS
13	21 June 2019	QM reviews feedback from Editor and communicates with PL	QM	GC
14	24 June 2019	PL addresses final comments	Author	JL
15	28 June 2019	Support Unit checks final formatting	Support Unit	DH
16	1 July 2019	Release to client with a cc. to the author, QM and editor@arrb.com.au	Project Leader	EVA
COMMENTS				

SUMMARY

Analytical models used to design and rehabilitate pavements are becoming increasingly sophisticated. The most appropriate process for verifying the accuracy and usefulness of these new analytical models (as well as for calibrating the parameters included in these models) is to observe the behaviour of pavements in the field. One economical approach is to use velocity transducers (geophones) for determining the displacement of a pavement section under actual loads. If used properly, geophones can provide accurate deflection-time history data.

The main aim of this project – which was funded by MRWA under its WARRIP program – was to acquire a better understanding of TSD deflection data by installing ground instrumentation (i.e. sensor arrays using geophones and accelerometers) and monitoring the ‘true’ surface response when heavy vehicle traffic or other deflection testing devices travel over the pavement. Two deflection validation sites (near Perth) were established where the ground response of different deflection equipment was measured using the embedded instrumentation arrays.

The main findings of the project were as follows.

- The deflection profile varies with pavement type.
- For the Kwinana Freeway, there was a good match between the deflection data collected using the TSD and FWD in the front end of the deflection bowl (0 to 600 mm). For the Leach Highway, the deflection in the front end of the deflection bowl collected using the TSD and FWD also has a good match between 0 to 900mm offset. Without further testing, a conclusive explanation of the difference in the field measurements cannot be made. However, several explanations can be postulated, including:
  - The shape of the deflection bowl was very different at the two sites, and the Signal-to-Noise (SNR) ratio may have been higher for the stiffer pavement at Site One (Kwinana Freeway).
  - The degree of subgrade non-linearity (Chai et al. 2015) is often observed in FWD deflection (beyond 900 mm offset). It is postulated that the TSD measurement is also affected by the subgrade non-linearity behaviour. This was also reported for TSD data collected on Queensland pavements (Chai et al. 2016). At this stage, because of the different type of dynamic loading imposed by the two devices, the extent of this effect cannot be quantified at this point in time.
- To date, TSD data has been collected at 41–77 km/h in Kwinana Freeway, whilst on the Leach Highway, because of the limited post speed of 70 km/h, the TSD operated at 48–65 km/h. The results do not support the fact that the pavement response is significantly affected by the speed of testing. Additional tests are needed to confirm this statement.
- In summary, the geophone is more immune to amplification than the accelerometer. This is primarily because the accelerometer does not have a casing to protect it against any compression from the wheel load. Furthermore, the accelerometer is generally installed much closer to the pavement surface than the geophone.

- A system needs to be developed to assist the driver of the TSD to travel as close as possible to the instrumentation array and to minimise wander.
- The predominant frequency of both the FWD and TSD (at 77 km/h) is between 20 and 30 Hz. When the TSD travelled at a lower speed (48 km/h), a lower predominant frequency of 10 to 20 Hz was recorded. It is important that the predominant frequencies are not filtered during the subsequent signal processing.

Recommendations for future research are also presented in the report.

CONTENTS

TABLES

FIGURES

1 INTRODUCTION

1.1 Background

Pavement deflection testing has historically been carried out using Benkelman Beams, Le Croix-type deflectographs or, particularly in more recent times by, Falling Weight Deflectometer. All three of these technologies collect data at low travelling speeds and are therefore poorly suited to the collection of continuous data along large lengths of road or of entire road networks.

The Traffic Speed Deflectometer (TSD) system developed by Greenwood Engineering in Denmark represents the first commercially available system that collects near continuous pavement deflection data at highway traffic speeds. As of 2019 there are two additional devices that can collect deflection data at highway speeds – ARA Rolling Wheel Deflectometer (RWD), Dynatest's RAPTOR™ Rolling Weight Deflectometer (RWD) – but neither of these are available for commercial purchase.

In 2014, the Australian Road Research Board (ARRB) acquired a TSD. After commissioning of the acquired TSD, ARRB added extra functional condition assessing sensors and integrated these into a single data acquisition system and denoted the resultant fully integrated function and structural assessment testing vehicle the iPAVe.

Since then, the iPAVe has been conducting annual network surveys in Queensland, New South Wales, and New Zealand. After a successful demonstration in 2016, Main Roads Western Australia (MRWA) commissioned ARRB to conduct a whole-of-network iPAVe survey of Western Australia's state-controlled roads.

Separate to the MRWA survey, a WARRIP project was established to investigate the differences in pavement response to the loads applied by the Falling Weight Deflectometers that MRWA were experienced in using, and the TSD component of the iPAVe system.

This report describes the installation of sensors within the pavements at two on-road sites located close to Perth. A comparison of the deflection bowls measured by the two deflection technologies and the in-pavement sensors is also included.

Note, as the only component of the integrated ARRB iPAVe system being examined in this report is the TSD component, and to enable the report to relevant to an international audience, this report will use the term TSD to denote both the deflection measuring system and the vehicle within which it was contained.

1.2 Research Aim

Analytical models used to design and rehabilitate pavements are becoming increasingly sophisticated. The most appropriate process for verifying the accuracy and usefulness of these new analytical models (a well as for calibrating the parameters included in these models) is to observe the behaviour of pavements in the field. One economical alternative is to use velocity transducers (geophones) for determining the displacement of a pavement section under actual loads. If used properly, geophones can provide quite accurate deflection-time history data (Nazarian & Bush 1989).

The main aim of this project – which was funded by MRWA under its WARRIP program – was to acquire a better understanding of TSD deflection data by installing ground instrumentation (i.e. sensor arrays using geophones, accelerometers, and strain gauges) and monitoring the 'true' surface response when heavy vehicle traffic or other deflection testing devices travel over the pavement. Two deflection validation sites (near Perth) were established where the ground response of different deflection equipment was measured using the embedded instrumentation arrays.

1.3 Report Structure

Section 1 of the report provides the background of the TSD and outlines the research aim of this project. In Section 2, details of the TSD measurement sensors and the analysis method adopted in Australia is presented. Section 3, presents details of the sensor selection and installation procedure used at both the instrumentation sites. Section 4, presents the work carried out to identify the locations of the two instrumentation sites, and the results of the field experimental work (collected by the instrumentation array, FWD and TSD) are presented. The correlation between the TSD and the FWD deflections from this study and from a recent NACoE study is presented in Section 6. Lastly, conclusion and future recommended work presented in Section 7.

2 TSD MEASUREMENT SENSORS AND DEFLECTION DATA

TSD applies a 10 tonne load via a single axle with dual tyres located as the trailer axle of a semi-trailer vehicle travelling at traffic speed (nominally 80 m/h). The measurement system uses Doppler lasers to measure the vertical surface velocity of the deflected pavement resulting from this applied load. The ARRB TSD system uses lasers fixed at six locations along the mid-line of the rear left dual tyres and in front of the axle (at 100, 200, 300, 600 and 900 mm offsets). D_o is defined as the deflection directly underneath the rear axle. The seventh Doppler laser, known as the reference laser, is positioned 3 500 mm away from the rear axle load. The reference laser is presumed to remain relatively unaffected by the load applied by the axles and, as such, it measures very little vertical pavement deflection velocity.

The TSD measures the vertical velocity of the pavement surface while traveling at traffic speed (nominally 80 km/h). A deflection bowl can be obtained by integrating the velocity slopes from each of the doppler lasers. Parameters such as the maximum deflection, curvature, and other structural condition indices can then be derived from the deflection bowl. Two methods are available for converting TSD deflection velocity slope to deflection:

- Euler-Bernoulli beam model (Rasmussen et al. 2008), more commonly known as the 'Greenwood Model'.
- ARRB 'area under the curve' (AUTC) method (Muller & Roberts 2013).

During operations, the Doppler sensors measure vertical velocities of the deflected pavement surface at discrete points and, when divided by the instantaneous vehicle speed, they produce deflection slopes (V_v/V_h) at those points (Rasmussen et al. 2008). Figure 2.1 shows the pavement deflection velocity vectors under a rolling wheel. Together with the deflection velocity, the corresponding deflection bowl is shown in Figure 2.2, where deflection slopes (tangents) are displayed. The pavement deflections can be determined by integrating the deflection slope curve using a closed-form solution of a mechanical model such as an elastic beam on a Winkler foundation (Rasmussen et al. 2008).

Figure 2.1: Pavement deflection velocity under a rolling load (Rasmussen et al. 2008)

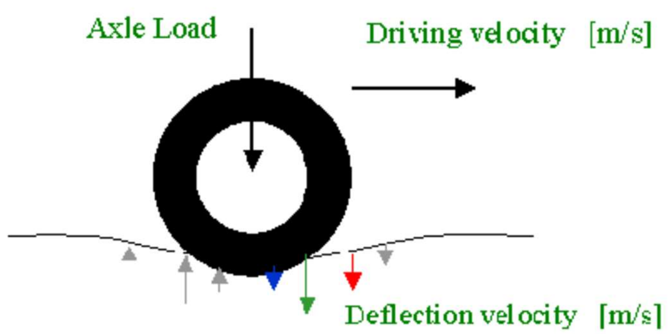

Figure 2.2: Pavement deflection velocity and deflection bowl with deflection slopes (tangents) (Rasmussen et al. 2008)

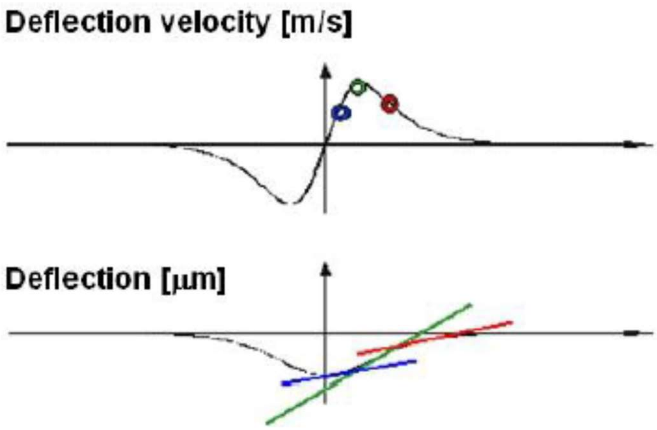

The current algorithm being used by the manufacturer is based on a statistical method that fits a curve through the TSD data (Pedersen 2013); it also accounts for asymmetry in the deflection bowl (Nasimifar et al. 2016).

Various additional algorithms are available to compute pavement vertical surface deflection from surface velocity data. The main methods are the Euler-Bernoulli beam model (Rasmussen et al., 2008), ARRB "Area Under the Curve" (AUTC) method (Austroads 2014) and (Muller & Roberts 2013), and the Weibull functional form method (Zofka et al. 2014).

Additionally, recent research conducted in the United States (Nasimifar et al. 2016) presented two methods, namely the velocity-based and the deflection-based approaches to estimate the pavement layer moduli for network-level analysis using the TSD. Furthermore, a deflection-based approach to back-calculate the layer moduli from TSD measured deflections is currently being investigated by ARRB in Queensland to explore the use of TSD technology in pavement rehabilitation design.

2.1 Details of AUTC Method

The AUTC method was first developed following the initial TSD trials conducted in Australia in 2010 (Muller & Roberts 2013). The method involves fitting the TSD slope measurements and numerically integrating them over the length of the deflection bowl, working towards the wheel load. Details are as follows:

- The base TSD data consists of a set of vertical pavement velocities, referenced against horizontal offset spaced along the axis of the wheelpath and away from the loading of the dual-tyred truck wheels. This data is termed the velocity profile.
- The value of the velocity at each point is a function of the pavement strength, the offset of the Doppler laser, the velocity sensor from the centre point of loading, and the horizontal speed of the TSD vehicle (which affects the speed of the vertical loading).
- The slope is the ratio between the vertical and horizontal velocities at each measurement point and the actual physical slope of the pavement surface within the deflection bowl centred under the moving TSD's rear wheel.
- By plotting slope values against the offsets from the load point as a slope profile curve (analogous to the previously-mentioned velocity profile), it is possible to show that the cumulative area under the slope profile working from the tail is exactly equal to the vertical deflection at that point.
- The vertical difference between any two deflection points, such as for the bowl curvature, (D_0–D_{200}), is equal to the area under the slope profile curve between these two points.

The AUTC method has been used when reporting TSD data in Australia. Therefore, only the AUTC method will be used in this report.

3 SENSOR SELECTION AND INSTALLATION

3.1 Introduction

SLR Consulting Australia Pty Ltd (SLR) was engaged by ARRB to assist with the permanent installation of instrumentation arrays in two pavements in the greater Perth area. A report prepared by SLR and reproduced in Appendix C, presents details of the installation. The locations of the sites are:

- Site One – southbound left lane (L2) of the Kwinana Freeway (H015)
- Site Two – southbound left lane of the Leach Highway (H012), an urban arterial in the southern suburb of Shelley in Perth.

The sensors were installed at night on 11–12 September 2018 (Site One) and 12–13 September 2018 (Site Two).

3.2 Sensor Selection and Calibration

The sensors in Site One (Kwinana Freeway) were installed 500 mm from the edge line marking, whilst, in Site Two (Leach Highway), they were located 1 m from the road kerbs. Details of the instrumentation are presented in Table 3.1, while Table 3.2 provides a brief description of the types of sensors used in the study. After the installation of the sensors, polyurethane resin (PU200) was poured into the drilled holes.

Table 3.1: Details of Sensors in Site One (Kwinana Highway) and Site Two (Leach Highway)

Label on the drilled hole	Sensor Type	Dimensions of drilled holes		Spacing to adjacent sensor (mm)
		Diameter (mm)	Depth (mm)	
B	Geophone	70	70	200
C	Accelerometer	50	30	200
D	Accelerometer/geophone	70	30 & 70	100
E	Accelerometer	50	30	150
F	Accelerometer	50	30	150
G	Accelerometer	50	30	300
H	Accelerometer	50	30	200
I	Thermocouples	50	40	

Table 3.2: Sensor descriptions

Label on drilled hole	Sensor type	Brief description
B, D	Geophone	Geophones with an internal resistance of 400 ohm were used to measure vertical velocity. Shaker tests were carried out on all geophones and their natural frequency was nominally 10.5 Hz with nominal sensitivity of 28 V per m/s above the natural frequency. The terminals of the geophones were coated with resin for moisture protection. Subsequently, a protective cap was glued over the terminals of each geophone. An M8 anchor was cold-welded (JB Weld) to the underside of each geophone. On-site, 9 mm pilot holes were drilled into the bottom of each hole. The pilot hole was filled with epoxy glue (5 min Araldite) and the anchor was glued into the hole. Epoxy glue was also used to level the contact zone between the geophone and the bottom of the hole. A protective plastic cup was glued over the geophones to ensure that the resin does not directly touch the geophone due to concerns that stresses imposed on the geophones' bodies may give rise to incorrect readings.
C,E,F,G,H	Accelerometer	Dytran model 3305A3 accelerometers with a nominal sensitivity of 500 mV/g were used for measuring the vertical acceleration. The accelerometers were attached to microdot leads and coated in a protective resin. Subsequently, the lead to the accelerometer connection was heat-shrinked. The accelerometers were cold-welded (JB Weld) into steel enclosures and fixed at the correct angle within the enclosure with bolts. Once the cold-weld had cured, the bolts were removed and more cold-weld was injected through the bolt holes. M8 anchors were bolted into the steel enclosures. The anchors protruded typically by 40–50 mm. 9 mm pilot holes were drilled into the bottom of each hole. The pilot hole was filled with epoxy glue (5 minute Araldite) and the anchor was glued into the hole. Epoxy glue was also used to level the contact zone of the steel enclosure and the bottom of the hole.
I	Thermocouples	Welded tip 'gas and watertight' PTFE thermocouples Type K with 10 m leads were used. The thermocouples were pushed into holes drilled into the pavement and epoxy glued in place to ensure they stayed in place as the resin was poured. The thermocouples were used to measure the asphalt temperature.

3.2.1 Selection of accelerometers

Accelerometers can also be used to monitor the vertical acceleration of the pavement surface. By double-integrating the measured acceleration time history, deflection (or displacement) profiles can be determined.

With modern solid-state accelerometer units, the size of the accelerometer can be very small (similar to the one used in this project) and it is able to withstand high G forces upon impact. The other attractive feature of using accelerometers is the simple calibration procedure that covers a wide range of frequencies, plus only a single calibration curve (Volt per g) is needed.

3.2.2 Selection of geophones

The monitoring of long-term pavement performance has been conducted by many road agencies worldwide. An alternative method for collecting deflection-time history pavement performance data is to install and monitor geophones (velocity transducers). Geophones were selected for this project because:

- they can be used effectively to monitor deflections in a pavement
- the method used to measure the deflection of a pavement is similar to that used by the FWD.

A study using geophones to measure pavement deflection was conducted by Nazarian & Bush (1989) in Texas. The study reviewed the different methods that may be used to determine the deflection-time history of a pavement section from geophone (velocity transducer) data.

A brief overview of the methods presented in their paper is presented here. The two methods used are: (a) Impulse Method, and (b) Frequency Response Method.

The **impulse method** is adopted from the shock engineering discipline. In this approach, the maximum response is only considered rather than the complete time history or the frequency content of the response. To implement this method, the impulse was analysed in the frequency domain. This process is repeated to determine the shock response spectrum (SRS). The SRS is the relationship between the ratio of the maximum response and the maximum input, versus the natural frequency of the system for a given damping ratio. The geophone has a natural frequency of 4.73 Hz and the damping ratio is 0.64.

The geophone generates a voltage that is related to the velocity of the geophone. The following steps are involved in converting the voltage to deflection:

1. Convert the voltage to velocity by dividing the record by the transductivity of the geophone.
2. Divide the converted velocity time record by the adjustment factor, C_g, to compensate for the effect of the geophone on the signal.
3. Integrate the signal with respect to time to obtain the maximum deflection.

The following formula is used to compute the deflection:

$$\text{DEFLECTION} = \text{FACTOR} * \text{INTVOLT} \tag{1}$$

$$\text{FACTOR} = 1/(T_g * C_g)$$

where

DEFLECTION = Deflection of pavement at geophone base

FACTOR = $1/(T_g*C_g)$, the correction factor for shape and duration of impulse and transductivity of the geophone

INTVOLT = Maximum output voltage after integration of raw geophone signal saved in the recording device.

Nazarian and Bush (1989) provided an example of how the maximum deflection computed from voltage output from the geophone was compared with the deflections measured by the FWD. The results were as follows:

INTVOLT = 3.37 mv.msec

T_g = 0.57

C_g = 0.75

FACTOR = $1/(T_g*C_g)$ = 2.33

Deflection = 3.37 * 2.33 = 7.9 mil (0.20066 mm)

Actual FWD maximum deflection = 7.7 mil (0.19558 mm) (3 percent difference between the two values)

The **Frequency Response method** uses the Fourier transform algorithm. The advantage of this method over the impulse method is that the entire displacement time history can be determined, whereas, with the impulse method, only the maximum deflection could be found. In the frequency response method, no simplifying assumption about the nature of the load is made. As such, the results are more accurate than those obtained using the impulse method.

The procedure for determining deflections from the geophone response is as follows:

- The geophone is calibrated using the procedure outlined below.
- Fourier transform was used to convert the time domain signal into the frequency domain.

- The Fourier-transformed signal is divided by the calibration curve.
- The result is then inverse-Fourier transformed to obtain the deflection time history and the maximum deflection.

To implement the two methods, **calibration of the geophone** is required. The commonly-used method of calibration is to use a shake-table. In this method of calibration, a reference accelerometer is rigidly connected to the shake-table and the geophone, which is in turn rigidly connected to either the accelerometer or the shake-table. The shake-table is vibrated with a sweep-sine steady-state source. The response of the accelerometer is integrated to obtain its response in term of velocity. The ratio of the geophone output voltage and the integrated accelerometer record at each frequency is the calibration curve for the geophone. To normalise the curve, the calibration value is divided by the tranductivity of the geophone (denoted by T_g), which is 0.57 volt/in./sec.

The deflections determined from the calibrated geophones, using both the impulse and frequency response methods, are presented in Table 3.3. The corresponding deflection values obtained directly from the FWD testing are also shown.

Table 3.3: Comparison of deflections obtained from impulse method, frequency response, and FWD tests using two calibrated geophones

Deflection, mil			
Sensor number	Impulse method	Frequency response method	FWD
2 R	7.3	7.4	6.9
3	6.6	6.8	6.6
2 R	7.2	7.4	7.3
4	5.9	6.0	5.9
2 R	7.2	7.3	7.2
5	5.3	4.7	5.3
2 R	7.2	7.3	7.2
6	4.6	4.7	4.6
2 R	7.1	7.3	7.4
7	4.0	4.1	4.1
Average Reference	7.20 (+0.07)	7.34 (0.05)	7.22 (0.19)

Source: (Nazarian & Bush 1989).

From the test, it can be observed that, at each sensor location, the three methods yielded deflections that were within 4% of one another. Therefore, the study demonstrated the precision and accuracy of the methods used to determine the pavement deflection using geophones (velocity transducers).

3.3 Sensor Calibration

When compared with an accelerometer, a geophone is a simple mass-on-spring system that is fairly reliable. However, the downside is that the voltage signal is only linearly proportional to the measured velocity if the frequency range of interest is well above the resonant frequency of the system. The calibration curve of the geophone used in this project is shown in Figure 3.1. This geophone has a resonant frequency of around 12–15 Hz, and the calibration curve is only expected to be flat for frequencies over 40 Hz. In other words, using a geophone requires an extra step in the analysis process. The extra step involves calibrating each geophone on a dynamic shaker-table to accurately determine the calibration curve for the region between 5–40 Hz (i.e. the frequency range over which most of the FWD and TSD measurements were conducted). This is discussed further in Section 3.6.

It is also worth noting that, while a geophone with a very low resonant frequency can be purchased off-the-shelf (e.g. 1 Hz and 2 Hz geophone/seismograph), they are usually very large mass and soft spring systems which would be too big for use in this project.

Figure 3.1: Laboratory calibration of a geophone unit

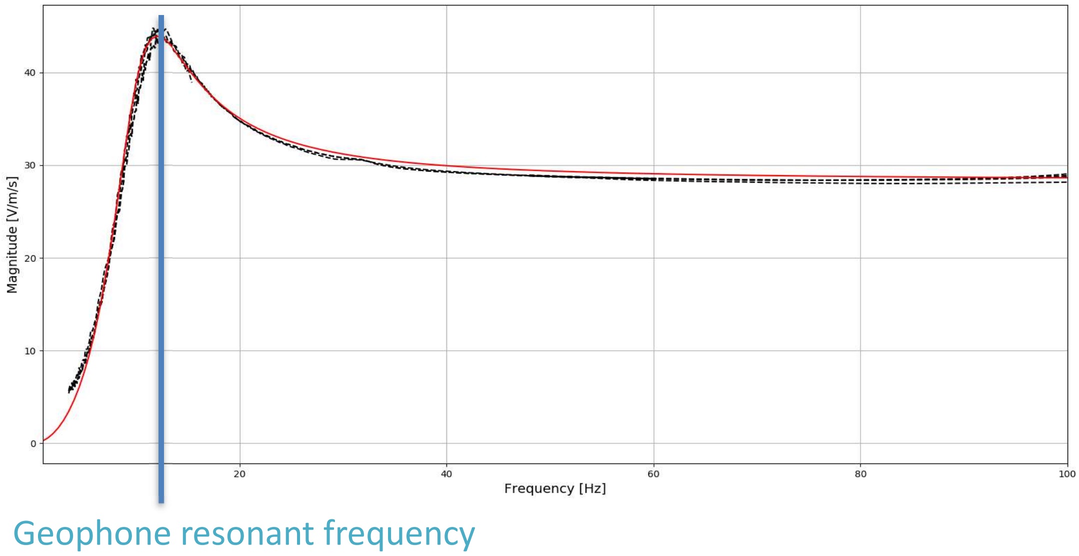

3.4 Sensor Preparation and Installation

Before the sensors were installed in the field, several modifications were needed to improve the reliability and longevity of the sensors. The off-the-shelf accelerometers and geophones required waterproofing and strengthening before they could be embedded in the pavement. In this section, the preparation work undertaken by SLR Consulting is outlined. For further details, readers are referred to Appendix C.

Figure 3.2 is a photograph of the installed sensors after they had been embedded in the pavement. The sensors measure the vertical acceleration (using accelerometers), vertical velocity (using geophones), and asphalt temperatures (using thermocouples).

Figure 3.2: Photograph of an accelerometer, geophone, and thermocouple installed

The weakest link in a solid-state accelerometer is often at the junction of the small connector between the accelerometer and the cables. In order to reduce moisture ingress and faulty cable connections, each accelerometer was protected by a layer of thick resin coat, as shown in Figure 3.3.

Figure 3.3: Close-up Dytran accelerometer with a resin coating to improve waterproofing at the connection

	
Moisture protecting resin coat (sticky tape was removed once the resin cured)	Heat shrink over connector but loose over microdot lead.

To further strengthen the accelerometer, each accelerometer was encapsulated in a steel casing. One of the concerns at the start of the project was that the shallow asphalt surfacing cover over the accelerometer may not be adequate to secure the sensor in the pavement under live heavy vehicle traffic. The encapsulate system design also included an anchor to secure the sensor in the pavement layer. During installation, a hole in the pavement was predrilled, and the anchor was epoxied into position. Figure 3.4 shows the finished accelerometer configuration.

Figure 3.4: Photograph of a Dytran accelerometer welded in a protective steel casing and anchoring system

Arrangement prior to the accelerometer being cold-welded into the enclosure. The two bolts were removed and the through-holes were used to inject more cold-weld.

Accelerometer prior to installation (above) and installed in hole before being covered with resin (below).

Similar to the accelerometer, protection and anchoring systems were needed for the geophones before they could be deployed in the field. Figure 3.5 and Figure 3.6 show the completed geophone and the configuration embedded at both sites.

Figure 3.5: Photograph of a geophone and the protective cap and anchoring system

Geophone terminals (uncoated)

Geophone with protective cap in place and anchor cold-welded.

Figure 3.6: Photograph of a geophone with the protective cap and epoxy in the pavement

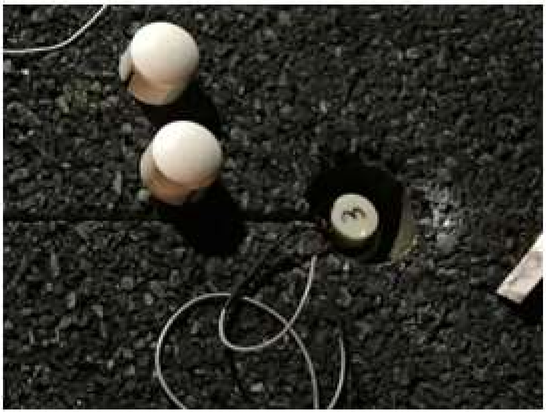 Geophone glued into hole without the protective caps. The protective caps are shown to the left.	 Geophone installation with protective cap in place. The slot for the lead was sealed with tape before the resin was poured.

The success of this project relied on paying attention to the installation of the sensors. Meetings were held between ARRB and MRWA staff to agree on the installation details as shown in Figure 3.7, Figure 3.8 and Figure 3.9. It is worth noting that one of the holes in the instrumentation array included both a geophone and an accelerometer (Figure 3.9). The purpose of this hole was to confirm that both the accelerometer and the geophone reported the same response.

Figure 3.7: Installation details for accelerometers

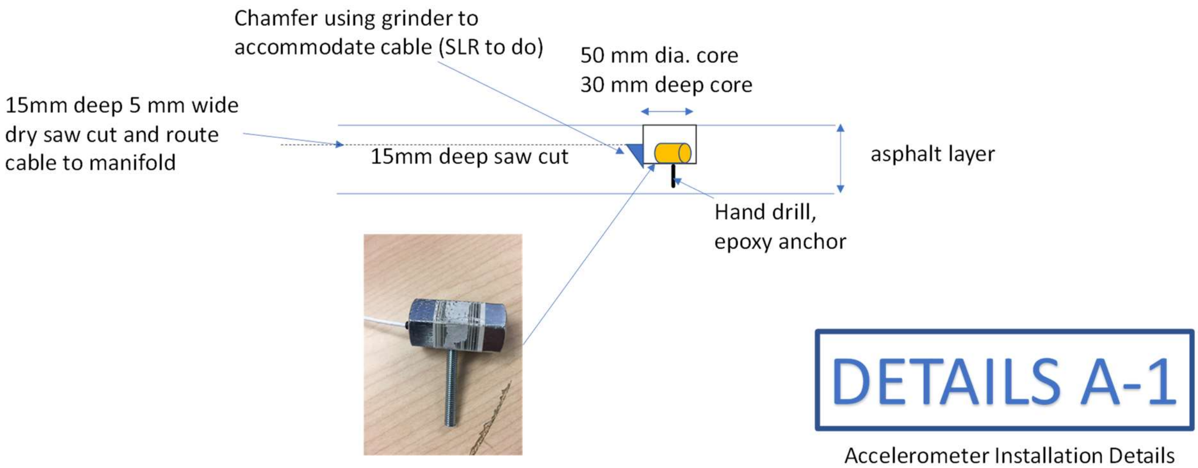

- A bedding layer at the bottom of the corehole (e.g. using PU200) may be needed to achieve a flat and horizontal surface.
- The core hole depth shown did not allow for additional bedding thickness. The depth of the corehole will need to be increased on-site to achieve the minimum core depth to accommodate the sensor after bedding is in place.

Figure 3.8: Installation details for geophones

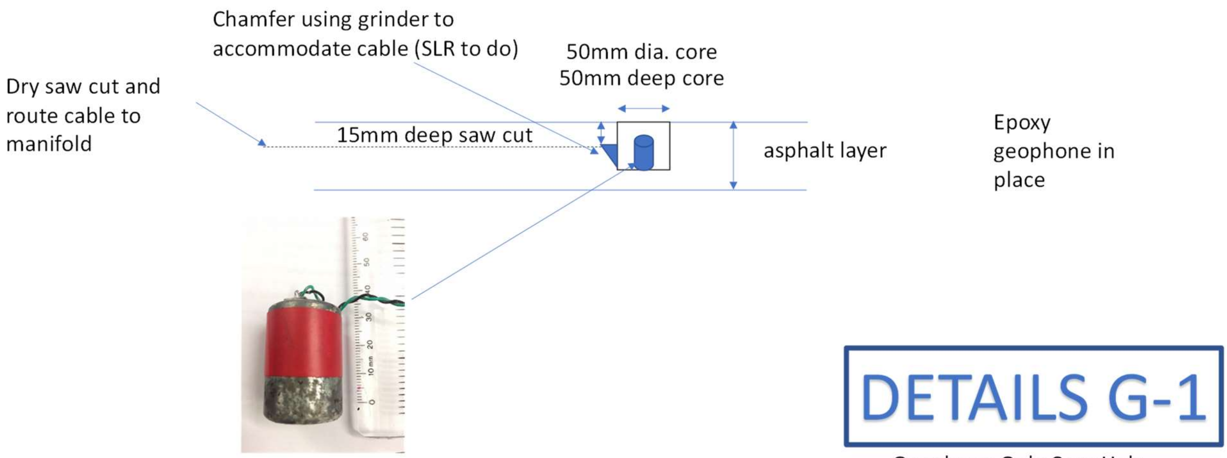

- A bedding layer at the bottom of the corehole (e.g. using PU200) may be needed to achieve a flat and horizontal surface.
- The core hole depth shown did not allow for additional bedding thickness. The depth of the corehole will need to be increased on-site to achieve the minimum core depth to accommodate the sensor after bedding is in place.

Figure 3.9: Installation details for location of both accelerometer and geophone in the same hole

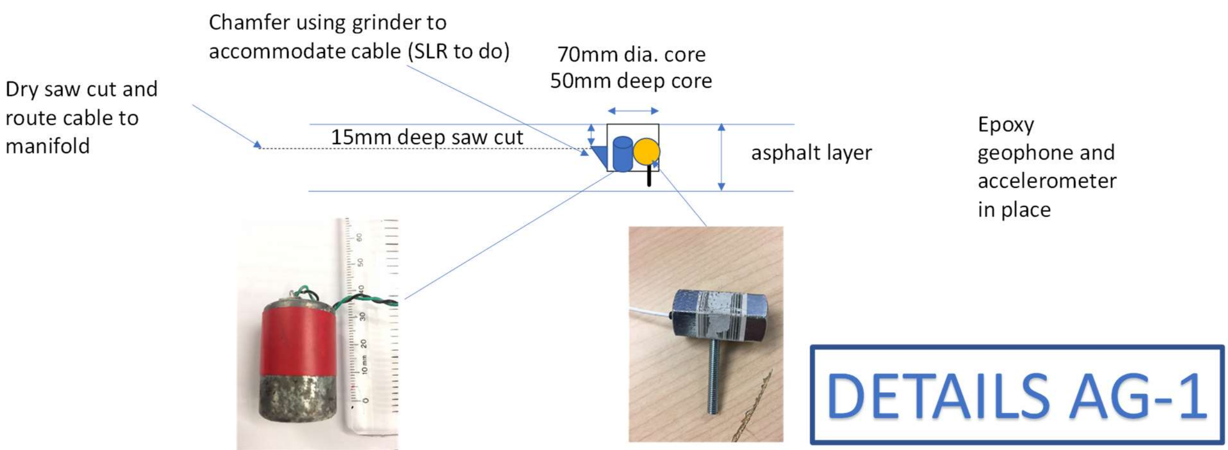

- A bedding layer at the bottom of the corehole (e.g. using PU200) may be needed to achieve a flat and horizontal surface.
- The core hole depth shown did not allow for additional bedding thickness. The depth of the corehole will need to be increased on-site to achieve the minimum core depth to accommodate the sensor after bedding is in place.

The sensors were installed between 13–15 September 2018. A photograph of the lateral and longitudinal offsets is shown in Figure 3.10. The longitudinal layout (in the direction of TSD travel) was designed to match the offset spacing of the TSD on-board doppler lasers.

Figure 3.10: Annotated photograph of the installation site located on Leach Highway, near Shelley WA

3.5 Data Acquisition System

After careful review of available data acquisition (DAQ) systems, the project team selected the National Instruments (NI) Compact-DAQ system. The DAQ system is self-contained with a built-in computer running Windows 7. When combining the versatile and powerful software system Labview™ from NI, the system can capture and analyse the fast waveforms that this project needed. All the dynamic signals were captured with a sampling frequency of 2048 Hz. A photograph of the data acquisition system is shown in Figure 3.11.

The NI equipment modules purchased for this project included:

- Compact DAQ Controller (cDAQ-9133) – a data acquisition unit that includes Intel Atom dual-core processing for data-logging and embedded monitoring using different cDAQ input modules.
- Analog Vibration Input Module (NI-9234) – measures signal from Integrated Electronics Piezo-Electric (IEPE) such as accelerometers and non-IEPE sensors such as geophones.
- Strain/Bridge Input Module (NI-9237) – measures up to four bridge-based strain sensors with supporting signal conditioning.
- Temperature Input Module (NI-9211) – measures temperature readings from thermocouples.

Figure 3.11: Photograph of National Instruments data acquisition system

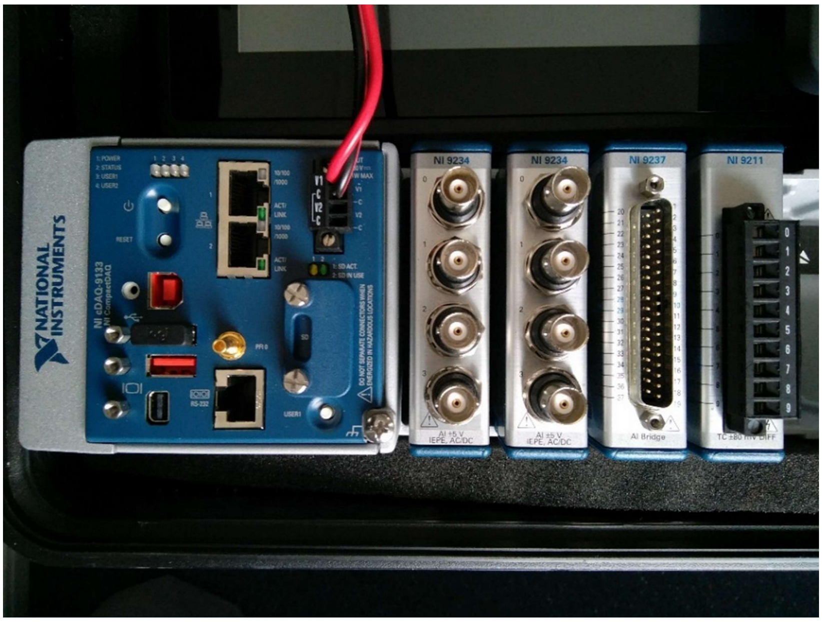

3.6 Signal Processing

The typical time record and the frequency content of the TSD operating at 77 km/h and 48 km/h are shown in Figure 3.12 and Figure 3.13 respectively. A similar time and frequency domain record of a TSD is shown in Figure 3.14.

Figure 3.12: Time domain and frequency power response of TSD traveling at 77 km/h

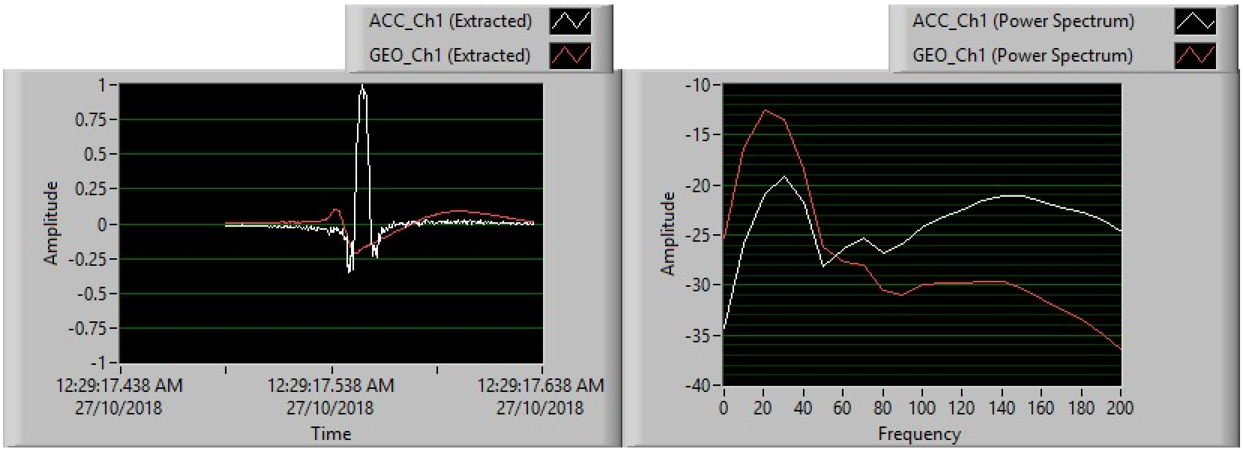

Figure 3.13: Time domain and frequency power response of TSD traveling at 48 km/h

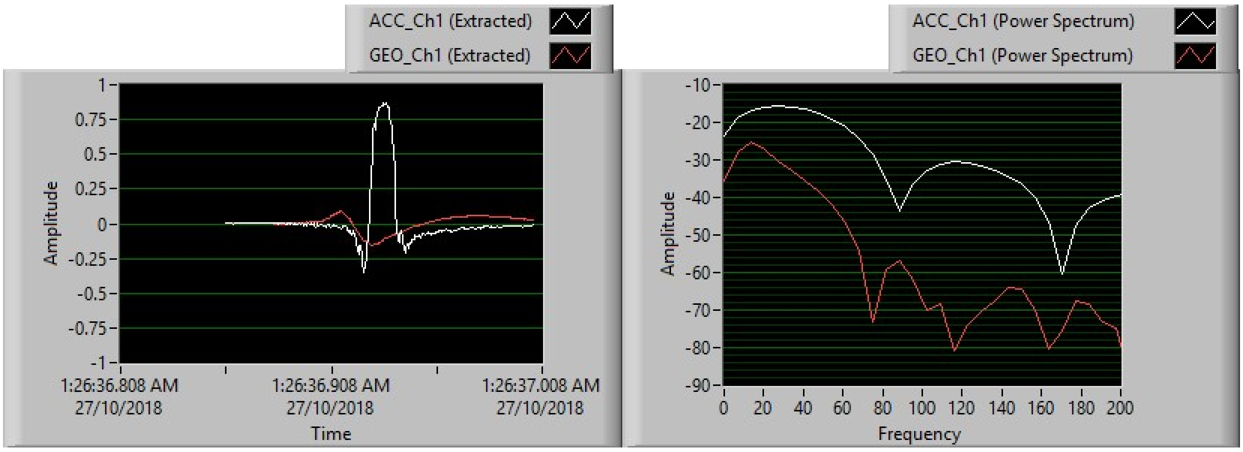

Figure 3.14: Time domain and frequency power response of FWD

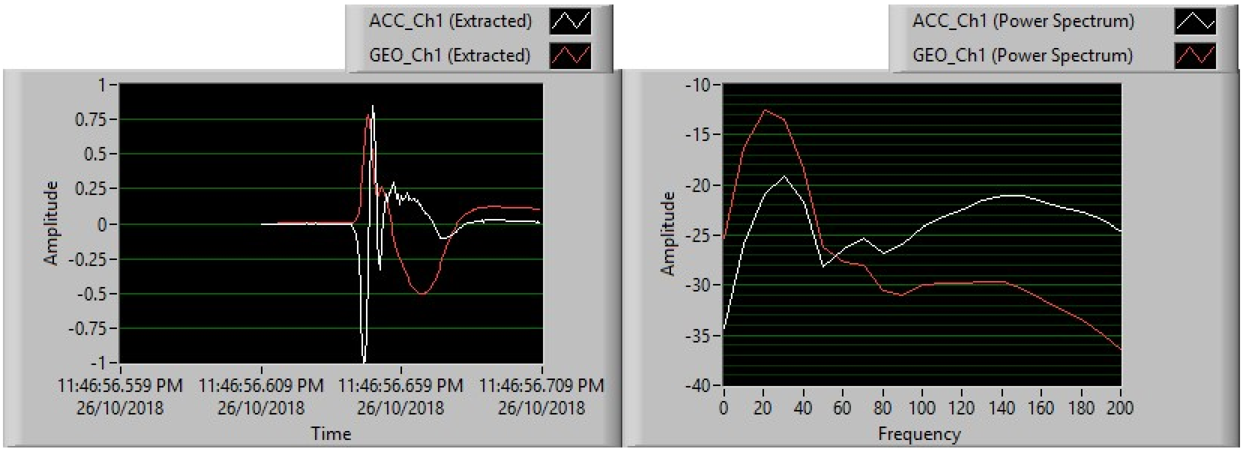

The predominant frequency of both the FWD and TSD (at 77 km/h) was between 20 and 30 Hz. As the TSD travels at a lower speed (48 km/h), a lower predominant frequency of 10 to 20 Hz was measured. During the subsequent signal processing, it was important that the predominant frequencies were not filtered.

The signal outputs obtained from a geophone and an accelerometer are different. As a result, the geophone data was bandpass filtered between 1 Hz and 500 Hz, and then integrated to displacements and differentiated to accelerations. The accelerometer data passed through a bandpass filter with cut-off frequencies between 5–500 Hz. The displacements were computed by double-integrating the acceleration data.

4 FIELD INVESTIGATION

The primary focus of this project is to measure and compare the deflection measurement made using a Traffic Speed Deflectometer (TSD), a Falling Weight Deflectometer (FWD), and the surface deflection obtained from the ground instrumentation array.

4.1 Selection of Instrumentation Sites

Two ground instrumentation sites near Perth were selected for this project. The criteria considered when selecting the sites were as follows:

- the site had a relatively uniform deflection profile and was free of surface defects
- the site was not going to be resurfaced and rehabilitated in the short term
- the TSD would be testing the section in the next three years
- structural responses cover both weak and stiff pavement structures.

After discussion with MRWA staff, the project team identified two sites. The first site was located along the Kwinana Freeway approximately 1.5 km south of the Paganoni Road exit. It was near the 'Trial Mile' section which MRWA had been monitoring over the past few years. The second site was a section of the Leach Highway, near Shelley in Perth.

4.1.1 Site One – Kwinana Freeway (H015)

The first site was located along the southbound left lane (L2) of the Kwinana Freeway. An aerial photograph showing the test site location is shown in Figure 4.1. The pavement structure comprises a full-depth asphalt pavement over a limestone subbase. A pavement core was taken at SLK 56.73, and the core thicknesses are summarised in Table 4.1. The section has an average annual daily traffic (AADT) of 15,941 and 11.1% of heavy vehicles (2012). The posted speed of this section is 110 km/h.

Figure 4.1: Aerial photograph of Kwinana Freeway test site

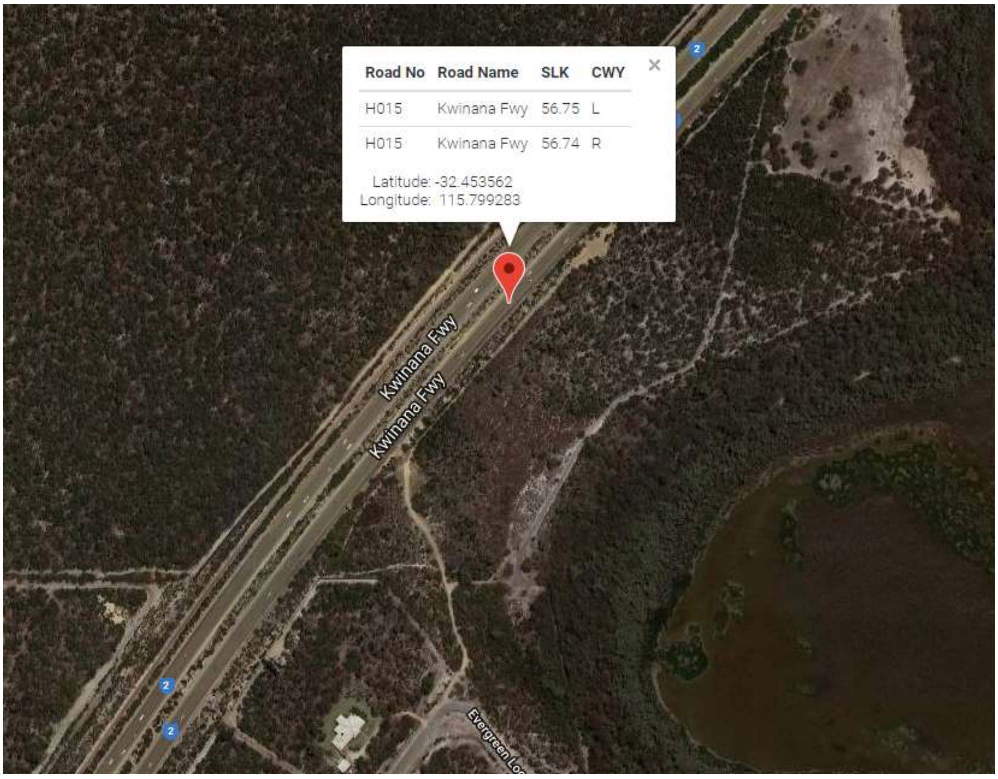

Table 4.1: Layer thicknesses of core taken at SLK 56.73 along Kwinana Freeway

Material Type	Average Depth (mm)	Average Layer Thickness (mm)
Asphalt	0–280	280
Limestone	280–500	220
Sand	500 +	

4.1.2 Site Two – Leach Highway (H012)

The Leach Highway is an urban arterial in the southern suburb of Shelley in Perth. The instrumentation was installed in the southbound outer lane (L3). An aerial photograph showing the test site location is shown in Figure 4.2. The pavement structure comprises a thin asphalt wearing course over a bitumen-stabilised limestone layer and a limestone subbase. A pavement core was taken at SLK 12.28, and the core thicknesses are summarised in Table 4.2. The section has an Average Annual Daily Traffic (AADT) of 19,232 and 8% of heavy vehicles (2016). The posted speed of this section is 70 km/h.

Figure 4.2: Aerial photograph of Leach Highway test site

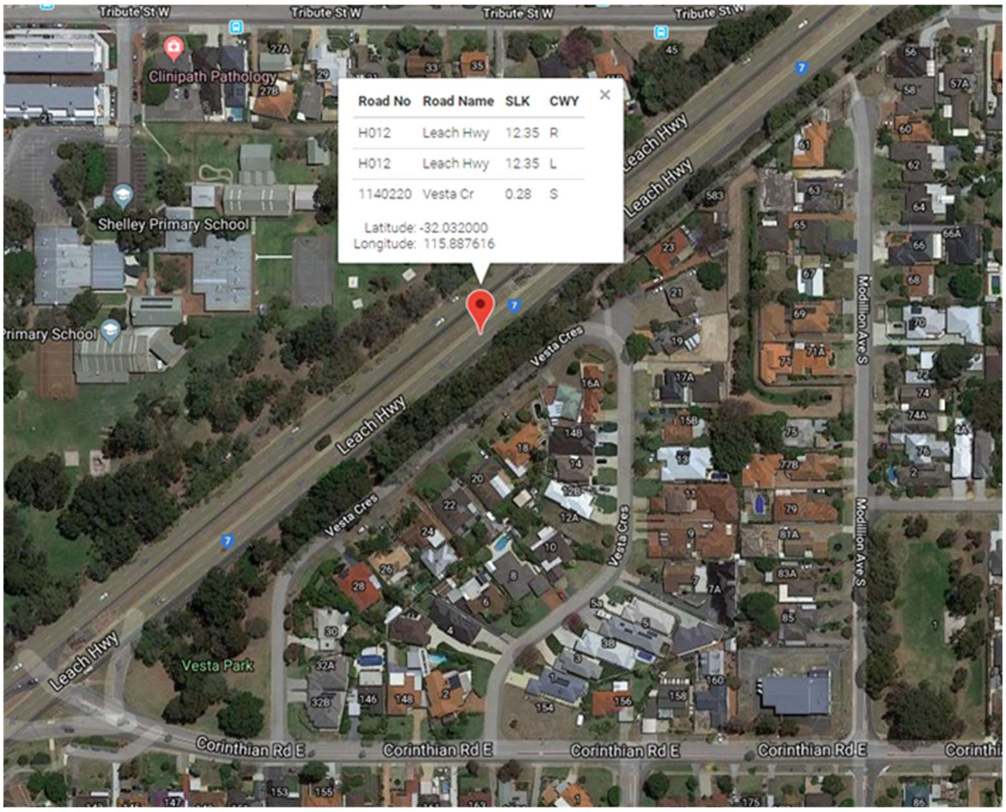

Table 4.2: Layer thicknesses of core taken at SLK 12.28 along Leach Highway

Material Type	Average Depth (mm)	Average Layer Thickness (mm)
Asphalt	0–40	40
Bitumen stabilised limestone (BSL)	40–190	150
Limestone	190–330	140
Sand	330 +	

4.2 Field Testing Program

The primary focus of this project was to measure and compare the deflections measured using a Traffic Speed Deflectometer (TSD), a Falling Weight Deflectometer (FWD), and the surface deflection obtained from the ground instrumentation array. Details of the sensor selection and sensor installation were reported in Section 3. In this section, different stages of the testing are listed and explained further in the sub-sections:

- identify pavement sites in Perth and check uniformity
- install instrumentation array and validate installation using an FWD and instrumented impact hammer
- monitor ground instrumentation output during TSD pass-by and FWD testing.

4.2.1 Identify pavement sites and check uniformity

At the time of this project, the post-processing software from Greenwood Engineering limited the reporting length to 10 m. In other words, each deflection reading from the TSD was an average value over a 10 m length of pavement. This difference needs to be highlighted when comparing the data with the discrete readings recorded the ground instrumentation array. Each sensor within the array measures the surface response for a single location spatially. In order to have a fair comparison between the TSD deflections and the deflections measured by each in-ground sensor, the project team selected areas that had uniform deflection.

To minimise the cost of lane closures, a screening exercise was carried out across the WA metro Perth network. As part of the TSD demonstration trial conducted in April 2018, several MRWA-controlled roads were surveyed, and deflection data collected from the Kwinana Freeway and the Leach Highway was made available to the project team. This data was used to identify potential candidate sites. The deflection data for the section along the Kwinana Freeway collected on 14 April 2018 is shown in Figure 4.3. The red box highlights the location where it was proposed to install the ground instrumentation array.

The deflection data for the section along Leach Highway was collected on 11 April 2018, as shown in Figure 4.4. The data from the preliminary metropolitan scan was very important because it indicated the likely deflection at the instrumented site after the gauges were installed.

After the installation, the uniformity of each section was checked by running the FWD along the section at 5 m increment spacings. Further details of the FWD testing is presented in Section 5 of this report.

Figure 4.3: TSD preliminary metropolitan scan along Kwinana Freeway (H015)

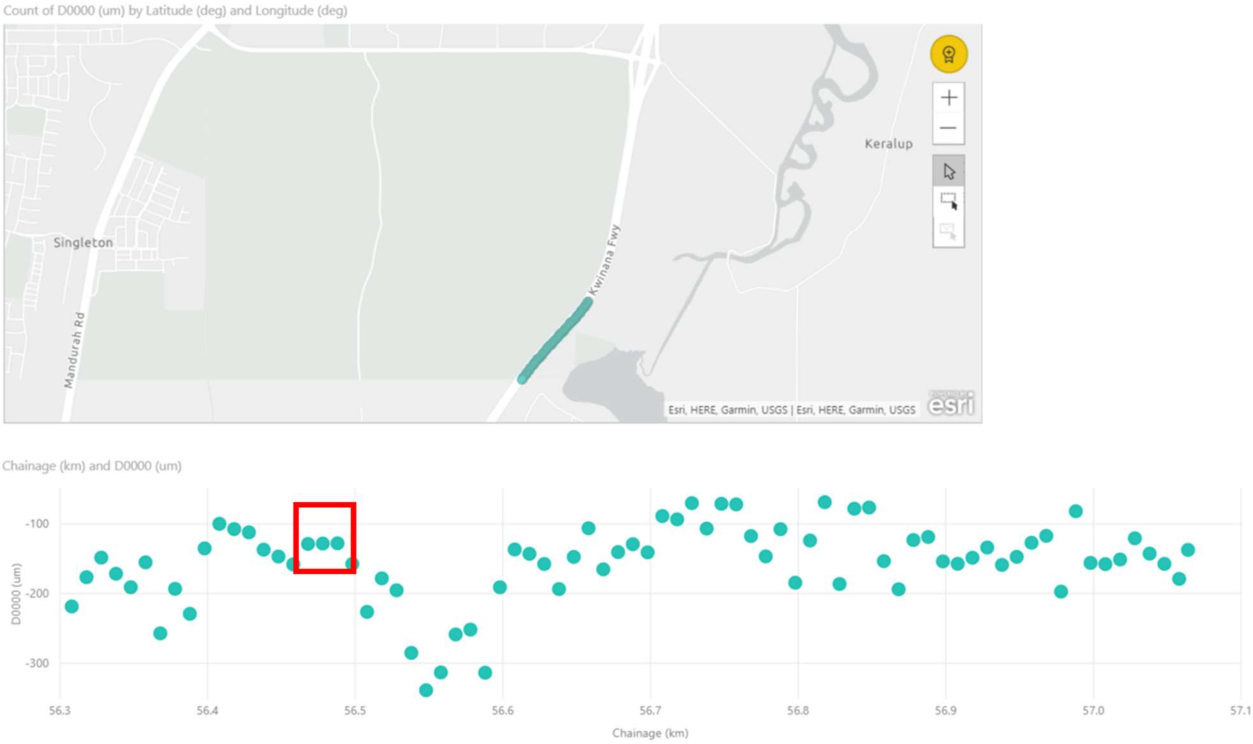

Figure 4.4: TSD preliminary metropolitan scan along Leach Highway (H012)

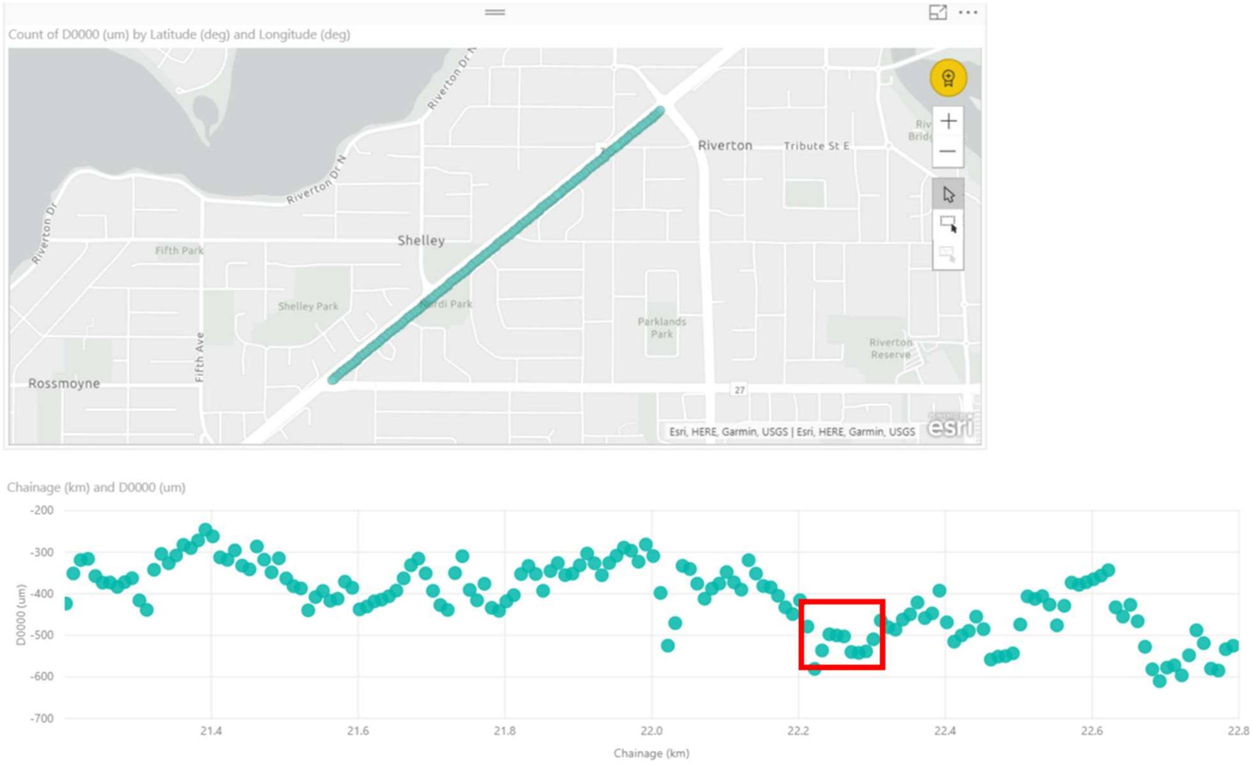

4.2.2 Validate instrumentation array installation shortly after sensor installation

For two consecutive nights between 13–15 September 2018, the project team carried out the sensor installation on both the Kwinana Freeway and Leach Highway. A detailed discussion of the sensor installation was presented in Section 3.4 of this report. In this section, the activities conducted to validate that the instrumentation array was functional are reported.

Immediately after the installation (i.e. after the polyurethane epoxy infill had cured), several impact loads including the FWD and an instrumented hammer were applied to the pavement and the outputs of the instrumentation array compared. The FWD and the instrumented hammer were selected because the mechanics of these two methods are well understood and can be used as a reference load/test.

Table 4.3 presents the comparison between an FWD measured deflection profile and a profile measured by the instrumentation array. It can be seen that the in-ground sensor was reporting similar deflections to the FWD deflections, apart from a few measurements near the centre of the FWD loading plate. At the time of the testing, the reason for this anomaly was not clearly understood, and so further tests were carried out in October 2018 (refer Section 4.2.3).

Table 4.3: Comparison of sensor and FWD results after initial instrumentation array installation

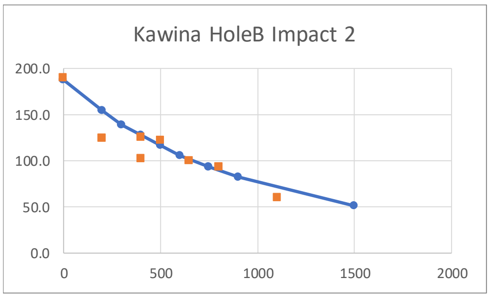	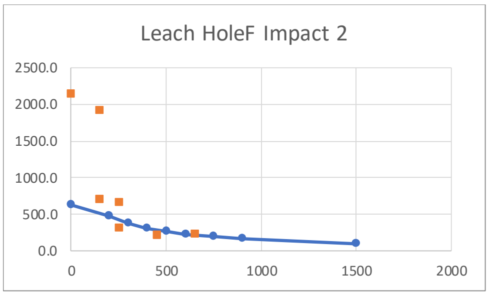
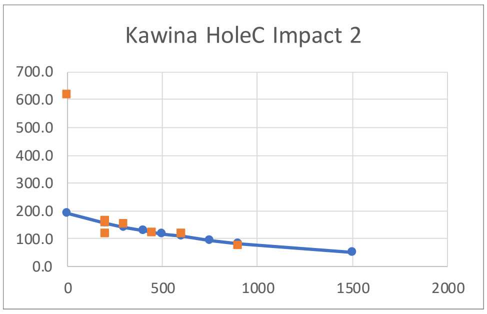	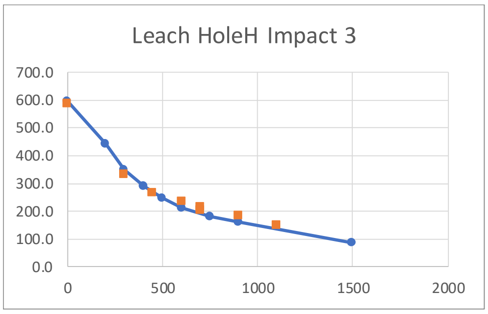
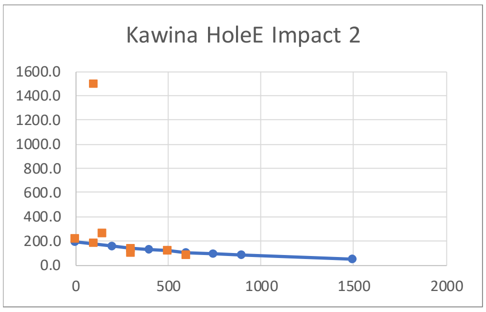	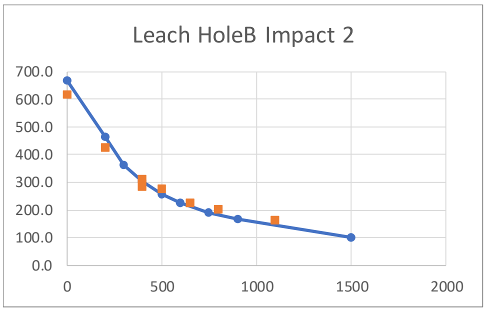
Note: FWD measured deflection profile is shown in blue colour	
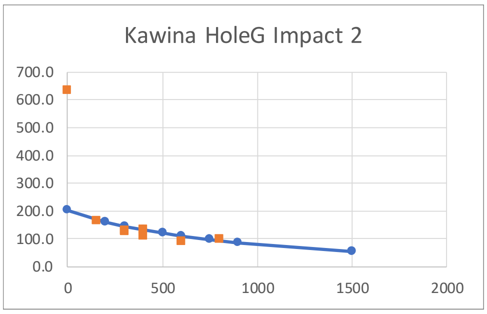	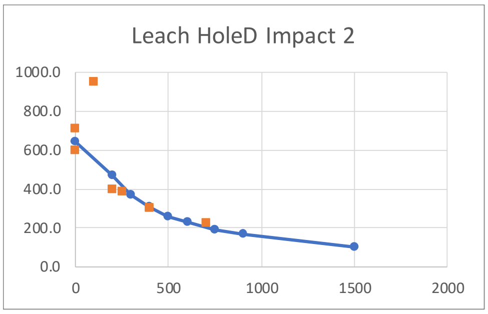
Note: FWD measured deflection profile is shown in blue colour	

During the sensor installation, impact hammer tests were also carried out at selected locations. The force and the acceleration response immediately adjacent to the impact location were recorded. The acceleration spectra were calculated and subsequently converted to mobility and receptance spectra. The results from the impact hammer, expressed in terms of receptance (deflection over applied force in m/N), are shown in Figure 4.5 and Figure 4.6. As the inverse of the receptance spectrum is the dynamic stiffness spectrum, the dynamic stiffness spectra were then calculated. The lower the inverse of the receptance spectrum, the higher the pavement stiffness.

Figure 4.5: Impact hammer results: Kwinana Freeway

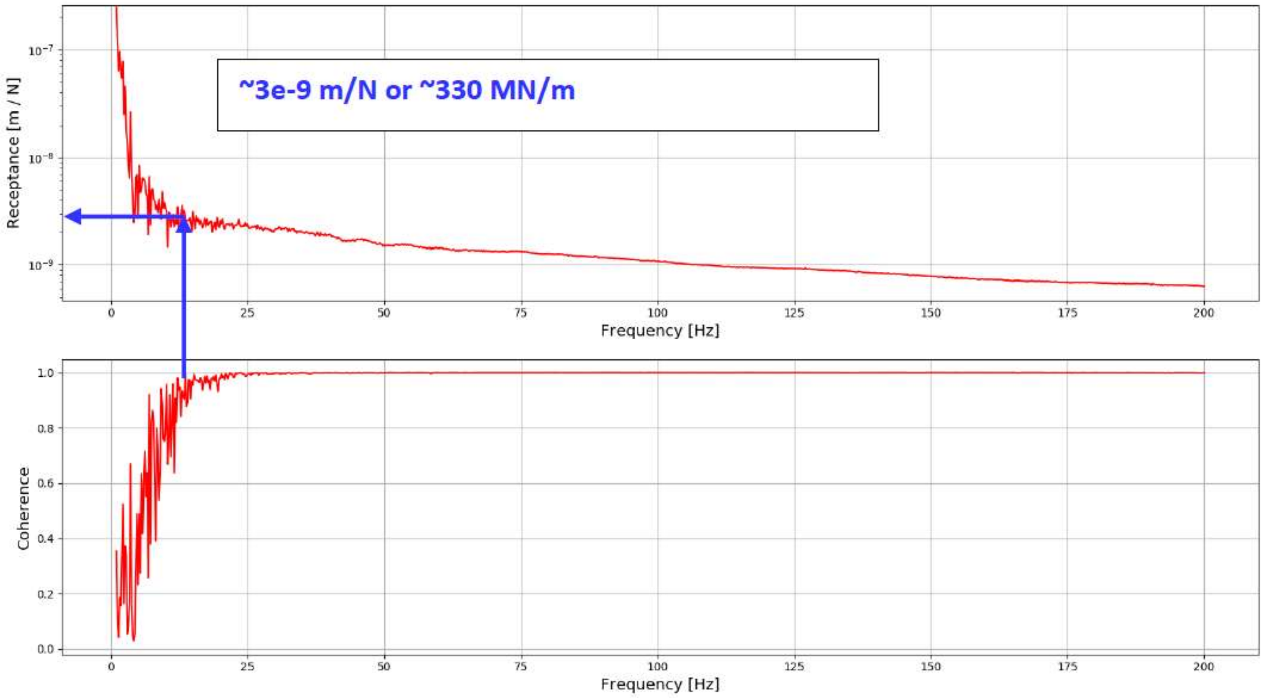

Figure 4.6: Impact hammer results: Leach Highway

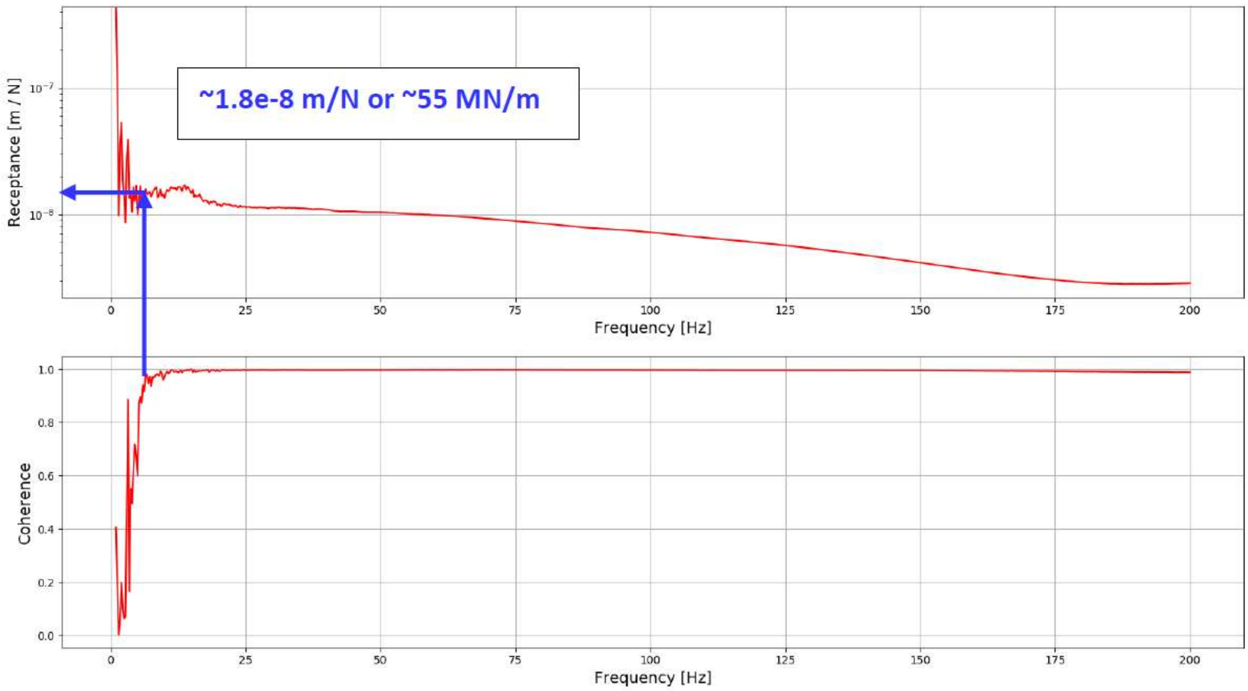

It was confirmed that the Kwinana Freeway (330 MN/m) had a much higher stiffness than the Leach Highway (55 MN/m). While the load level and impact frequency of an impact hammer are very different from an FWD; it would still be worthwhile to compare the stiffness measured using the two different methods.

For the Kwinana Freeway, the impulse hammer gives a stiffness of 330 MN/m. Based on a 50 kN FWD load, the stiffness can be converted to an equivalent deflection of about 150 microns. For the Leach Highway, a stiffness of 55 MN/m can be converted to an equivalent deflection of about 900 microns.

In terms of the FWD measurements made in September 2018 at the instrumentation array location, the Kwinana Freeway reported a normalised deflection of 183 microns, and the Leach Highway had an equivalent deflection of 620 microns. The results from the Kwinana Freeway were similar, but there was a large difference in the weaker Leach Highway because of the high non-linearity, as would be expected.

4.2.3 Monitoring Ground Instrumentation Output During TSD Pass-by and FWD Tests

After the successful installation of the instrumentation array in September 2018, the project team organised additional FWD tests and multiple runs by the TSD were also carried out. On the night on 27 October, the project team conducted the following tests:

- FWD testing at 5 m spacings to check the deflection uniformity in the vicinity of the instrumentation array
- FWD testing at different lateral offset as illustrated in Figure 4.7
- Multiple TSD runs at different speeds.

Figure 4.7: Diagram illustrating the different FWD loading plate positions used in October 2018

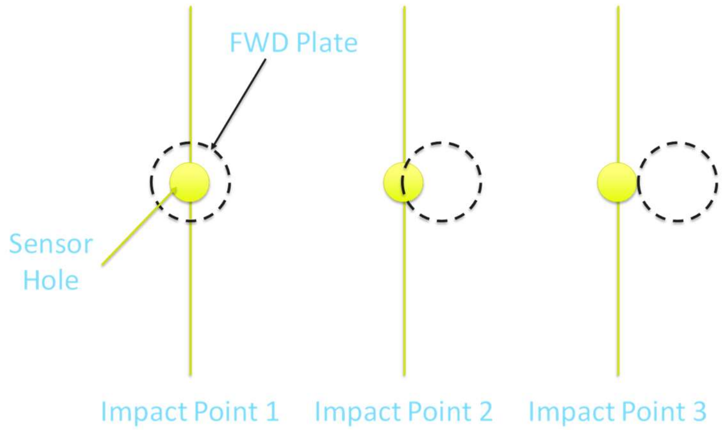

5 RESULTS OF FIELD TEST

5.1 Site Uniformity and Repeatability

For the reasons provided in Section 4.2.1, in order to allow a fair comparison between the TSD deflection (i.e. every TSD deflection point is an average value over a 10 m spacing) and discrete response from an FWD and the ground instrumentation sensors, the deflection in the test site needs to be fairly uniform.

The FWD deflections were collected at 5 m spacing, from 25 m before and 25 m after the location of the instrumentation array. The normalised maximum deflections (ND0) and normalised curvatures (NDCURV) for both the Kwinana Freeway and Leach Highway sites are shown in Figure 5.1. The measurements, conducted the night before the TSD past over the site, confirmed the uniformity of both test sites.

Figure 5.1: FWD maximum deflection and curvature

Deflection measurements are often used to monitor the deterioration of a pavement asset. Other than normal degradation of the pavement asset, deflection measurements can be affected by environmental factors such as temperature and moisture conditions. The repeatability of deflection measurements from multiple TSD runs is therefore an important aspect of this study. As shown in Figure 5.2 (maximum deflection and curvature), multiple TSD testing was conducted to confirm the repeatability of the measurements. For the Kwinana Freeway, the TSD operating speed was between 41 and 75 km/h whilst, at the Leach Highway, the operating speeds ranged between 48 and 65 km/h.

Although the results did not exactly match, it demonstrated that the TSD was very repeatable. When evaluating the results, it is important to recognise that, within the limit of the TSD driver, consecutive TSD runs may not be aligned perfectly along with the instrumentation array.

Future research should aim to improve the monitoring and guidance of the TSD to minimise wandering when passing an instrumentation array.

Figure 5.2: TSD maximum deflection collected at Kwinana Freeway and Leach Highway

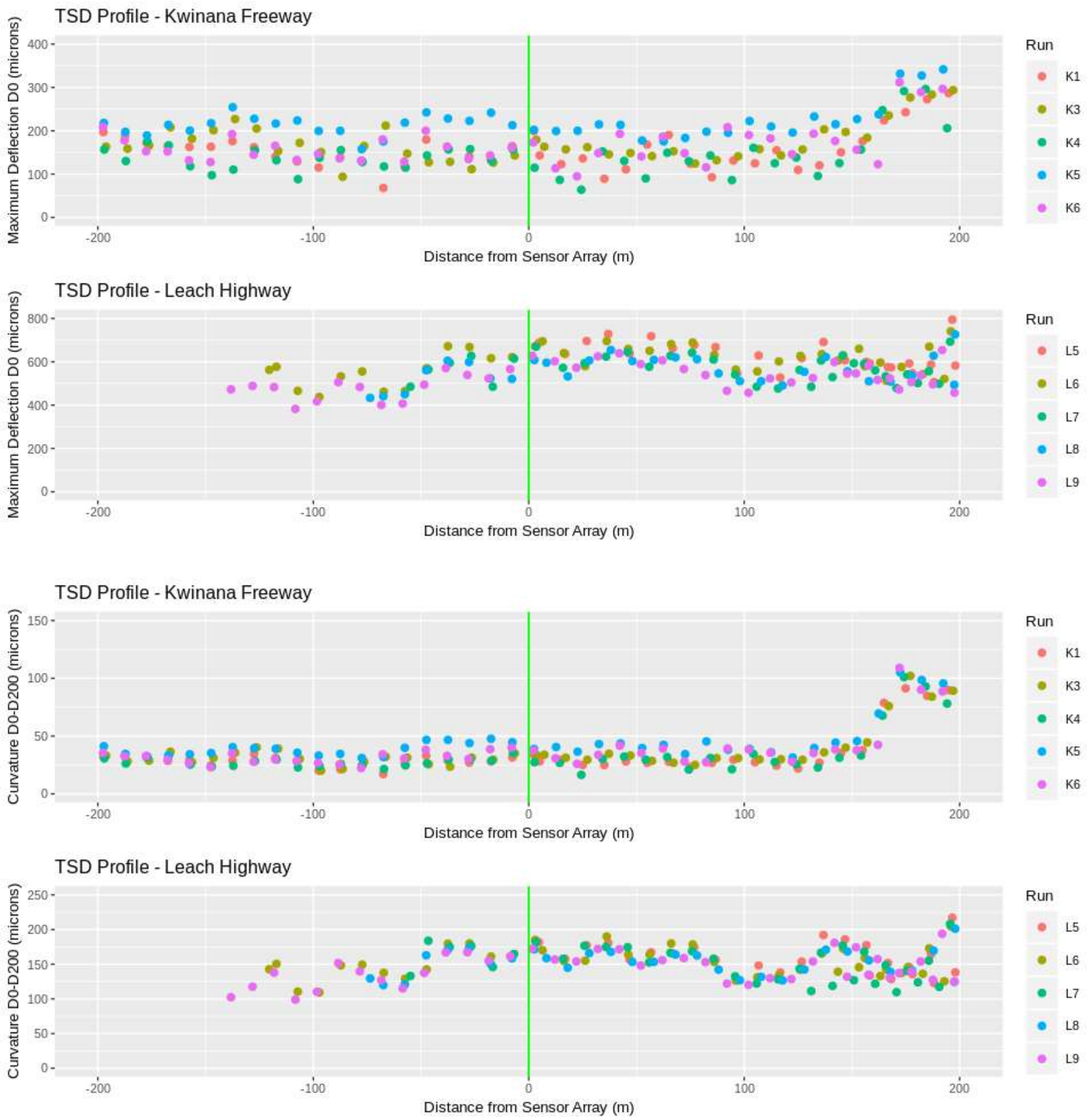

Figure 5.3 shows the Doppler laser in the leading side of the TSD rear axle.

Figure 5.3: Photograph of Doppler laser in front of the rear dual-tyre axle

To illustrate the variability of the TSD traffic paths, laser images obtained from the onboard Automatic Crack Detection (ACD) were analysed. The ACD images collected in subsequent TSD runs along the Kwinana Freeway and the Leach Highway are shown in Figure 5.4 and Figure 5.5, respectively. Red lines in the figures denote the approximate lateral position of the Doppler laser. Based on the ACD images and field observations, the TSD driver had more difficulty lining up the Doppler laser with the instrumentation array on the Kwinana Freeway than the Leach Highway. A possible reason for this could be that the TSD was traveling at a higher along the Kwinana Freeway and the site is located in a rural area where there were no kerbs and limited road furniture to help guide the driver. Nevertheless, the fifth run (K5) on the Kwinana Freeway was very close to the instrumentation array, whilst the eighth run (L8) was the closest on the Leach Highway. The project team believed that the lateral variability explained the variability in deflection of subsequent TSD runs. In the future, ACD images should be used to determine the location of the Doppler laser in relation to the instrumentation array.

Figure 5.4: ACD images from subsequent TSD runs along Kwinana Freeway

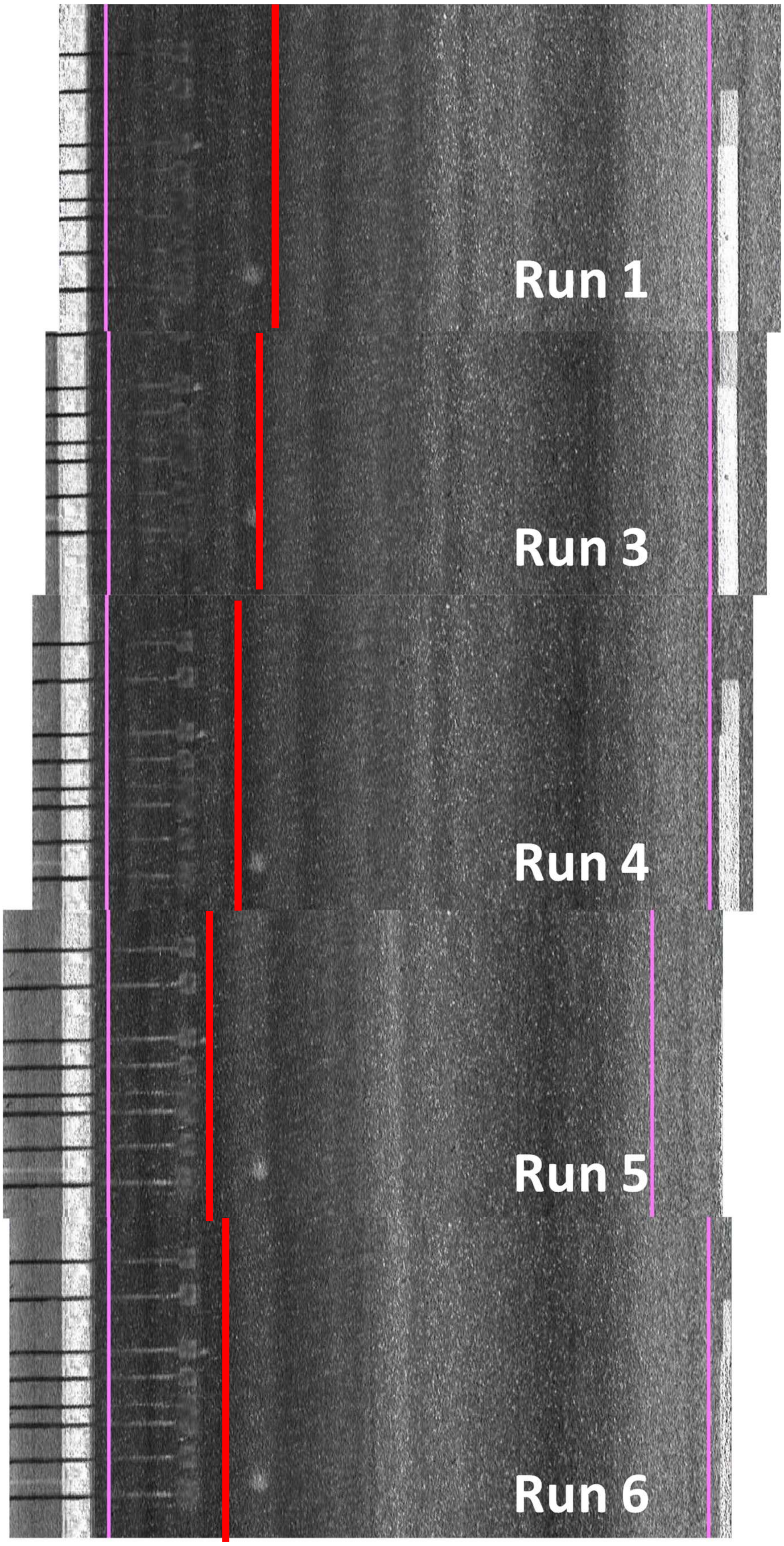

Figure 5.5: ACD images from subsequent TSD runs along Leach Highway

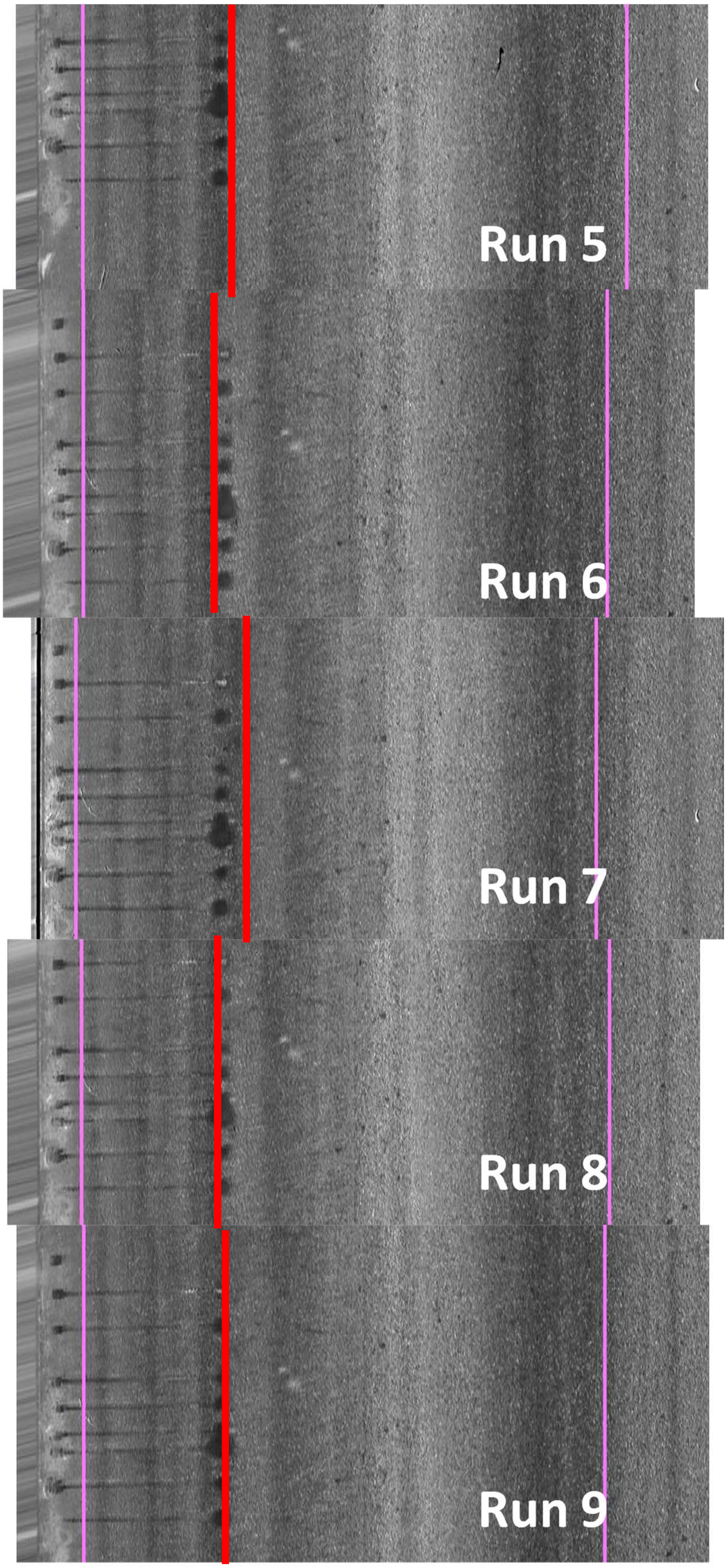

5.2 Typical Time Histories Collected from the Instrumentation Array

As discussed in Section 3.5, a high-precision data acquisition system was used in this project. During all the FWD testing and TSD pass-by runs, each geophone and accelerometer channel was sampling at a rate of more than 2 000 Hz. At this sampling rate, very detailed time-history data can be captured. An example of the velocity-time record captured by a geophone during a TSD pass-by is shown in Figure 5.6. The peaks in the time histories represent the pavement response induced by the first, second and third axle of the TSD as it travelled past the instrumentation array (left to right of the horizontal axis). The velocity record can be converted into the displacement record (refer Figure 5.7) through integration with respect to time. Furthermore, the acceleration record can be determined from the velocity record by differentiating with respect to time, as shown in Figure 5.8.

Figure 5.6: Typical velocity time history when TSD passes by instrumentation array

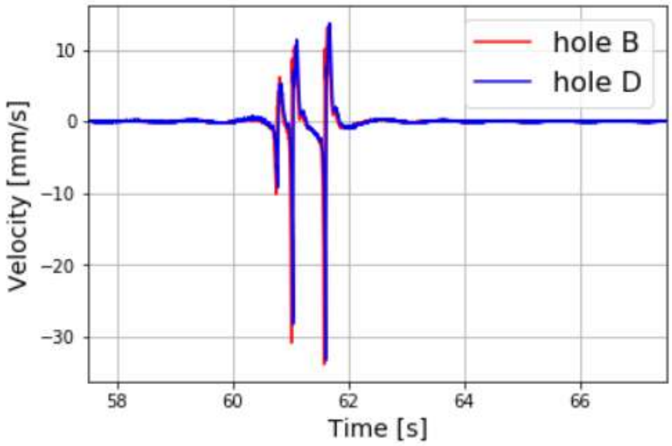

Figure 5.7: Typical displacement time history when TSD passes by instrumentation array

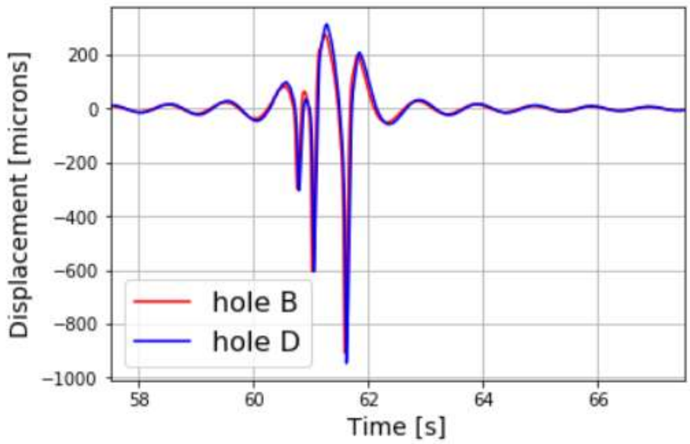

Figure 5.8: Typical acceleration time history when TSD passes by instrumentation array

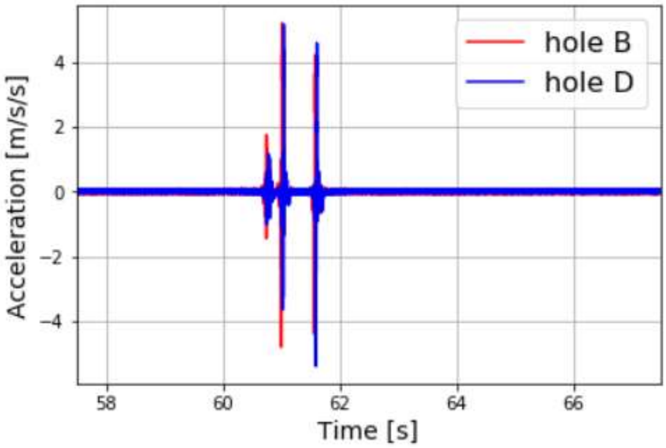

Other than a TSD run, typical velocity and acceleration time records collected during an FWD test are also shown in Figure 5.9. It is worth noting that, for the same impulse load, the velocity time history has a lower frequency content than the acceleration history.

Figure 5.9: Typical velocity and acceleration time history of an FWD impact load

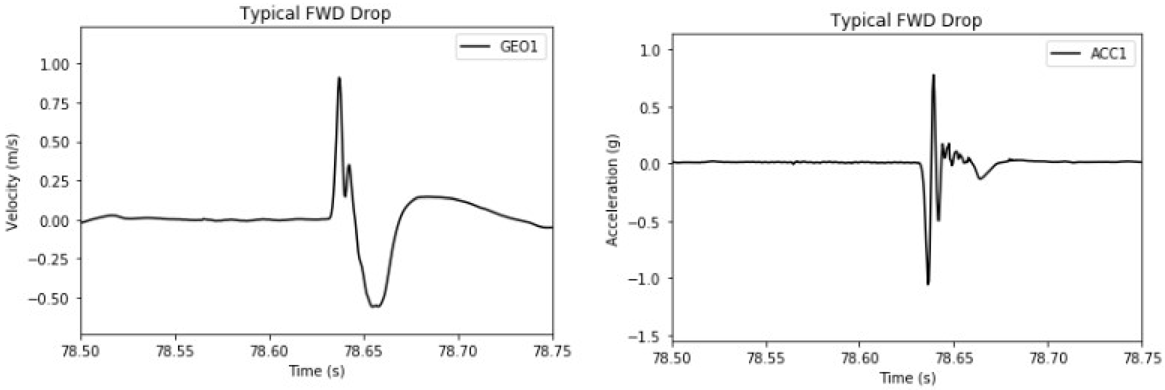

The instrumentation array captures the response from all three TSD axles. However, the deflection measured by the TSD only considers the loading from the last axle (single axle dual tyre). The velocity and acceleration time records from the TSD and the FWD are shown side-by-side in Figure 5.10. It is evident that the waveform from an FWD is different to a TSD from a time domain perspective. The TSD time record is a function of the travel speed of the device. Further analysis in the future can be carried out in the frequency domain to improve our understanding in this area.

Figure 5.10: Comparison of velocity and acceleration time records

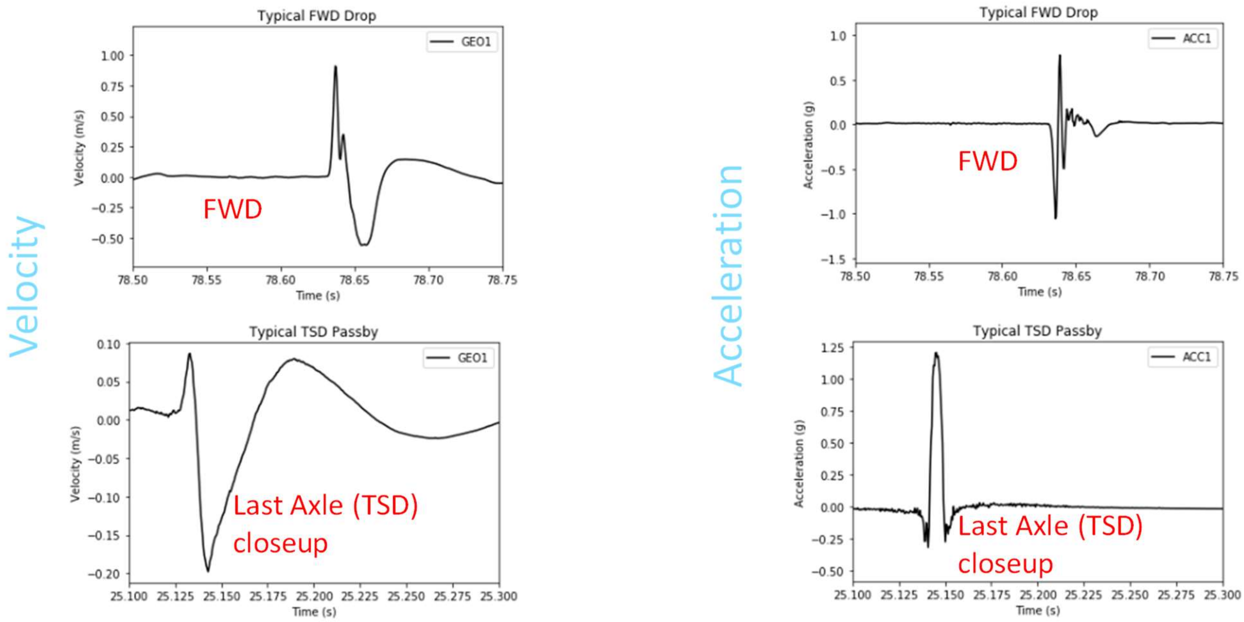

It is worth further investigating the time history when the last TSD axle travels passed the instrumentation array, the deflection bowl shown in Figure 5.11 indicated an asymmetric rolling deflection bowl. It is characterized by rapid loading as the TSD approaches the instrumentation array, with the pavement rebounding slowly as the last axle leaves the instrumentation array.

Figure 5.11: Asymmetric rolling deflection bowl measured by the instrumentation array

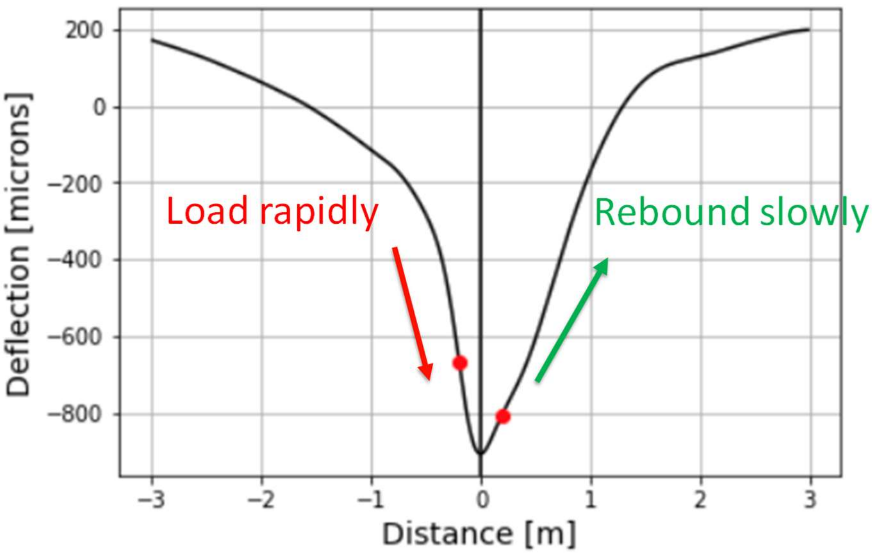

Figure 5.12 shows the time histories as all three axles travelled past the instrumentation array on the Kwinana Freeway and Leach Highway. As expected, the displacement measured on the Leach Highway was higher than the displacement measured on the Kwinana Freeway. The last axle (far right axle) is heavier than the front and second axles. Therefore, the displacement measured is also of a similar pattern.

It is also important to note that the velocity and acceleration caused by the second axle (middle axle) return to zero before the last axle. This confirms that each axle is responding independently at both sites.

Figure 5.12: Acceleration, velocity and displacement time histories of TSD passing the test array along Kwinana Freeway (left) and Leach Highway (right)

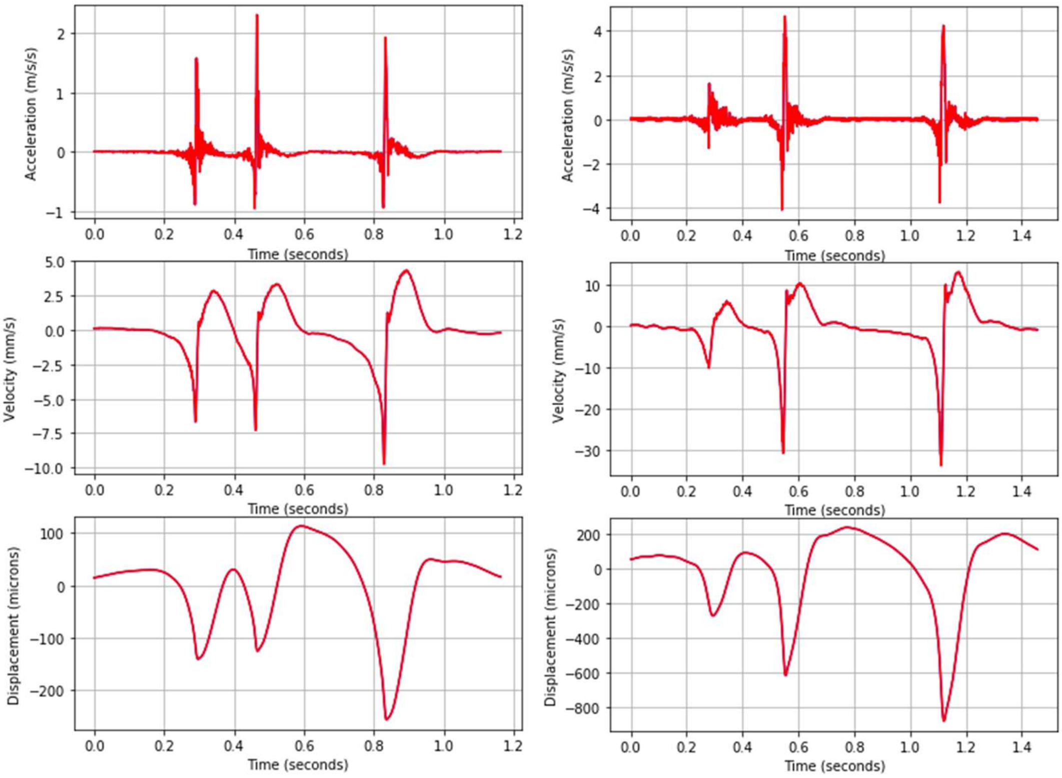

5.3 Comparison Between TSD and FWD Results

Based on the time records presented in the previous section, it is evident that a TSD pass-by is different from an FWD impulse load, with respect to the load duration, the shape of the waveform and the energy content in the frequency domain. To further complicate the issue, the response induced by the TSD is also dependent on the operating speed.

It is common practice to evaluate a relatively new device against an established testing device. In this case, one of the most commonly asked questions is how do the TSD measurements compare with the FWD measurements. Despite all the fundamental differences, at certain operating conditions, the net effects of these factors can cancel each other out.

A comparison of the maximum TSD and FWD deflections and curvatures at the two sites is shown in Figure 5.13 and Figure 5.14, respectively. For simplicity, only a single TSD run is shown for the Kwinana Freeway (left Figures) and Leach Highway (right of the Figures). The curvature function is of interest to MRWA because there is an emphasis of utilising this function for pavement acceptance purposes.

Figure 5.13: Comparison of maximum deflections on Kwinana Freeway (left) and Leach Highway (right)

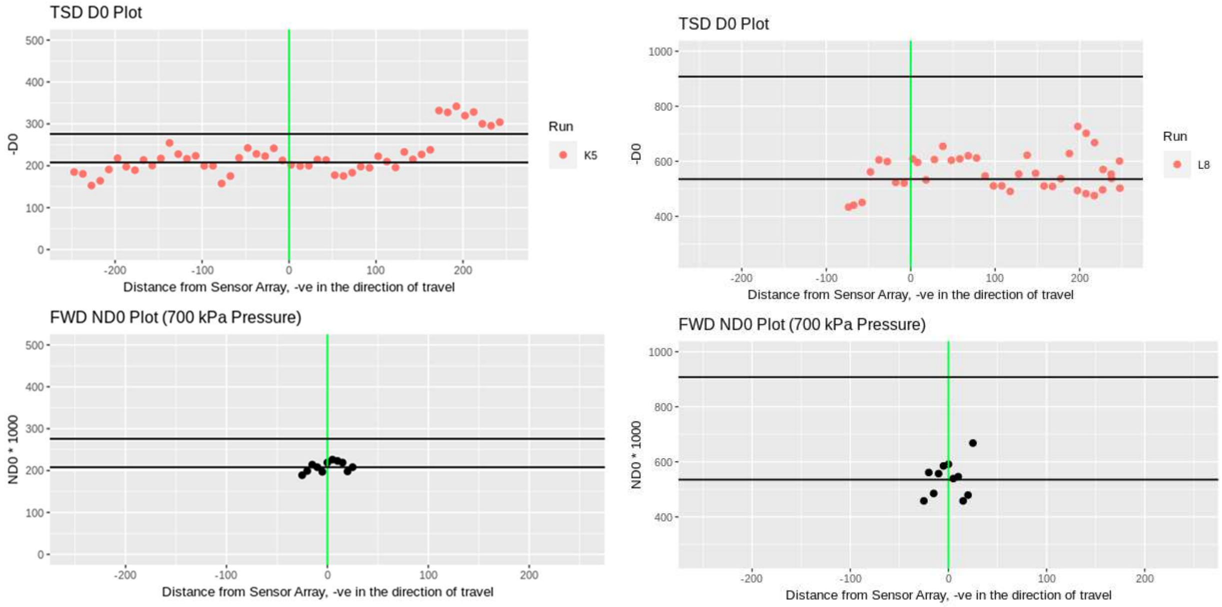

Figure 5.14: Comparison of curvature function (D0 – D200) on Kwinana Freeway and Leach Highway

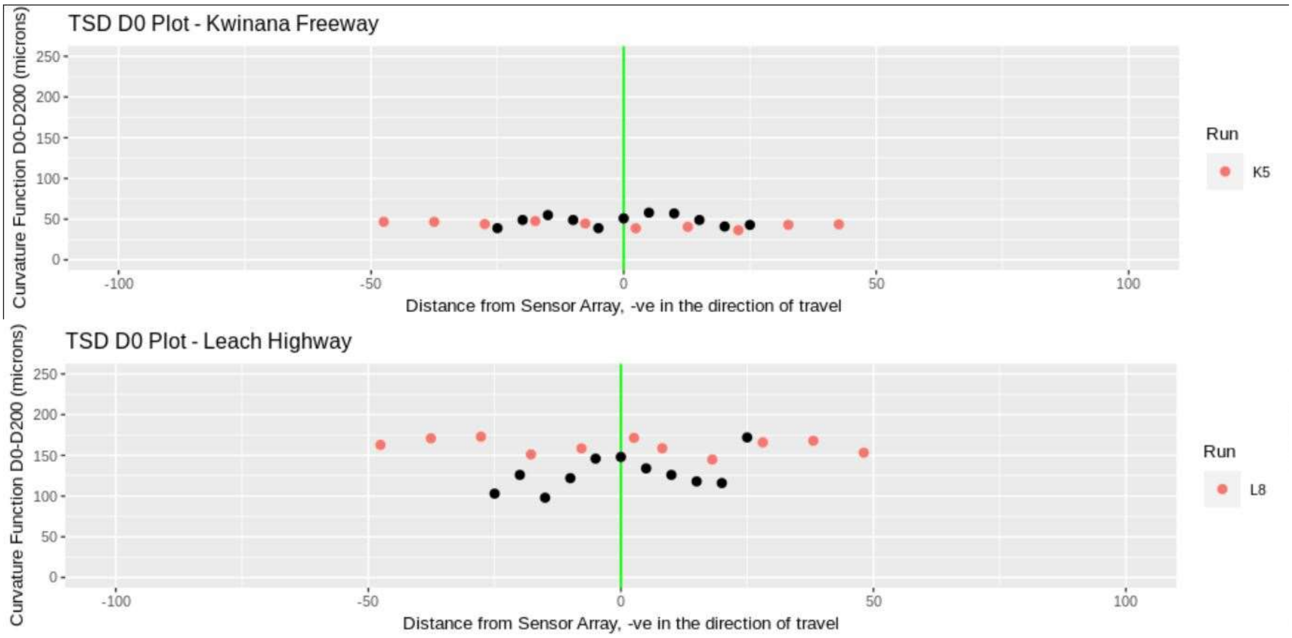

These Figures only compare the maximum deflections and the curvature functions, which only applies to the front part of the deflection bowl. The full deflection bowls from both devices are shown in Figure 5.15; they confirm the remarkable match in the front part of the deflection bowl.

Figure 5.15: Comparison of selected deflection bowls collected from TSD and FWD

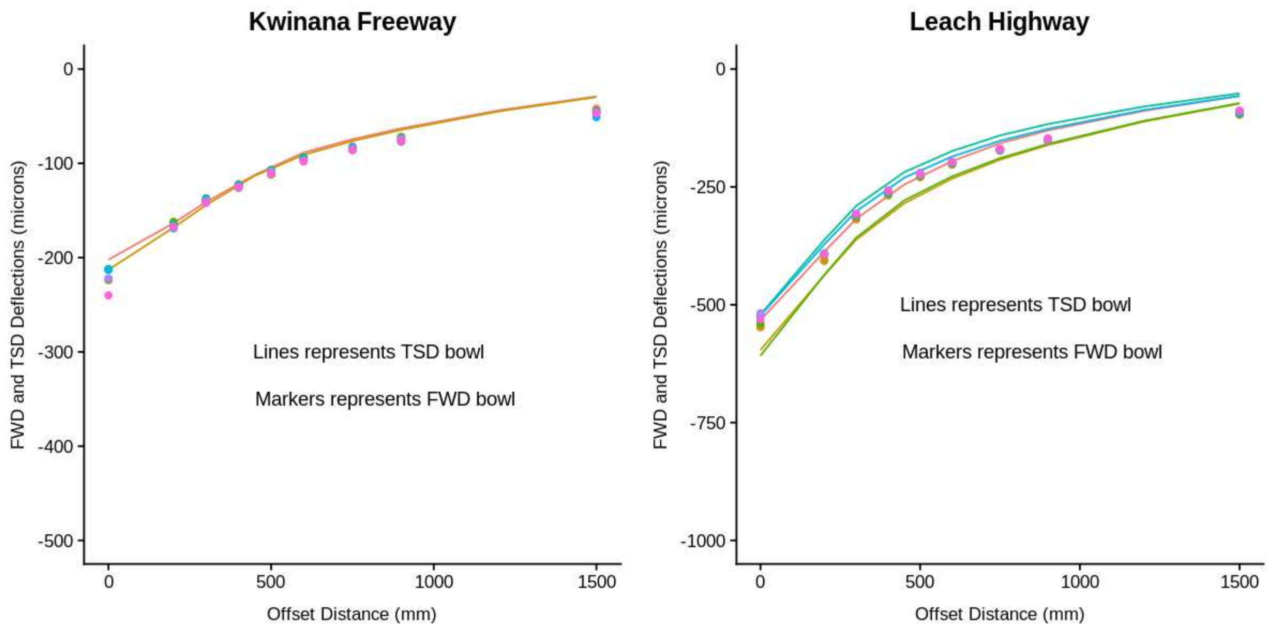

The deflection bowl for both the Kwinana Freeway and Leach Highway are compared in Figure 5.16 and Figure 5.17. It is worth noting that the tail end data (i.e. deflection beyond 900 mm offset) does not match well at the Kwinana Freeway site. Two recommendations for future study are suggested:

- Future research should focus on the linear viscoelastic behaviour of the Kwinana pavement with relatively thick asphalt layers.
- The study should include the subject of time-dependent asphalt layer properties subjected to the dynamic moving loads associated with the TSD. The effects of viscoelastic behaviour are expected to be more profound in the case of thick asphalt pavements.

The deflection measurements on the Leach Highway showed a much better match to at least 900 mm offset from the centre of the load. It is envisaged that a good TSD-FWD correlation can be developed from the deflection data collected at the Leach Highway.

Without further data, the project team cannot conclusively explain the difference in the field measurement at the Kwinana site. However, several explanations can be postulated here:

- The deflection bowl is very different at the two sites, and the Signal-to-Noise (SNR) ratio may be higher for stiff pavement at Site One (Kwinana Freeway).
- The degree of subgrade non-linearity (Chai et al. 2015) is often observed in FWD deflection (beyond 900 mm offset). It is postulated that the TSD measurement is also affected by the subgrade non-linearity behaviour. This was also reported for TSD data collected on Queensland pavements (Chai et al. 2016). At this stage, because of the different type of dynamic loading imposed by the two devices, the extent of this effect cannot be quantified at this point in time.

Lee & Conaghan (2016), in a study in Queensland, raised concerns as to whether linear regression is adequate to represent the relationship between TSD and FWD measurements in the tail end of the deflection bowl.

Figure 5.16: TSD deflection and FWD deflection comparison at different offsets along Kwinana Freeway

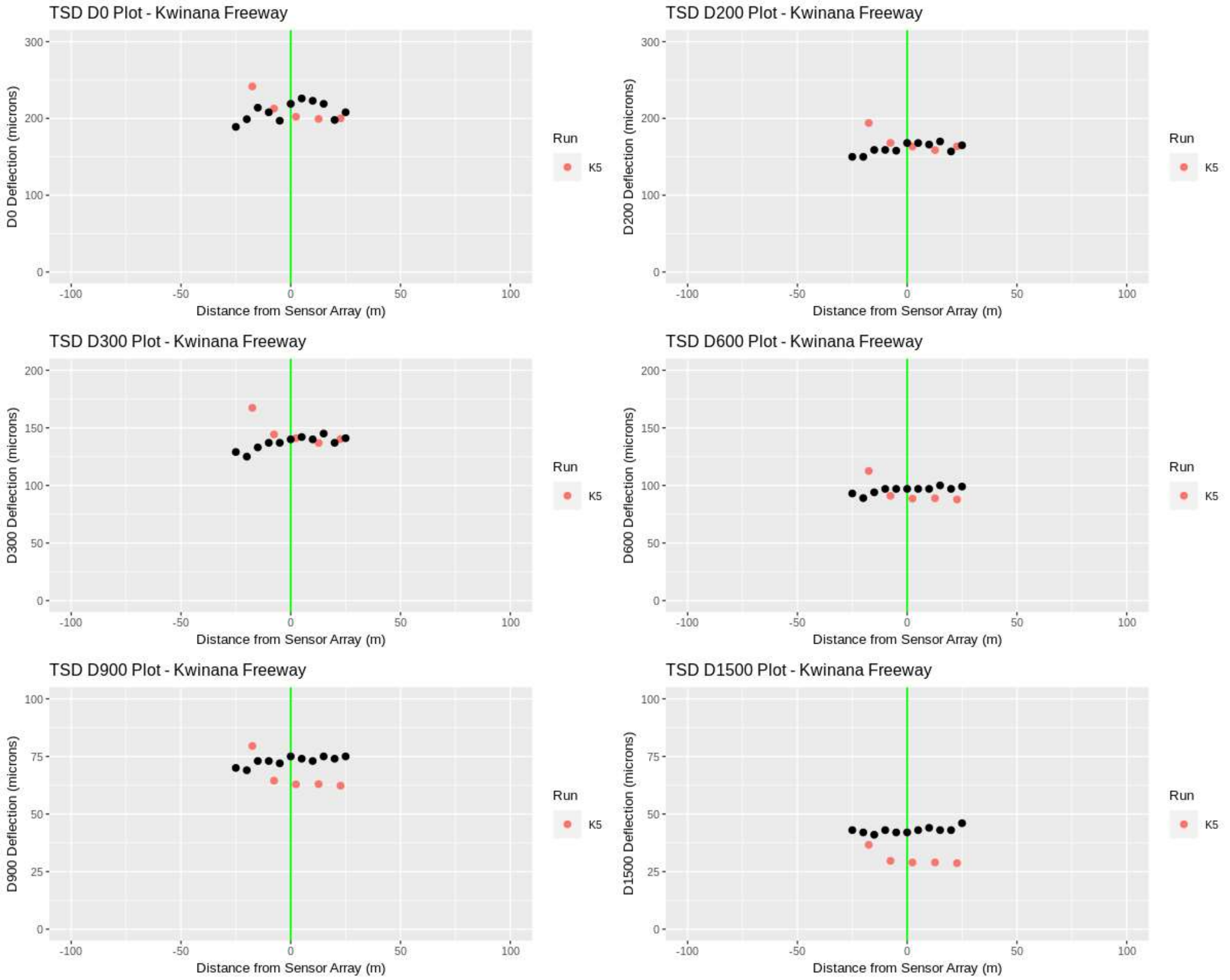

Figure 5.17: TSD deflection and FWD deflection comparison at different offsets along Leach Highway

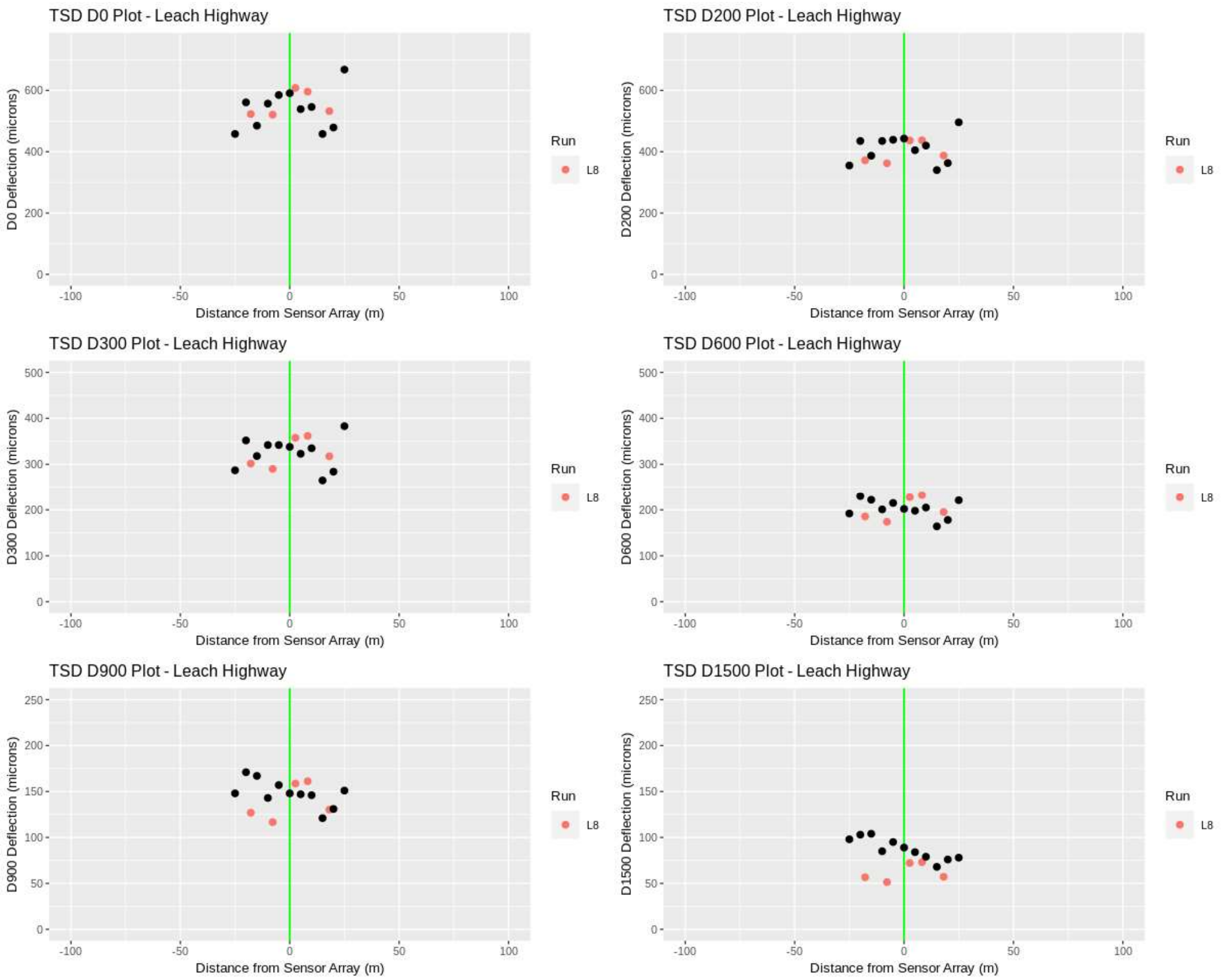

5.4 Comparison of TSD and Ground Instrumentation

In the previous section, the TSD and FWD deflections were compared and showed reasonable agreement. While it is helpful to relate the TSD deflection with a traditional deflection testing device such as the FWD, the aim of this project is to set up an instrumentation array and demonstrate that in-ground sensors can validate the TSD or FWD measurement independently. In this section, the TSD data will be compared with the response measured by the instrumentation array.

Multiple TSD runs were carried out on 27 October 2018. The results of the TSD runs and the response measured by the instrumentation array along the Kwinana Freeway and Leach Highway are shown in Table 5.1. On the Kwinana Freeway, the TSD operated at 41–77 km/h, whilst on the Leach Highway, because of the limited post speed of 70 km/h, the TSD operated at 48–65 km/h.

Table 5.1: Measured instrumentation array response (geophone)

Site	Run	Average speed (km/h)	Maximum displacement (microns)	Maximum velocity (mm/s)	Maximum acceleration (mm/s2)
Kwinana Freeway	1	73	207.91	4.12	0.38
	2	77	268.69	9.99	1.62
	3	76	247.01	8.90	1.06
	4	76	233.23	7.02	1.05
	5	76	258.58	9.74	1.49
	6	41	259.55	5.48	0.62
	7	48	275.82	6.93	0.75
Leach Highway	1	62	535.22	14.34	1.63
	2	65	686.32	29.70	5.85
	3	62	821.40	32.50	4.25
	4	65	847.20	42.13	9.21
	5	65	772.57	37.30	8.97
	6	64	829.03	36.90	6.07
	7	48	876.00	31.00	5.30
	8	50	907.42	33.90	4.81

The deflection bowl measured by the TSD in each subsequent runs through the instrumentation site is presented in Figure 5.18 and Figure 5.19, for Kwinana Freeway and Leach Highway respectively. The deflection bowl measured by the instrumentation array using a geophone is also plotted for comparison.

Figure 5.18: Comparison of TSD runs and instrumentation response: Kwinana Freeway

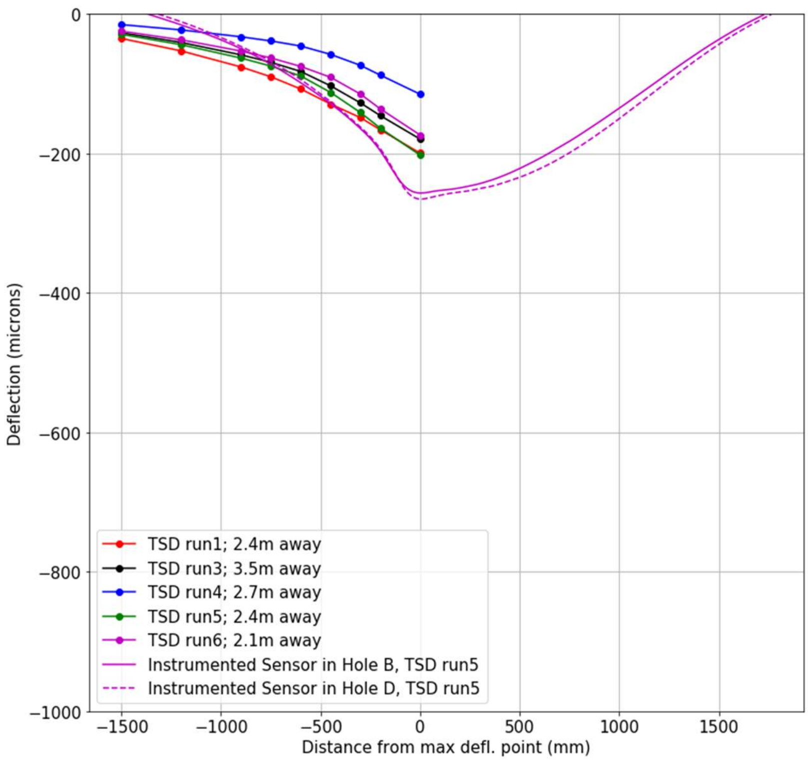

Figure 5.19: Comparison of TSD runs and instrumentation response: Leach Highway

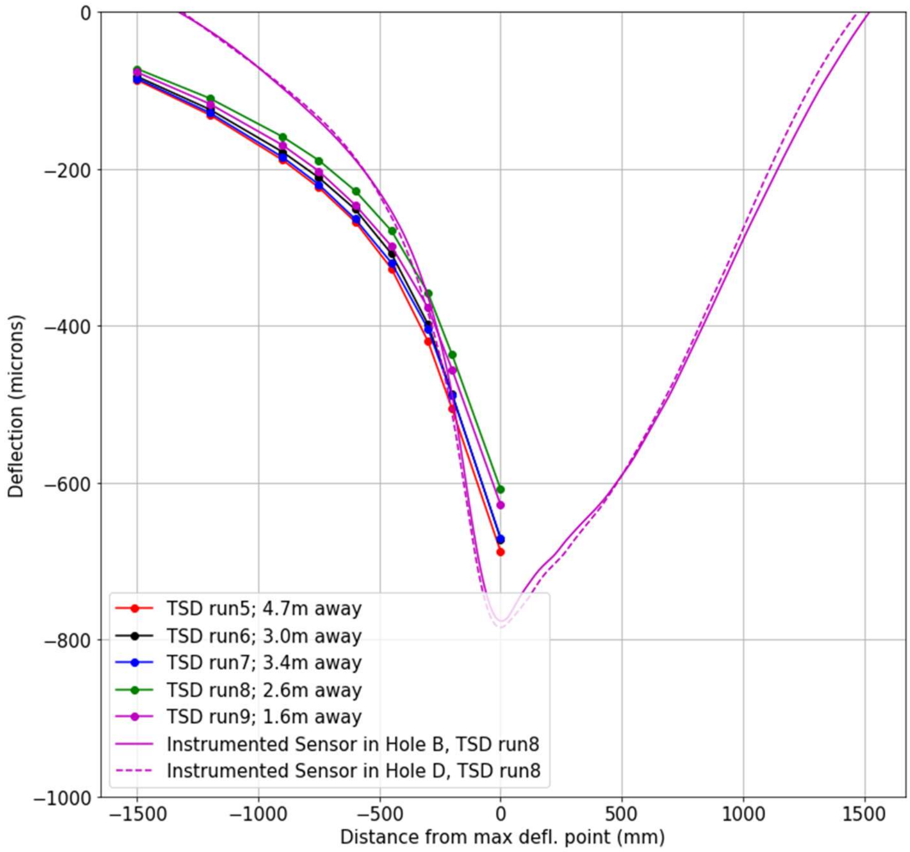

5.5 Comparison Between FWD and Ground Instrumentation

A similar comparison between the FWD and instrumentation measurements is shown in Figure 5.20 and Figure 5.21, for the Kwinana Freeway and Leach Highway respectively. All the FWD deflections measured by the instrumentation array are presented. The response measured by the geophone in Hole B and Hole D is also plotted. It is noted that, in order to construct the entire deflection bowl based on a point measurement, a different part of the time record from the instrumentation array was obtained as the dual-tyres of the wheel travelled through the array. The FWD and instrumentation array results from both sites compare well.

Figure 5.20: Comparison of FWD measurements and instrumentation array: Kwinana Freeway

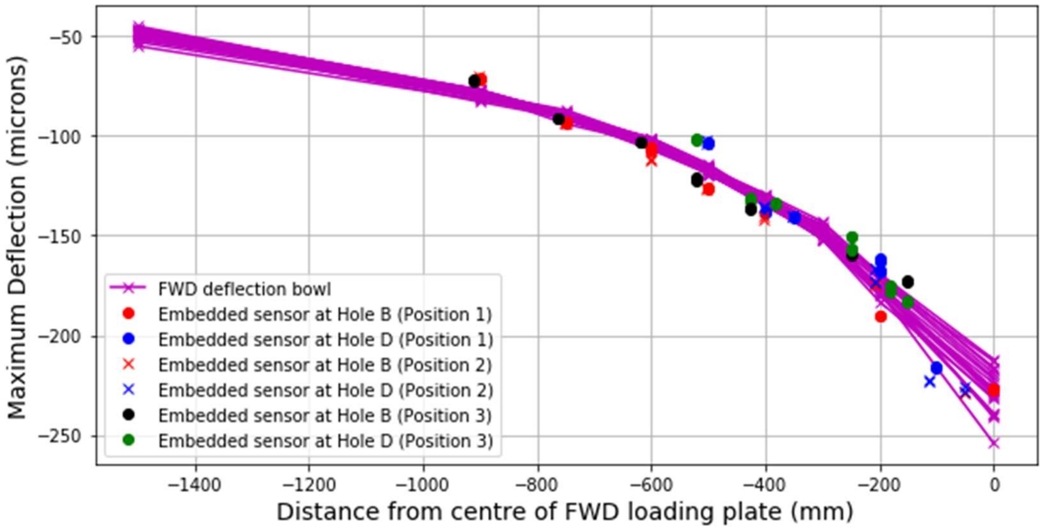

Figure 5.21: Comparison of FWD measurements and instrumentation array: Leach Highway

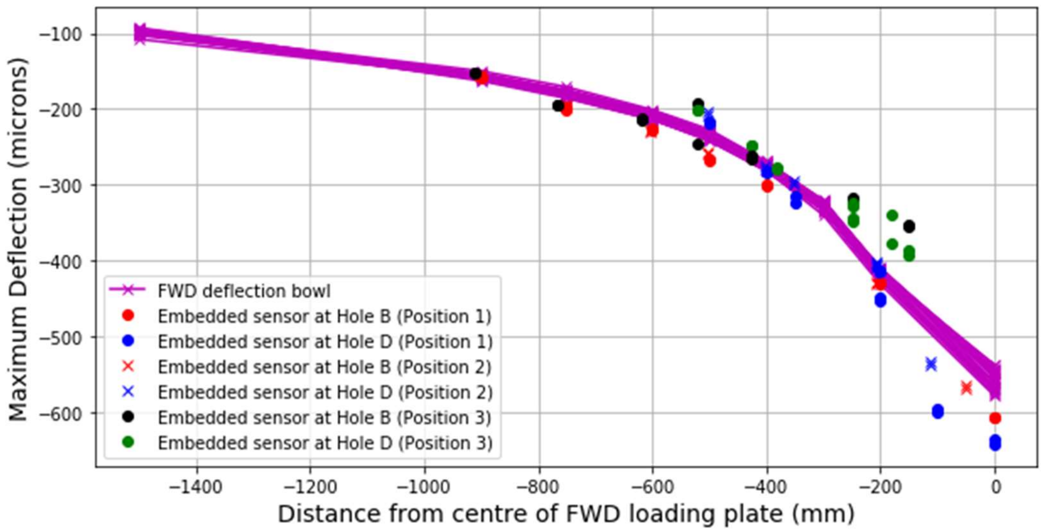

5.5.1 Near Field Sensor Amplification

One of the phenomena mentioned earlier in this report (refer Section 4.2.2) is that, when the FWD loading plate is located directly over the instrumentation array, the instantaneous response measured by the instrumentation array is higher than the reported FWD deflection. As soon as the wheel departs the instrumentation array, the response from the FWD and the in-ground sensor agrees very well. This was not well understood by the project team at the time of the sensor installation. In order to better understand the reasons behind this, in October 2018, additional FWD testing was undertaken. Three series of tests, as denoted in Figure 5.22, with different lateral positions, were conducted.

The results collected by the geophones are shown in Figure 5.23, and the results collected by the accelerometers are shown in Figure 5.24. For the geophones, the measurements are slightly different at positions 1 and 2 (i.e. the FWD loading plate is either fully or partially covering the hole).

For the accelerometers, when the loading plate was at positions 1 and 2, the response was amplified significantly at the corresponding holes (i.e. when impacting at Hole B, the response in Hole B was higher than expected). At position 3, the FWD loading plate was not pressing against the hole, and the response reported by the instrumentation array was as expected.

In summary, the geophone was more immune to amplification compared to the accelerometer. This is primarily because the accelerometer does not have a casing to protect it against any compression from the wheel load. Furthermore, the accelerometer was generally embedded much closer to the pavement surface compared the geophone. Improvement to the installation details would therefore need to be addressed in future installations.

Figure 5.22: Comparison of selected deflection bowls collected from TSD and FWD

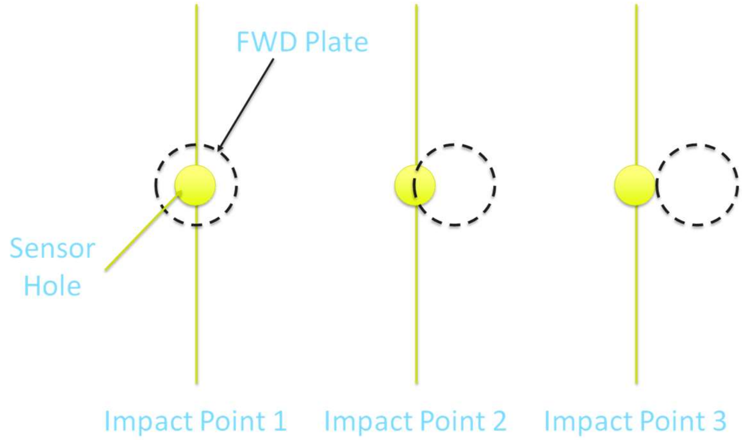

Figure 5.23: Comparison of displacement measured by geophones in the array when FWD impacted at different lateral positions

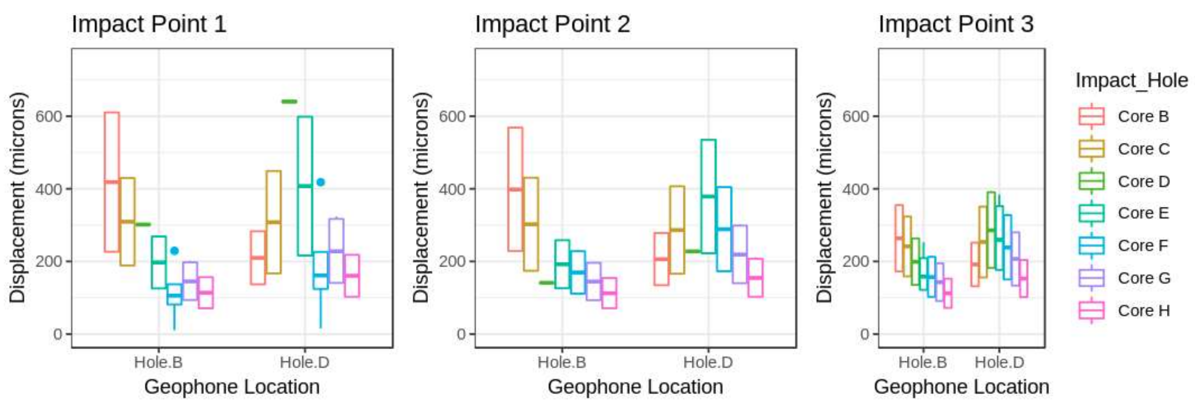

Figure 5.24: Comparison of displacement measured by accelerometers in the array when FWD was impacted at different lateral positions

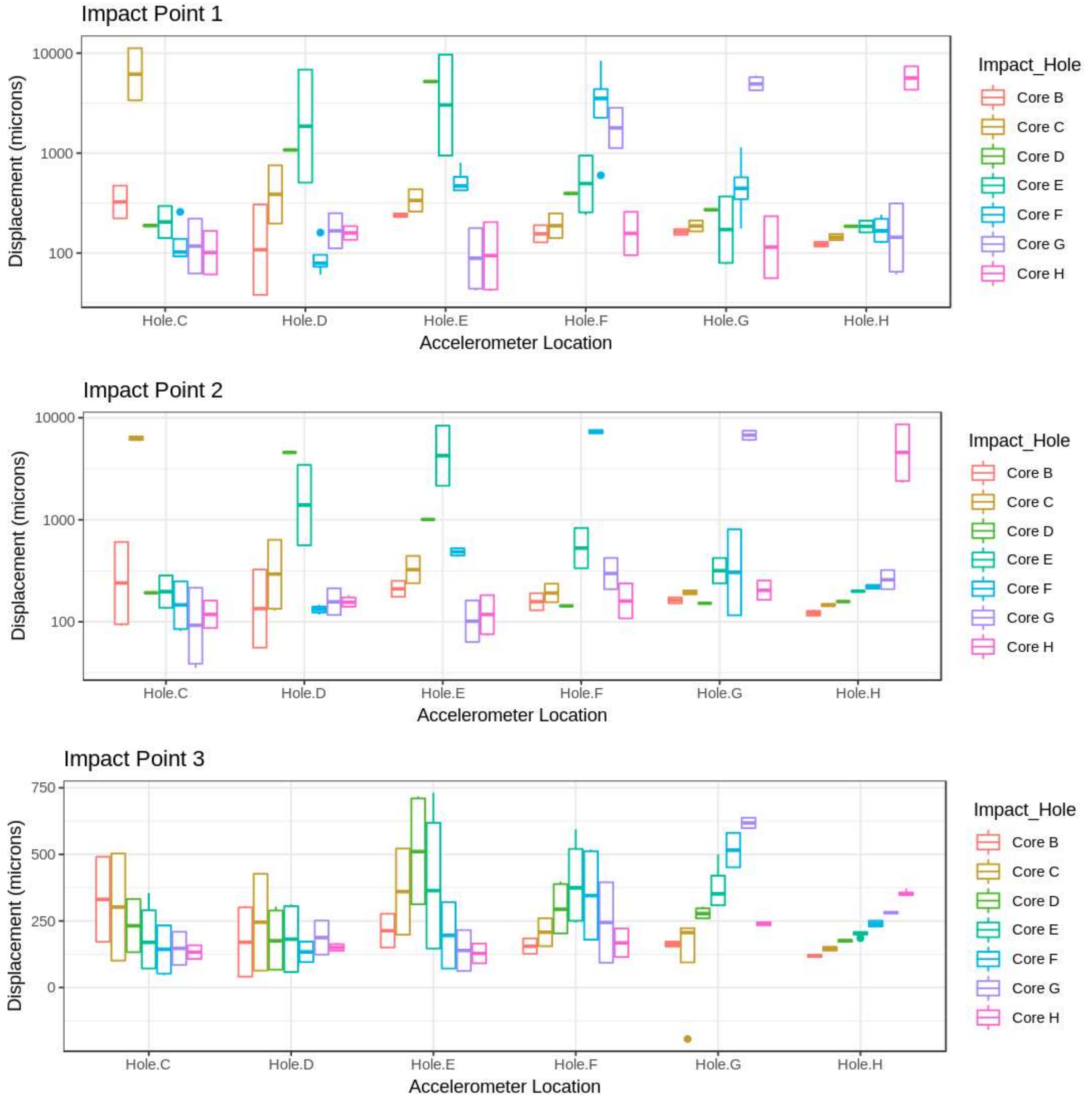

6 DEFLECTION BOWL COMPARISON AND CORRELATION STUDY

In a previous National Assets Centre of Excellence (NACoE) study in Queensland study (Lee & Conaghan 2016), several conversion curves were produced to relate the deflections measured with a FWD to the deflections measured under a TSD (Figure 6.1). The study was based on deflection data collected at nine different sites with a range of different pavement compositions.

Figure 6.1: Correlation Chart – NACOE

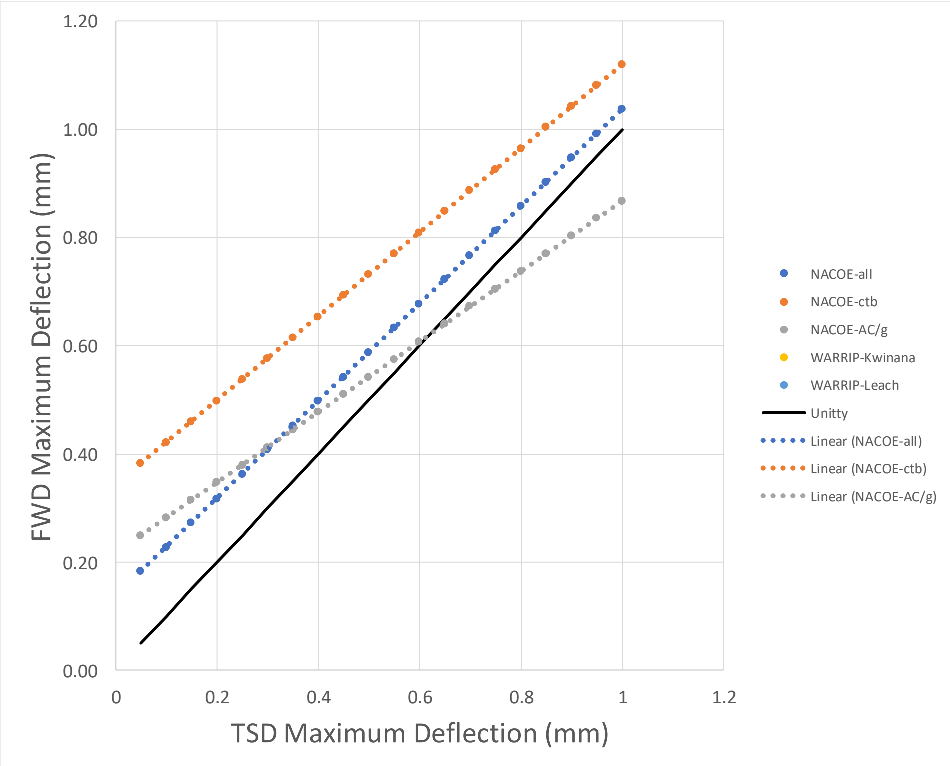

The testing in October 2018 was conducted on a full-depth asphalt pavement and an asphalt pavement over the granular base. The TSD and FWD data collected at both sites is plotted in Figure 6.2, together with the correlation developed in the previous study. It can be seen that the TSD and FWD maximum deflection is closer to the line of unity.

Since MRWA is placing a strong emphasis on the FWD curvature data, the curvature (D0–D200) data collected from the TSD was compared with the FWD data, and the results are shown in Figure 6.3. It can be seen that there is an excellent correlation between the two devices.

The observations made in this study are based on limited data collected in October 2018. Further work is recommended to ensure that any variability during testing, and any seasonal and environmental influence, are properly taken into account.

Figure 6.2: Correlation between TSD and FWD maximum deflection

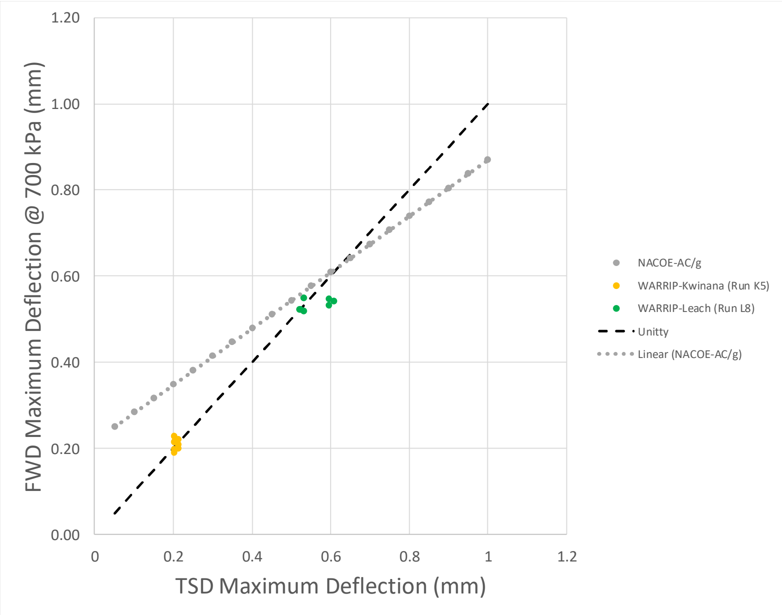

Figure 6.3: Correlation between TSD and FWD curvature function (D0–D200)

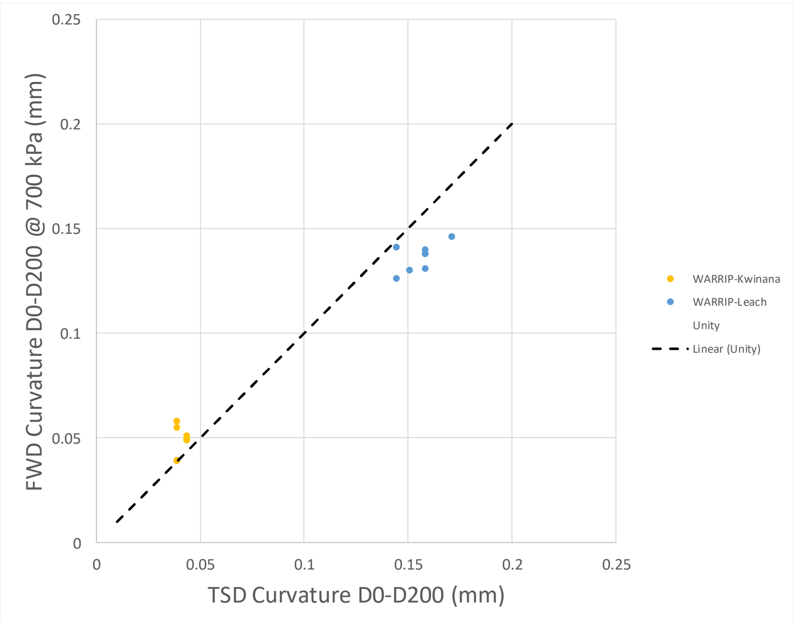

7 CONCLUSIONS AND RECOMMENDATIONS

The main aim of the project – which was funded by MRWA under its WARRIP program – was to acquire a better understanding of TSD deflection data by installing ground instrumentation (i.e. sensor arrays using geophones and accelerometers) and comparing the 'true' surface response when heavy vehicle traffic or other deflection testing devices travel over the pavement. Two deflection validation sites were established where the ground response of different deflection equipment was measured using the embedded instrumentation arrays. This was the first attempt in Australia to validate the deflection measurements made by a Traffic Speed Deflectometer (or commonly known as iPAVE).

The main findings of the project were as follows.

- The deflection profile varies with pavement type.
- For the Kwinana Freeway, there was a good match between the deflection data collected using the TSD and FWD in the front end of the deflection bowl (0 to 600 mm). For the Leach Highway, the deflection in the front end of the deflection bowl collected using the TSD and FWD also has a good match between 0 to 900mm offset. Without further testing, a conclusive explanation of the difference in the field measurements cannot be made. However, several explanations can be postulated, including:
  - The shape of the deflection bowl was very different at the two sites, and the Signal-to-Noise (SNR) ratio may have been higher for the stiffer pavement at Site One (Kwinana Freeway).
  - The degree of subgrade non-linearity (Chai et al. 2015) is often observed in FWD deflection (beyond 900 mm offset). It is postulated that the TSD measurement is also affected by the subgrade non-linearity behaviour. This was also reported for TSD data collected on Queensland pavements (Chai et al. 2016). At this stage, because of the different type of dynamic loading imposed by the two devices, the extent of this effect cannot be quantified at this point in time.
- To date, TSD data has been collected at 41–77 km/h in Kwinana Freeway, whilst on the Leach Highway, because of the limited post speed of 70 km/h, the TSD operated at 48–65 km/h. The results do not support the fact that the pavement response is significantly affected by the speed of testing. Additional tests are needed to confirm this statement.
- In summary, the geophone is more immune to amplification than the accelerometer. This is primarily because the accelerometer does not have a casing to protect it against any compression from the wheel load. Furthermore, the accelerometer is generally installed much closer to the pavement surface than the geophone.
- A system needs to be developed to assist the driver of the TSD to travel as close as possible to the instrumentation array and to minimise wander.
- The predominant frequency of both the FWD and TSD (at 77 km/h) is between 20 and 30 Hz. When the TSD travelled at a lower speed (48 km/h), a lower predominant frequency of 10 to 20 Hz was recorded. It is important that the predominant frequencies are not filtered during the subsequent signal processing.

7.1 Future Work

Even though the main objectives of this project have been met, there are a few activities that can be considered for future research work:

- Take more measurements using the instrumentation array when the TSD travels past the sites in the future.

- The deflection profile differed according to pavement type. It is recommended that additional instrumentation sites be established in other pavement types. For example, granular base with thin bituminous surfacing, and asphalt over granular subbase.
- The experimental method developed in this project can be used to monitor the movement in the pavement materials. It can be used to track the response under a range of vehicular loadings.
- Develop and improve the design of the accelerometer housing case.
- In order to automate the data collection process, a cabinet should be designed to provide all-weather storage of the data acquisition system in the field, including a live data upload link to the internet for long-term storage.
- Develop an improved travel path tracking system to determine any lateral offset between the TSD Doppler laser array and the in-ground sensor. Testing during the day would help.
- The curvature function is of interest to MRWA because there is an emphasis on utilising this function for pavement acceptance purposes. Only limited data was collected in this project, and it is recommended that further studies be conducted.

REFERENCES

Austroads 2014, *Traffic speed deflectometer: data review and lessons learnt*, AP-T279-14, Austroads, Sydney, NSW.

Chai, G, Kelly, G, Huang, A, Chowdhury, SH, Manoharan, S & Golding, A 2015, ‘New approaches for modelling non-linearity of subgrade in asphalt pavements’, *Transportation Research Board annual meeting, 94th, 2015, Washington, DC, USA*, TRB, Washington, DC, USA, 13 pp.

Chai, G, Manoharan, S, Golding, A, Kelly, G & Chowdhury, SH 2016, ‘Evaluation of the traffic speed deflectometer data using simplified deflection model’, *Transport Research Procedia*, vol. 14, Elsevier, Amsterdam, Netherlands, pp. 3031–9.

Lee, J & Conaghan, A 2016, *P40 benefits of traffic speed deflectometer data in pavement analysis (TSD and FWD correlation study and investigation to 'ground truth' instrumentation) (year 2: 2015/2016)*, contract report 010554, National Asset Centre of Excellence, Brisbane, Qld.

Muller, WB & Roberts, J 2013, ‘Revised approach to assessing traffic speed deflectometer data and field validation of deflection bowl predictions’, *International Journal of Pavement Engineering,* vol. 14, no. 4, pp. 388–402.

Nasimifar, M, Thyagarajan, S, Siddharthan, RV & Sivaneswaran, N 2016, ‘Robust deflection indices from traffic-speed deflectometer measurement to predict critical pavement responses for network-level pavement management system application’, *Journal of Transportation Engineering*, vol. 142, no. 3, 11 pp.

Nazarian, S & Bush, A 1989, ‘Determination of deflection of pavement systems using velocity transducers’, *Transportation Research Record*, no. 1227, pp. 147–58.

Pedersen, L 2013, ‘Viscoelastic modelling of road deflections for use with the traffic speed deflectometer’, PhD thesis, Technical University of Denmark, Lyngby, Denmark.

Rasmussen, S, Aagaard, L, Baltzer, S & Krarup, J 2008, ‘A comparison of two years of network level measurements with the Traffic Speed Deflectometer’, *Transport Research Arena Europe*, *2008*, *Ljubljana, Slovenia*, TRA, Ljubljana, Slovenia, 8 pp.

Zofka, A, Sudyka, J, Maliszewski, M, Harasim, P & Sybilski, D 2014, ‘Alternative approach for interpreting traffic speed deflectometer results’, *Transportation Research Record*, no. 2457, pp. 12–8.

APPENDIX A FWD TEST RESULT SUMMARY – KWINANA FREEWAY

Station	Surface	Air	Time	Latitude	Longitude	Height	Stress	ND0	ND200	ND300	ND400	ND500	ND600	ND750	ND900	ND1500
0.05	10.2	13	12/09/2018 20:28	-32.4535183	115.799295	3.535	700.00	170.84	145.63	130.70	119.93	110.26	99.13	87.01	77.22	45.65
0.05	10.2	13	12/09/2018 20:28	-32.4535183	115.799295	3.535	700.00	168.13	144.25	129.63	119.50	109.13	98.88	87.38	76.75	46.13
0.05	10.2	13	12/09/2018 20:28	-32.4535183	115.799295	3.535	700.00	168.29	143.05	129.63	119.27	109.27	98.54	86.83	76.10	45.61
0.05	10.2	13	12/09/2018 20:28	-32.4535183	115.799295	3.535	700.00	171.29	143.81	129.47	119.94	108.91	99.48	88.05	77.52	47.13
0.05	10.2	13	12/09/2018 20:28	-32.4535183	115.799295	3.535	700.00	167.98	144.81	128.57	119.24	108.61	99.89	87.45	78.72	47.44
0	10.4	13	12/09/2018 20:37	-32.4531866	115.799657	3.311	700.00	167.88	140.00	124.90	115.53	104.70	94.59	81.08	71.22	42.97
0	10.4	13	12/09/2018 20:37	-32.4531866	115.799657	3.311	700.00	165.57	139.50	123.74	114.56	104.88	93.71	80.55	71.49	41.21
0	10.4	13	12/09/2018 20:37	-32.4531866	115.799657	3.311	700.00	167.16	139.26	123.95	115.31	104.94	93.33	80.49	71.85	42.35
0	10.4	13	12/09/2018 20:37	-32.4531866	115.799657	3.311	700.00	167.16	139.40	124.52	115.34	104.55	94.76	82.88	72.90	45.53
0	10.4	13	12/09/2018 20:37	-32.4531866	115.799657	3.311	700.00	168.85	140.20	124.83	115.31	104.01	94.99	83.48	73.17	44.92
0.005	10.6	13	12/09/2018 20:38	-32.4532162	115.799624	3.23	700.00	189.69	155.17	135.84	123.11	110.14	98.76	85.54	73.55	42.59
0.005	10.6	13	12/09/2018 20:38	-32.4532162	115.799624	3.23	700.00	190.25	155.00	134.88	122.00	111.13	99.38	86.50	74.13	45.88
0.005	10.6	13	12/09/2018 20:38	-32.4532162	115.799624	3.23	700.00	185.67	153.03	132.30	120.02	109.34	96.93	84.52	70.50	46.54
0.005	10.6	13	12/09/2018 20:38	-32.4532162	115.799624	3.23	700.00	186.13	152.54	133.58	120.34	110.01	98.18	85.64	73.01	46.43
0.005	10.6	13	12/09/2018 20:38	-32.4532162	115.799624	3.23	700.00	186.37	151.57	131.13	118.26	109.99	96.92	85.66	70.50	50.06
0.01	10.9	13	12/09/2018 20:39	-32.4532512	115.799587	3.264	700.00	185.84	152.21	133.15	121.94	111.60	100.77	87.31	75.48	44.47
0.01	10.9	13	12/09/2018 20:39	-32.4532512	115.799587	3.264	700.00	183.63	153.63	127.00	120.25	112.00	99.63	83.63	70.25	46.50
0.01	10.9	13	12/09/2018 20:39	-32.4532512	115.799587	3.264	700.00	183.41	152.61	128.75	120.71	112.05	100.05	84.84	71.86	44.89
0.01	10.9	13	12/09/2018 20:39	-32.4532512	115.799587	3.264	700.00	181.29	152.28	127.93	120.42	112.30	100.74	86.03	73.45	49.00
0.01	10.9	13	12/09/2018 20:39	-32.4532512	115.799587	3.264	700.00	180.83	149.06	132.63	121.38	110.83	100.67	87.62	76.77	46.30
0.015	10.8	14	12/09/2018 20:40	-32.4532867	115.799547	3.237	700.00	153.04	131.27	120.44	111.09	104.45	94.11	82.43	74.80	43.55
0.015	10.8	14	12/09/2018 20:40	-32.4532867	115.799547	3.237	700.00	153.34	131.19	120.42	110.63	104.02	94.23	81.99	75.51	43.32
0.015	10.8	14	12/09/2018 20:40	-32.4532867	115.799547	3.237	700.00	150.55	130.44	119.65	109.84	103.63	93.46	81.91	75.34	43.69
0.015	10.8	14	12/09/2018 20:40	-32.4532867	115.799547	3.237	700.00	152.10	132.03	120.73	112.87	104.29	95.12	84.32	75.35	45.49
0.015	10.8	14	12/09/2018 20:40	-32.4532867	115.799547	3.237	700.00	152.72	131.79	121.07	112.56	104.25	95.24	84.22	76.21	45.77
0.02	10.6	14	12/09/2018 20:41	-32.4533175	115.799515	2.832	700.00	151.79	134.96	121.21	114.46	104.26	93.33	85.23	75.16	45.56
0.02	10.6	14	12/09/2018 20:41	-32.4533175	115.799515	2.832	700.00	148.22	133.27	120.94	113.22	104.13	94.29	84.95	74.61	45.46
0.02	10.6	14	12/09/2018 20:41	-32.4533175	115.799515	2.832	700.00	149.50	134.28	119.43	114.07	104.33	92.77	84.73	74.99	43.46
0.02	10.6	14	12/09/2018 20:41	-32.4533175	115.799515	2.832	700.00	151.43	134.08	121.15	114.23	104.80	94.47	85.64	75.72	46.73
0.02	10.6	14	12/09/2018 20:41	-32.4533175	115.799515	2.832	700.00	150.95	134.72	119.39	114.31	104.95	93.30	86.43	76.37	47.00
0.025	10.1	14	12/09/2018 20:42	-32.4533548	115.799475	2.731	700.00	155.46	133.69	121.08	111.80	102.03	92.88	82.49	73.59	44.40
0.025	10.1	14	12/09/2018 20:42	-32.4533548	115.799475	2.731	700.00	155.04	132.17	119.98	111.03	102.45	92.13	82.31	73.36	44.64
0.025	10.1	14	12/09/2018 20:42	-32.4533548	115.799475	2.731	700.00	156.02	131.99	120.40	110.30	102.17	92.43	82.45	73.70	45.11
0.025	10.1	14	12/09/2018 20:42	-32.4533548	115.799475	2.731	700.00	151.72	132.63	119.49	110.91	105.05	92.63	82.12	74.95	49.60
0.025	10.1	14	12/09/2018 20:42	-32.4533548	115.799475	2.731	700.00	151.85	132.83	117.50	109.93	105.45	92.01	81.35	75.28	52.48
0.03	10.1	13	12/09/2018 20:42	-32.4533827	115.799445	2.89	700.00	161.72	134.04	119.89	110.21	101.15	90.98	80.92	70.25	43.81
0.03	10.1	13	12/09/2018 20:42	-32.4533827	115.799445	2.89	700.00	158.59	133.51	120.29	109.93	99.45	91.84	79.86	72.62	43.92
0.03	10.1	13	12/09/2018 20:42	-32.4533827	115.799445	2.89	700.00	160.18	133.60	120.07	110.23	99.53	91.04	80.21	70.98	43.18
0.03	10.1	13	12/09/2018 20:42	-32.4533827	115.799445	2.89	700.00	163.30	135.16	121.74	111.66	101.37	92.80	82.31	73.73	45.09
0.03	10.1	13	12/09/2018 20:42	-32.4533827	115.799445	2.89	700.00	160.24	136.15	123.02	111.07	100.11	94.39	81.85	76.81	46.90
0.035	10.1	13	12/09/2018 20:43	-32.4534219	115.799403	3.048	700.00	168.39	139.63	125.93	116.38	104.88	96.31	85.30	75.02	45.03
0.035	10.1	13	12/09/2018 20:43	-32.4534219	115.799403	3.048	700.00	168.37	138.39	124.39	114.60	103.20	95.65	84.87	74.21	45.72
0.035	10.1	13	12/09/2018 20:43	-32.4534219	115.799403	3.048	700.00	167.75	138.40	124.04	115.44	103.16	95.79	85.23	74.91	46.30
0.035	10.1	13	12/09/2018 20:43	-32.4534219	115.799403	3.048	700.00	166.93	140.30	125.88	116.80	104.70	97.44	87.05	76.46	50.03
0.035	10.1	13	12/09/2018 20:43	-32.4534219	115.799403	3.048	700.00	165.33	139.10	124.34	116.97	102.21	97.22	87.25	77.18	52.65
0.04	10.9	13	12/09/2018 20:45	-32.4534521	115.799371	2.975	700.00	170.66	144.96	127.96	118.03	105.99	97.30	88.49	75.96	46.05
0.04	10.9	13	12/09/2018 20:45	-32.4534521	115.799371	2.975	700.00	169.70	142.10	127.31	118.43	106.36	96.50	88.86	76.16	45.72
0.04	10.9	13	12/09/2018 20:45	-32.4534521	115.799371	2.975	700.00	169.40	141.74	127.54	117.58	106.87	96.90	88.81	75.98	45.46
0.04	10.9	13	12/09/2018 20:45	-32.4534521	115.799371	2.975	700.00	170.98	141.49	128.18	118.16	107.53	98.10	89.66	77.05	50.24
0.04	10.9	13	12/09/2018 20:45	-32.4534521	115.799371	2.975	700.00	170.30	143.54	128.69	118.59	107.88	98.08	88.38	77.17	48.08
0.045	10.1	13	12/09/2018 20:46	-32.4534853	115.799335	2.893	700.00	165.12	138.76	125.45	117.37	106.18	97.10	86.66	80.20	44.51
0.045	10.1	13	12/09/2018 20:46	-32.4534853	115.799335	2.893	700.00	162.54	139.38	125.30	116.58	106.37	96.53	86.44	78.72	44.47
0.045	10.1	13	12/09/2018 20:46	-32.4534853	115.799335	2.893	700.00	161.79	139.37	125.47	117.46	106.82	97.30	86.91	80.64	45.46
0.045	10.1	13	12/09/2018 20:46	-32.4534853	115.799335	2.893	700.00	162.93	137.46	125.39	117.78	106.72	96.99	87.65	82.68	47.28
0.045	10.1	13	12/09/2018 20:46	-32.4534853	115.799335	2.893	700.00	164.58	137.37	124.93	117.14	106.21	97.01	87.40	82.34	47.54
0.05	10	13	12/09/2018 20:46	-32.45352	115.799296	2.983	700.00	172.68	147.16	132.96	122.28	111.10	100.66	90.23	77.67	46.25
0.05	10	13	12/09/2018 20:46	-32.45352	115.799296	2.983	700.00	170.88	146.52	130.90	121.05	110.47	99.40	90.30	77.01	45.64
0.05	10	13	12/09/2018 20:46	-32.45352	115.799296	2.983	700.00	170.62	146.67	130.37	120.25	109.88	98.89	88.27	76.42	45.56
0.05	10	13	12/09/2018 20:46	-32.45352	115.799296	2.983	700.00	177.41	150.26	132.46	122.20	112.64	101.98	91.52	79.76	48.28
0.05	10	13	12/09/2018 20:46	-32.45352	115.799296	2.983	700.00	173.65	148.81	131.39	122.37	111.46	101.65	90.73	79.31	48.67
0.055	10.6	13	12/09/2018 20:48	-32.4535516	115.799261	3.229	700.00	176.67	147.81	132.81	122.78	111.26	100.23	88.09	77.93	46.09
0.055	10.6	13	12/09/2018 20:48	-32.4535516	115.799261	3.229	700.00	175.56	146.79	131.85	121.98	110.74	99.75	88.27	78.15	45.31
0.055	10.6	13	12/09/2018 20:48	-32.4535516	115.799261	3.229	700.00	172.02	145.59	130.82	120.64	110.71	98.55	87.62	77.45	44.06
0.055	10.6	13	12/09/2018 20:48	-32.4535516	115.799261	3.229	700.00	173.70	147.70	133.50	123.90	113.20	100.90	90.00	80.10	47.60
0.055	10.6	13	12/09/2018 20:48	-32.4535516	115.799261	3.229	700.00	172.54	147.23	134.28	124.63	113.79	99.63	89.38	79.84	51.12
0.06	9.9	13	12/09/2018 20:49	-32.453586	115.799226	3.189	700.00	179.15	148.81	132.95	122.25	111.04	100.22	87.25	76.04	44.06
0.06	9.9	13	12/09/2018 20:49	-32.453586	115.799226	3.189	700.00	180.49	148.29	133.05	121.95	110.85	100.12	87.80	76.95	48.41
0.06	9.9	13	12/09/2018 20:49	-32.453586	115.799226	3.189	700.00	183.88	146.50	132.25	119.88	112.13	100.50	87.75	76.63	52.88
0.06	9.9	13	12/09/2018 20:49	-32.453586	115.799226	3.189	700.00	181.14	147.64	133.16	122.50	113.95	101.38	88.20	77.44	59.94
0.06	9.9	13	12/09/2018 20:49	-32.453586	115.799226	3.189	700.00	181.18	145.02	132.57	119.01	110.37	101.43	87.47	77.83	63.97
0.065	9.9	13	12/09/2018 20:50	-32.4536201	115.799188	3.468	700.00	179.47	153.61	137.18	125.66	113.40	102.61	90.47	80.67	47.08
0.065	9.9	13	12/09/2018 20:50	-32.4536201	115.799188	3.468	700.00	176.95	151.31	135.35	124.29	111.85	101.29	89.10	80.56	45.87
0.065	9.9	13	12/09/2018 20:50	-32.4536201	115.799188	3.468	700.00	177.59	151.09	135.56	123.24	111.90	101.06	89.47	79.00	46.71
0.065	9.9	13	12/09/2018 20:50	-32.4536201	115.799188	3.468	700.00	176.36	152.12	136.57	124.85	113.54	104.04	91.21	80.51	48.99
0.065	9.9	13	12/09/2018 20:50	-32.4536201	115.799188	3.468	700.00	177.55	152.88	137.50	125.82	114.94	105.65	92.67	82.38	50.83
0.07	9.9	13	12/09/2018 20:51	-32.453652	115.799153	3.455	700.00	162.38	139.50	125.95	116.87	107.55	97.73	86.54	77.09	46.63
0.07	9.9	13	12/09/2018 20:51	-32.453652	115.799153	3.455	700.00	160.78	140.12	127.39	117.49	109.08	98.94	88.18	78.29	48.36
0.07	9.9	13	12/09/2018 20:51	-32.453652	115.799153	3.455	700.00	162.39	140.74	128.37	119.10	109.95	100.92	89.42	79.89	49.96
0.07	9.9	13	12/09/2018 20:51	-32.453652	115.799153	3.455	700.00	162.54	139.40	127.14	117.86	108.19	99.42	87.75	78.48	48.56
0.07	9.9	13	12/09/2018 20:51	-32.453652	115.799153	3.455	700.00	159.20	138.70	126.60	117.20	107.90	98.80	87.80	78.60	48.80
0.075	9.9	13	12/09/2018 20:52	-32.4536864	115.799116	3.404	700.00	169.82	144.07	129.52	120.16	109.31	100.07	88.61	78.38	47.57
0.075	9.9	13	12/09/2018 20:52	-32.4536864	115.799116	3.404	700.00	170.58	143.81	129.44	120.23	109.05	100.70	88.54	78.72	48.02
0.075	9.9	13	12/09/2018 20:52	-32.4536864	115.799116	3.404	700.00	167.19	143.44	129.30	119.46	109.37	100.02	88.82	78.98	47.36
0.075	9.9	13	12/09/2018 20:52	-32.4536864	115.799116	3.404	700.00	168.00	143.73	130.13	120.46	110.69	101.53	90.04	79.97	49.25
0.075	9.9	13	12/09/2018 20:52	-32.4536864	115.799116	3.404	700.00	168.39	144.34	130.34	120.87	110.82	101.45	90.41	79.96	49.39
0.08	10	13	12/09/2018 20:53	-32.4537183	115.799082	3.602	700.00	170.66	147.20	131.93	121.26	111.70	101.28	89.49	79.18	47.78
0.08	10	13	12/09/2018 20:53	-32.4537183	115.799082	3.602	700.00	171.03	146.70	131.81	121.01	111.21	101.52	89.49	79.31	47.29
0.08	10	13	12/09/2018 20:53	-32.4537183	115.799082	3.602	700.00	171.32	147.00	132.02	121.33	111.75	101.32	90.26	79.58	47.77
0.08	10	13	12/09/2018 20:53	-32.4537183	115.799082	3.602	700.00	175.25	148.59	134.14	123.74	113.33	103.54	92.02	81.92	50.51
0.08	10	13	12/09/2018 20:53	-32.4537183	115.799082	3.602	700.00	175.80	148.48	133.72	123.65	112.98	103.90	91.94	82.17	49.86
0.085	10.4	13	12/09/2018 20:54	-32.4537497	115.799049	3.441	700.00	167.06	143.10	129.57	118.53	109.59	99.79	87.87	78.19	46.79
0.085	10.4	13	12/09/2018 20:54	-32.4537497	115.799049	3.441	700.00	164.52	141.60	127.92	117.94	108.70	98.96	87.38	77.39	45.97
0.085	10.4	13	12/09/2018 20:54	-32.4537497	115.799049	3.441	700.00	166.40	142.09	129.07	117.53	109.54	99.23	87.93	77.61	46.54
0.085	10.4	13	12/09/2018 20:54	-32.4537497	115.799049	3.441	700.00	166.01	142.21	129.05	118.81	110.17	100.03	88.78	78.54	48.21
0.085	10.4	13	12/09/2018 20:54	-32.4537497	115.799049	3.441	700.00	166.07	142.41	128.87	119.54	109.21	100.49	88.75	79.53	48.44
0.091	10.3	13	12/09/2018 20:55	-32.4537911	115.799007	3.524	700.00	174.26	149.56	134.04	123.37	111.21	101.90	89.36	79.93	46.79
0.091	10.3	13	12/09/2018 20:55	-32.4537911	115.799007	3.524	700.00	174.50	149.43	134.79	123.62	111.58	101.65	89.24	80.55	46.29
0.091	10.3	13	12/09/2018 20:55	-32.4537911	115.799007	3.524	700.00	171.95	149.45	133.29	123.46	110.91	101.46	89.15	79.57	48.12
0.091	10.3	13	12/09/2018 20:55	-32.4537911	115.799007	3.524	700.00	172.70	149.81	134.69	124.88	112.31	103.42	90.95	82.06	49.46
0.091	10.3	13	12/09/2018 20:55	-32.4537911	115.799007	3.524	700.00	171.33	149.84	134.98	125.04	113.29	103.24	91.09	82.35	49.51
0.095	10.3	13	12/09/2018 20:55	-32.4538212	115.798975	3.699	700.00	182.72	152.47	134.94	123.46	112.47	102.72	89.63	80.37	49.63
0.095	10.3	13	12/09/2018 20:55	-32.4538212	115.798975	3.699	700.00	182.12	151.77	135.04	122.78	112.74	102.34	88.09	80.78	49.56
0.095	10.3	13	12/09/2018 20:55	-32.4538212	115.798975	3.699	700.00	182.84	152.22	133.83	124.44	112.22	102.72	89.14	80.00	49.88
0.095	10.3	13	12/09/2018 20:55	-32.4538212	115.798975	3.699	700.00	181.94	152.18	135.71	124.72	115.04	104.85	90.37	82.68	49.93
0.095	10.3	13	12/09/2018 20:55	-32.4538212	115.798975	3.699	700.00	181.66	152.23	135.23	123.69	114.64	103.81	89.89	82.23	50.71
0.1	10.3	13	12/09/2018 20:56	-32.453854	115.798942	3.432	700.00	169.18	142.88	127.23	118.96	108.69	99.68	88.16	79.14	46.58
0.1	10.3	13	12/09/2018 20:56	-32.453854	115.798942	3.432	700.00	167.53	143.18	127.40	119.44	107.69	99.74	88.11	79.79	46.50
0.1	10.3	13	12/09/2018 20:56	-32.453854	115.798942	3.432	700.00	167.75	143.50	128.25	120.25	109.00	100.13	89.00	79.50	47.25
0.1	10.3	13	12/09/2018 20:56	-32.453854	115.798942	3.432	700.00	168.69	143.43	129.29	120.91	110.00	101.21	89.49	80.00	48.28
0.1	10.3	13	12/09/2018 20:56	-32.453854	115.798942	3.432	700.00	167.26	143.32	129.14	120.89	109.73	100.68	89.11	79.96	48.38

Station	Surface	Air	Time	Latitude	Longitude	DropID	Stress	ND0	ND200	ND300	ND400	ND500	ND600	ND750	ND900	ND1500
0	8.3	14.4	14/09/2018 0:11	-32.4532	115.7997	1	700.00	155.56	131.06	116.90	107.96	97.51	89.39	79.05	70.35	40.75
0	8.3	14.4	14/09/2018 0:11	-32.4532	115.7997	2	700.00	153.17	128.29	115.98	105.73	95.61	88.90	78.29	68.05	43.17
0	8.3	14.4	14/09/2018 0:11	-32.4532	115.7997	3	700.00	153.06	129.28	115.23	105.99	96.13	88.61	78.13	69.88	41.53
0	8.3	14.4	14/09/2018 0:11	-32.4532	115.7997	4	700.00	153.44	129.37	116.43	110.72	96.68	88.95	79.63	73.21	39.71
0	8.3	14.4	14/09/2018 0:11	-32.4532	115.7997	5	700.00	153.50	129.40	115.40	110.70	96.50	89.00	79.90	72.60	42.30
0.005	8.4	14.4	14/09/2018 0:12	-32.4532	115.7996	6	700.00	168.89	139.64	123.46	115.67	103.68	96.61	83.07	77.43	44.59
0.005	8.4	14.4	14/09/2018 0:12	-32.4532	115.7996	7	700.00	168.42	138.40	123.64	114.90	104.69	96.08	84.15	75.17	45.27
0.005	8.4	14.4	14/09/2018 0:12	-32.4532	115.7996	8	700.00	166.39	137.56	122.29	113.73	103.96	95.41	82.95	75.86	44.59
0.005	8.4	14.4	14/09/2018 0:12	-32.4532	115.7996	9	700.00	167.39	138.99	124.17	114.94	105.30	96.48	84.30	77.20	46.16
0.005	8.4	14.4	14/09/2018 0:12	-32.4532	115.7996	10	700.00	166.96	138.10	123.92	114.04	105.15	97.06	83.68	79.29	46.83
0.01	7.9	14.4	14/09/2018 0:13	-32.4533	115.7996	11	700.00	178.02	145.92	129.34	119.75	107.66	98.54	86.58	75.57	44.89
0.01	7.9	14.4	14/09/2018 0:13	-32.4533	115.7996	12	700.00	175.61	142.68	127.93	117.56	106.34	97.20	85.12	75.00	43.78
0.01	7.9	14.4	14/09/2018 0:13	-32.4533	115.7996	13	700.00	174.44	142.74	127.19	117.25	106.68	97.35	85.67	74.72	44.01
0.01	7.9	14.4	14/09/2018 0:13	-32.4533	115.7996	14	700.00	174.90	145.01	128.27	119.44	108.51	99.18	87.95	76.92	46.43
0.01	7.9	14.4	14/09/2018 0:13	-32.4533	115.7996	15	700.00	177.30	142.10	130.20	117.60	108.70	99.20	87.40	77.00	46.10
0.015	7.7	14.3	14/09/2018 0:14	-32.4533	115.7995	16	700.00	150.85	129.86	118.53	109.83	99.10	93.25	80.14	74.29	45.55
0.015	7.7	14.3	14/09/2018 0:14	-32.4533	115.7995	17	700.00	148.57	129.11	117.48	109.16	99.37	92.88	81.50	73.67	45.28
0.015	7.7	14.3	14/09/2018 0:14	-32.4533	115.7995	18	700.00	148.05	128.41	116.95	109.39	100.37	92.56	81.59	73.29	45.00
0.015	7.7	14.3	14/09/2018 0:14	-32.4533	115.7995	19	700.00	149.92	129.59	119.67	110.25	101.43	94.49	82.69	76.05	46.90
0.015	7.7	14.3	14/09/2018 0:14	-32.4533	115.7995	20	700.00	150.04	129.66	118.61	109.27	99.93	93.70	81.35	75.22	46.40
0.02	7.8	14.4	14/09/2018 0:15	-32.4533	115.7995	21	700.00	150.27	130.68	119.33	111.21	102.85	94.73	82.42	75.14	46.11
0.02	7.8	14.4	14/09/2018 0:15	-32.4533	115.7995	22	700.00	148.37	129.05	117.61	110.11	101.37	93.25	81.44	74.43	44.41
0.02	7.8	14.4	14/09/2018 0:15	-32.4533	115.7995	23	700.00	148.24	129.17	118.35	110.35	101.37	93.50	82.43	74.55	46.87
0.02	7.8	14.4	14/09/2018 0:15	-32.4533	115.7995	24	700.00	147.03	129.45	118.71	110.57	102.74	94.51	82.55	75.82	47.50
0.02	7.8	14.4	14/09/2018 0:15	-32.4533	115.7995	25	700.00	145.71	130.39	119.47	111.66	102.85	94.84	84.12	75.51	46.57
0.025	7.7	14.3	14/09/2018 0:16	-32.4534	115.7995	26	700.00	147.41	128.41	118.02	108.34	98.31	91.62	78.48	72.63	44.68
0.025	7.7	14.3	14/09/2018 0:16	-32.4534	115.7995	27	700.00	145.35	127.57	115.75	106.31	97.10	91.39	79.57	72.61	45.51
0.025	7.7	14.3	14/09/2018 0:16	-32.4534	115.7995	28	700.00	147.14	127.82	117.24	106.66	97.43	92.88	78.61	73.20	45.27
0.025	7.7	14.3	14/09/2018 0:16	-32.4534	115.7995	29	700.00	147.43	128.95	117.80	109.07	99.73	93.40	81.45	74.32	46.40
0.025	7.7	14.3	14/09/2018 0:16	-32.4534	115.7995	30	700.00	147.22	129.72	118.45	108.46	99.76	94.12	81.37	74.65	46.77
0.03	7.7	14.3	14/09/2018 0:17	-32.4534	115.7994	31	700.00	153.71	129.45	114.77	106.88	95.60	88.32	79.95	68.42	44.64
0.03	7.7	14.3	14/09/2018 0:17	-32.4534	115.7994	32	700.00	152.59	127.90	114.44	105.93	95.93	87.41	79.51	67.53	43.83
0.03	7.7	14.3	14/09/2018 0:17	-32.4534	115.7994	33	700.00	152.06	126.47	113.92	106.05	96.94	88.82	79.23	68.65	44.04
0.03	7.7	14.3	14/09/2018 0:17	-32.4534	115.7994	34	700.00	153.86	128.55	115.70	107.36	98.42	89.99	81.05	70.60	46.10
0.03	7.7	14.3	14/09/2018 0:17	-32.4534	115.7994	35	700.00	152.69	128.92	116.33	108.17	98.60	89.84	80.47	70.30	46.53
0.035	7.6	14.4	14/09/2018 0:18	-32.4534	115.7994	36	700.00	164.14	135.78	121.78	113.21	103.79	95.34	83.76	74.10	45.98
0.035	7.6	14.4	14/09/2018 0:18	-32.4534	115.7994	37	700.00	157.59	134.18	120.67	111.75	102.58	94.28	83.26	73.72	45.96
0.035	7.6	14.4	14/09/2018 0:18	-32.4534	115.7994	38	700.00	157.81	134.31	121.08	111.80	102.77	94.24	83.23	74.20	46.25
0.035	7.6	14.4	14/09/2018 0:18	-32.4534	115.7994	39	700.00	160.52	135.88	123.61	113.45	104.60	96.25	84.89	75.73	47.87
0.035	7.6	14.4	14/09/2018 0:18	-32.4534	115.7994	40	700.00	161.10	135.10	123.00	113.10	104.30	95.90	84.50	75.50	47.50
0.04	7.7	14.4	14/09/2018 0:19	-32.4535	115.7994	41	700.00	161.97	138.20	124.87	114.19	105.90	96.17	84.53	77.20	45.63
0.04	7.7	14.4	14/09/2018 0:19	-32.4535	115.7994	42	700.00	159.88	136.54	123.21	112.84	104.81	95.43	83.21	77.28	45.31
0.04	7.7	14.4	14/09/2018 0:19	-32.4535	115.7994	43	700.00	160.23	136.90	123.62	112.94	105.62	95.57	83.65	76.08	45.30
0.04	7.7	14.4	14/09/2018 0:19	-32.4535	115.7994	44	700.00	158.39	138.27	125.07	114.60	106.88	97.33	84.83	78.74	47.04
0.04	7.7	14.4	14/09/2018 0:19	-32.4535	115.7994	45	700.00	157.98	137.66	124.86	114.70	106.27	97.13	85.24	76.91	47.24
0.045	7.6	14.4	14/09/2018 0:19	-32.4535	115.7993	46	700.00	157.99	135.14	122.62	113.75	104.39	95.40	82.76	77.41	46.79
0.045	7.6	14.4	14/09/2018 0:19	-32.4535	115.7993	47	700.00	157.13	133.17	121.13	111.70	103.39	94.57	82.16	75.96	44.31
0.045	7.6	14.4	14/09/2018 0:19	-32.4535	115.7993	48	700.00	152.75	132.64	121.37	111.19	103.35	94.40	82.38	76.74	44.50
0.045	7.6	14.4	14/09/2018 0:19	-32.4535	115.7993	49	700.00	155.85	133.50	122.83	112.37	104.75	95.70	83.21	79.85	45.52
0.045	7.6	14.4	14/09/2018 0:19	-32.4535	115.7993	50	700.00	157.30	131.55	121.90	110.23	104.09	95.34	82.87	81.57	46.16
0.05	7.2	14.4	14/09/2018 0:20	-32.4535	115.7993	51	700.00	176.69	145.55	130.47	120.93	109.83	97.40	87.98	78.81	46.22
0.05	7.2	14.4	14/09/2018 0:20	-32.4535	115.7993	52	700.00	166.86	143.98	129.56	119.24	109.29	96.86	87.28	78.58	45.88
0.05	7.2	14.4	14/09/2018 0:20	-32.4535	115.7993	53	700.00	173.11	142.64	128.04	119.23	109.03	96.19	87.63	79.44	46.83
0.05	7.2	14.4	14/09/2018 0:20	-32.4535	115.7993	54	700.00	171.11	144.29	130.13	121.45	110.28	99.12	89.44	80.47	47.66
0.05	7.2	14.4	14/09/2018 0:20	-32.4535	115.7993	55	700.00	174.30	144.63	130.85	122.10	110.53	99.77	89.81	80.96	49.08
0.055	7.7	14.4	14/09/2018 0:21	-32.4536	115.7993	56	700.00	167.83	143.43	127.74	119.40	109.47	98.20	87.53	78.34	46.95
0.055	7.7	14.4	14/09/2018 0:21	-32.4536	115.7993	57	700.00	166.88	141.86	126.25	116.96	108.16	96.64	86.48	78.30	45.72
0.055	7.7	14.4	14/09/2018 0:21	-32.4536	115.7993	58	700.00	167.50	142.48	126.50	117.82	110.27	97.88	87.96	80.65	47.08
0.055	7.7	14.4	14/09/2018 0:21	-32.4536	115.7993	59	700.00	167.76	143.98	126.53	117.86	115.92	99.18	91.53	85.61	50.51
0.055	7.7	14.4	14/09/2018 0:21	-32.4536	115.7993	60	700.00	166.20	142.70	126.40	117.50	114.70	98.40	90.40	83.70	49.90
0.06	7.7	14.3	14/09/2018 0:22	-32.4536	115.7992	61	700.00	173.40	142.59	128.79	118.06	108.20	97.85	87.01	76.41	45.97
0.06	7.7	14.3	14/09/2018 0:22	-32.4536	115.7992	62	700.00	173.53	141.96	127.88	117.12	107.69	97.41	86.40	76.24	45.77
0.06	7.7	14.3	14/09/2018 0:22	-32.4536	115.7992	63	700.00	173.46	140.86	127.53	116.91	107.53	96.91	86.30	76.30	45.68
0.06	7.7	14.3	14/09/2018 0:22	-32.4536	115.7992	64	700.00	172.19	142.15	128.55	118.34	108.12	99.12	87.07	77.66	47.42
0.06	7.7	14.3	14/09/2018 0:22	-32.4536	115.7992	65	700.00	171.16	143.14	128.47	118.96	108.64	99.54	88.31	78.29	47.85
0.065	7.4	14.3	14/09/2018 0:23	-32.4536	115.7992	66	700.00	176.46	148.17	132.68	123.78	111.22	99.63	90.98	76.46	46.83
0.065	7.4	14.3	14/09/2018 0:23	-32.4536	115.7992	67	700.00	173.02	147.42	131.10	122.56	110.69	99.43	90.41	76.80	46.63
0.065	7.4	14.3	14/09/2018 0:23	-32.4536	115.7992	68	700.00	173.13	147.25	131.00	123.63	109.88	99.38	91.13	76.50	47.13
0.065	7.4	14.3	14/09/2018 0:23	-32.4536	115.7992	69	700.00	176.34	147.92	133.56	123.17	112.38	102.87	91.29	80.40	48.51
0.065	7.4	14.3	14/09/2018 0:23	-32.4536	115.7992	70	700.00	174.45	147.93	131.76	125.24	111.38	100.83	92.70	77.73	49.41
0.07	7.3	14.3	14/09/2018 0:24	-32.4537	115.7992	71	700.00	155.77	136.97	123.74	115.13	105.18	96.45	87.71	78.98	47.07
0.07	7.3	14.3	14/09/2018 0:24	-32.4537	115.7992	72	700.00	156.09	137.11	124.17	115.12	105.57	96.89	87.97	80.05	48.26
0.07	7.3	14.3	14/09/2018 0:24	-32.4537	115.7992	73	700.00	155.46	134.64	122.47	112.61	105.55	95.69	85.58	75.84	46.50
0.07	7.3	14.3	14/09/2018 0:24	-32.4537	115.7992	74	700.00	155.32	135.99	123.88	115.46	106.55	98.04	86.82	77.61	48.37
0.07	7.3	14.3	14/09/2018 0:24	-32.4537	115.7992	75	700.00	154.30	136.35	123.97	115.45	107.03	97.90	86.94	77.91	48.39
0.075	7.4	14.3	14/09/2018 0:25	-32.4537	115.7991	76	700.00	160.02	140.86	126.61	118.02	107.95	98.98	87.19	76.88	47.04
0.075	7.4	14.3	14/09/2018 0:25	-32.4537	115.7991	77	700.00	166.05	140.12	127.41	118.15	108.89	99.14	88.02	77.16	46.79
0.075	7.4	14.3	14/09/2018 0:25	-32.4537	115.7991	78	700.00	159.20	138.88	126.74	116.71	108.16	98.62	86.85	76.44	46.71
0.075	7.4	14.3	14/09/2018 0:25	-32.4537	115.7991	79	700.00	159.39	140.10	127.45	119.29	108.37	100.20	88.06	78.37	48.27
0.075	7.4	14.3	14/09/2018 0:25	-32.4537	115.7991	80	700.00	162.53	140.50	127.48	119.37	109.06	100.34	88.73	79.21	48.87
0.08	7.5	14.3	14/09/2018 0:26	-32.4537	115.7991	81	700.00	168.64	142.94	128.99	118.83	109.28	98.64	86.52	76.00	46.75
0.08	7.5	14.3	14/09/2018 0:26	-32.4537	115.7991	82	700.00	167.75	142.33	127.35	118.75	109.91	96.65	85.60	74.30	46.91
0.08	7.5	14.3	14/09/2018 0:26	-32.4537	115.7991	83	700.00	165.22	141.23	126.34	117.61	108.51	96.94	85.75	75.41	47.49
0.08	7.5	14.3	14/09/2018 0:26	-32.4537	115.7991	84	700.00	170.12	142.82	129.32	119.76	110.79	99.51	88.53	78.56	48.65
0.08	7.5	14.3	14/09/2018 0:26	-32.4537	115.7991	85	700.00	168.24	142.52	128.20	119.42	110.45	99.05	88.26	78.37	49.32
0.085	7.6	14.2	14/09/2018 0:27	-32.4538	115.799	86	700.00	165.07	139.39	127.04	116.87	107.79	98.46	87.08	77.39	46.75
0.085	7.6	14.2	14/09/2018 0:27	-32.4538	115.799	87	700.00	160.65	137.92	126.20	115.93	107.50	98.22	87.96	78.55	46.42
0.085	7.6	14.2	14/09/2018 0:27	-32.4538	115.799	88	700.00	157.75	136.65	124.73	114.56	106.74	97.43	86.63	76.58	46.05
0.085	7.6	14.2	14/09/2018 0:27	-32.4538	115.799	89	700.00	160.88	138.31	126.58	116.73	107.59	99.53	88.20	78.55	47.93
0.085	7.6	14.2	14/09/2018 0:27	-32.4538	115.799	90	700.00	160.80	138.48	125.70	117.07	107.43	99.12	87.86	78.12	47.88
0.09	7.4	14.1	14/09/2018 0:28	-32.4538	115.799	91	700.00	169.70	144.99	130.63	119.79	110.17	100.68	87.41	78.16	45.90
0.09	7.4	14.1	14/09/2018 0:28	-32.4538	115.799	92	700.00	166.54	144.07	128.89	120.25	109.63	99.26	87.28	78.15	47.04
0.09	7.4	14.1	14/09/2018 0:28	-32.4538	115.799	93	700.00	170.92	143.96	129.86	120.09	108.71	100.18	88.80	78.29	46.63
0.09	7.4	14.1	14/09/2018 0:28	-32.4538	115.799	94	700.00	167.24	144.32	129.93	121.09	111.22	100.84	88.81	79.97	48.21
0.09	7.4	14.1	14/09/2018 0:28	-32.4538	115.799	95	700.00	167.82	145.09	130.13	122.45	111.78	101.01	88.45	80.67	48.36
0.095	7.3	14.1	14/09/2018 0:29	-32.4538	115.799	96	700.00	177.13	148.52	132.94	123.32	111.39	102.38	92.16	79.74	50.89
0.095	7.3	14.1	14/09/2018 0:29	-32.4538	115.799	97	700.00	175.25	145.18	127.18	119.54	106.73	100.07	89.60	76.04	48.68
0.095	7.3	14.1	14/09/2018 0:29	-32.4538	115.799	98	700.00	173.95	145.08	129.22	119.93	108.90	100.11	89.08	77.81	48.44
0.095	7.3	14.1	14/09/2018 0:29	-32.4538	115.799	99	700.00	175.56	147.15	129.88	122.42	109.96	103.01	92.18	79.71	50.58
0.095	7.3	14.1	14/09/2018 0:29	-32.4538	115.799	100	700.00	174.85	147.67	131.14	123.17	111.12	103.36	92.50	80.16	50.18
0.1	7.3	14.1	14/09/2018 0:30	-32.4539	115.7989	101	700.00	161.18	137.57	124.66	116.02	106.16	97.51	85.83	76.45	45.90
0.1	7.3	14.1	14/09/2018 0:30	-32.4539	115.7989	102	700.00	159.18	137.68	124.73	115.93	105.92	97.24	86.49	76.60	45.93
0.1	7.3	14.1	14/09/2018 0:30	-32.4539	115.7989	103	700.00	160.65	137.28	124.05	115.76	105.87	97.08	86.08	77.05	46.50
0.1	7.3	14.1	14/09/2018 0:30	-32.4539	115.7989	104	700.00	163.66	139.80	127.17	118.52	108.98	100.13	88.79	79.05	48.52
0.1	7.3	14.1	14/09/2018 0:30	-32.4539	115.7989	105	700.00	163.37	138.19	125.66	117.64	107.81	99.38	88.75	81.23	48.24

Comment	Surface	Air	Time	Latitude	Longitude	Height	DropID	Stress	ND0	ND200	ND300	ND400	ND500	ND600	ND750	ND900	ND1500
B	8.6	14	14/09/2018 0:44	-32.4535202	115.799299	3.319	1	700.00	181.48	145.42	130.93	119.97	108.89	98.16	83.91	75.19	45.61
B	8.6	14	14/09/2018 0:44	-32.4535202	115.799299	3.319	2	700.00	180.29	144.21	129.18	118.83	108.73	97.54	83.23	74.57	44.98
B	8.6	14	14/09/2018 0:44	-32.4535202	115.799299	3.319	3	700.00	177.27	144.03	129.93	119.76	109.48	98.50	86.22	76.35	46.73
B	8.6	14	14/09/2018 0:44	-32.4535202	115.799299	3.319	4	700.00	175.70	144.38	130.12	119.59	109.33	98.99	86.87	76.90	47.54
B	8.6	14	14/09/2018 0:44	-32.4535202	115.799299	3.319	5	700.00	176.81	142.64	126.81	116.39	106.67	95.28	80.97	72.78	42.92
B	8.6	14	14/09/2018 0:44	-32.4535202	115.799299	3.319	6	700.00	180.14	143.47	128.89	118.47	107.78	97.22	82.50	74.31	44.31
C	8.8	14	14/09/2018 0:46	-32.4535203	115.799297	3.498	7	700.00	177.06	145.24	129.77	119.16	108.18	97.70	85.35	75.12	49.29
C	8.8	14	14/09/2018 0:46	-32.4535203	115.799297	3.498	8	700.00	176.11	144.33	128.13	116.25	106.61	96.47	85.95	71.98	43.16
C	8.8	14	14/09/2018 0:46	-32.4535203	115.799297	3.498	9	700.00	176.50	144.59	129.63	119.26	107.89	98.52	87.35	74.59	45.77
C	8.8	14	14/09/2018 0:46	-32.4535203	115.799297	3.498	10	700.00	176.29	144.42	130.05	119.09	108.68	99.01	87.78	76.91	47.71
D	9.1	14	14/09/2018 0:48	-32.4535219	115.799296	3.182	11	700.00	182.93	144.67	130.04	118.72	106.05	96.82	86.36	74.80	42.81
D	9.1	14	14/09/2018 0:48	-32.4535219	115.799296	3.182	12	700.00	183.05	146.10	128.29	119.02	106.10	97.32	86.83	76.22	45.12
D	9.1	14	14/09/2018 0:48	-32.4535219	115.799296	3.182	13	700.00	181.70	145.44	130.13	120.06	107.47	98.00	87.63	76.95	46.13
D	9.1	14	14/09/2018 0:48	-32.4535219	115.799296	3.182	14	700.00	181.27	146.04	130.05	120.48	108.21	99.28	88.69	77.90	47.04
E	9.2	14	14/09/2018 0:49	-32.4535212	115.799297	3.438	15	700.00	179.29	147.21	130.18	118.49	106.68	97.35	86.91	76.96	44.14
E	9.2	14	14/09/2018 0:49	-32.4535212	115.799297	3.438	16	700.00	180.78	148.70	131.17	119.36	107.92	98.10	87.03	77.34	46.00
E	9.2	14	14/09/2018 0:49	-32.4535212	115.799297	3.438	17	700.00	180.00	147.88	131.41	119.60	108.08	100.40	89.39	79.49	45.66
E	9.2	14	14/09/2018 0:49	-32.4535212	115.799297	3.438	18	700.00	177.79	148.38	131.99	119.89	110.31	100.16	88.71	79.03	47.38
F	9.1	14	14/09/2018 0:50	-32.4535209	115.799297	3.815	19	700.00	180.84	146.52	130.90	119.95	108.01	97.07	84.76	75.17	49.33
F	9.1	14	14/09/2018 0:50	-32.4535209	115.799297	3.815	20	700.00	180.55	145.37	130.52	119.54	106.43	96.45	83.23	74.87	45.67
F	9.1	14	14/09/2018 0:50	-32.4535209	115.799297	3.815	21	700.00	180.79	146.66	131.70	120.83	108.43	97.88	85.78	76.76	47.96
F	9.1	14	14/09/2018 0:50	-32.4535209	115.799297	3.815	22	700.00	179.92	146.21	132.17	121.38	108.87	98.46	86.04	77.26	48.04
G	9.1	14	14/09/2018 0:51	-32.453522	115.799295	3.491	23	700.00	190.61	147.68	130.49	120.37	107.20	97.80	87.93	75.37	47.44
G	9.1	14	14/09/2018 0:51	-32.453522	115.799295	3.491	24	700.00	189.15	146.70	130.44	119.77	107.48	98.17	87.13	76.08	45.18
G	9.1	14	14/09/2018 0:51	-32.453522	115.799295	3.491	25	700.00	187.70	147.03	131.36	121.02	108.77	99.33	88.48	77.53	48.21
G	9.1	14	14/09/2018 0:51	-32.453522	115.799295	3.491	26	700.00	186.42	146.82	132.45	121.21	109.51	100.67	87.96	78.29	48.63
H	9.5	14	14/09/2018 0:53	-32.4535252	115.799294	3.674	27	700.00	197.90	150.37	132.96	121.36	109.14	99.51	87.41	76.67	46.91
H	9.5	14	14/09/2018 0:53	-32.4535252	115.799294	3.674	28	700.00	196.85	149.27	132.36	120.97	108.07	99.05	86.91	76.14	45.33
H	9.5	14	14/09/2018 0:53	-32.4535252	115.799294	3.674	29	700.00	194.87	149.28	133.24	122.05	109.34	100.76	87.75	78.17	49.02
H	9.5	14	14/09/2018 0:53	-32.4535252	115.799294	3.674	30	700.00	193.88	149.46	133.82	122.66	110.29	101.49	88.55	79.18	50.32

ARRB_ID	Chainage(m)	GPS		Date	Time	Temperatures		Drop No	Deflections (µm) Normalised To 700 kPa & Load Distace (mm)									Curvature	Comments
		Latitude	Longitude			Surface C	Air C		0	200	300	400	500	600	750	900	1500		
Run 1 kwinana sensors complete off_0.0	0	-32.4535	115.7993	26/10.0/2018	21:53	17	18.7	5	201	160	136	122	110	97	85	75	44	43	
Run 1 kwinana sensors complete off_0.0	0	-32.4535	115.7993	26/10.0/2018	21:54	17.2	18.7	5	205	161	139	125	109	95	85	75	47	46	
Run 1 kwinana sensors complete off_0.0	0	-32.4535	115.7993	26/10.0/2018	21:56	17.4	18.7	5	206	163	138	123	110	97	84	74	45	47	
Run 1 kwinana sensors complete off_0.0	0	-32.4535	115.7993	26/10.0/2018	21:57	17.5	18.6	5	210	163	139	124	110	98	84	74	45	51	
Run 1 kwinana sensors complete off_0.0	0	-32.4535	115.7993	26/10.0/2018	21:59	17.5	18.6	5	210	168	136	123	109	97	85	75	50	45	
Run 1 kwinana sensors complete off_0.0	0	-32.4535	115.7993	26/10.0/2018	22:00	17.5	18.7	5	212	165	139	125	110	98	85	75	47	50	
Run 1 kwinana sensors complete off_0.0	0	-32.4535	115.7993	26/10.0/2018	22:02	17.6	18.7	5	212	164	140	124	110	98	85	74	45	51	
Run 1 kwinana sensors offset_0.0	0	-32.4535	115.7993	26/10.0/2018	21:26	17.3	18.3	5	203	159	137	123	109	97	83	72	48	48	
Run 1 kwinana sensors offset_0.0	0	-32.4535	115.7993	26/10.0/2018	21:27	17.5	18.3	5	205	160	138	123	110	98	84	73	43	47	
Run 1 kwinana sensors offset_0.0	0	-32.4535	115.7993	26/10.0/2018	21:29	17.6	18.3	5	206	161	136	125	112	96	82	74	44	48	
Run 1 kwinana sensors offset_0.0	0	-32.4535	115.7993	26/10.0/2018	21:30	17.6	18.3	5	201	163	140	124	110	98	85	73	45	40	
Run 1 kwinana sensors offset_1.0	1	-32.4535	115.7993	26/10.0/2018	21:32	17.7	18.4	5	212	162	138	124	108	97	84	74	45	55	
Run 1 kwinana sensors offset_1.0	1	-32.4535	115.7993	26/10.0/2018	21:33	17.7	18.4	5	213	164	140	124	110	98	84	73	43	52	
Run 1 kwinana sensors offset_1.0	1	-32.4535	115.7993	26/10.0/2018	21:35	17.5	18.3	5	225	168	141	126	111	97	84	74	45	60	
Run 1 kwinana sensors on_0.0	0	-32.4535	115.7993	26/10.0/2018	21:41	17.1	18.5	5	224	164	138	126	111	96	82	73	42	64	
Run 1 kwinana sensors on_0.0	0	-32.4535	115.7993	26/10.0/2018	21:42	17.3	18.5	5	213	165	139	122	107	95	86	72	44	52	
Run 1 kwinana sensors on_0.0	0	-32.4535	115.7993	26/10.0/2018	21:43	17.5	18.5	5	223	162	141	123	112	94	84	72	45	66	
Run 1 kwinana sensors on_0.0	0	-32.4535	115.7993	26/10.0/2018	21:45	17.5	18.4	5	212	165	137	123	107	94	84	77	45	50	
Run 1 kwinana sensors on_0.0	0	-32.4535	115.7993	26/10.0/2018	21:46	17.5	18.5	5	213	169	140	123	109	96	83	76	51	47	
Run 1 kwinana sensors on_0.0	0	-32.4535	115.7993	26/10.0/2018	21:47	17.6	18.5	5	222	167	140	126	109	97	85	74	46	59	
Run 1 kwinana sensors on_0.0	0	-32.4535	115.7993	26/10.0/2018	21:49	17.5	18.6	5	240	168	142	125	111	98	86	77	47	76	
TSD Run Trough Site Kwinana_0.0	0	-32.4534	115.7995	26/10.0/2018	21:03	17.5	18.4	5	189	150	129	116	102	93	80	70	43	42	
TSD Run Trough Site Kwinana_5.0	5	-32.4534	115.7994	26/10.0/2018	21:04	17.9	18.5	5	199	150	125	112	99	89	75	69	42	52	
TSD Run Trough Site Kwinana_10.0	10	-32.4534	115.7994	26/10.0/2018	21:06	17.5	18.6	5	214	159	133	119	104	94	83	73	41	57	
TSD Run Trough Site Kwinana_15.0	15	-32.4535	115.7994	26/10.0/2018	21:07	17.6	18.6	5	208	159	137	122	109	97	83	73	43	51	
TSD Run Trough Site Kwinana_20.0	20	-32.4535	115.7993	26/10.0/2018	21:08	17.6	18.6	5	197	158	137	121	107	97	83	72	42	39	
TSD Run Trough Site Kwinana_25.0	25	-32.4535	115.7993	26/10.0/2018	21:09	17.6	18.5	5	219	168	140	127	111	97	84	75	42	51	
TSD Run Trough Site Kwinana_30.0	30	-32.4536	115.7993	26/10.0/2018	21:10	17.5	18.5	5	226	168	142	125	109	97	84	74	43	58	
TSD Run Trough Site Kwinana_35.0	35	-32.4536	115.7992	26/10.0/2018	21:11	17.6	18.6	5	223	166	140	125	109	97	84	73	44	58	
TSD Run Trough Site Kwinana_40.0	40	-32.4536	115.7992	26/10.0/2018	21:12	17.7	18.6	5	219	170	145	128	113	100	85	75	43	49	
TSD Run Trough Site Kwinana_45.0	45	-32.4537	115.7991	26/10.0/2018	21:13	17.4	18.7	5	198	157	137	123	110	97	84	74	43	42	
TSD Run Trough Site Kwinana_50.0	50	-32.4537	115.7991	26/10.0/2018	21:14	17.5	18.5	5	208	165	141	126	112	99	85	75	46	44	

APPENDIX B SUMMARY OF FWD TEST RESULTS – LEACH HIGHWAY

Station	Surface	Air	Time	Latitude	Longitude	DropID	Stress	ND0	ND200	ND300	ND400	ND500	ND600	ND750	ND900	ND1500
0	11.8	13.2	11/09/2018 20:35	-32.03206253	115.8875676	1	700.00	575.34	440.33	366.68	317.62	274.40	242.02	203.43	179.57	106.89
0	11.8	13.2	11/09/2018 20:35	-32.03206253	115.8875676	2	700.00	565.25	432.83	361.48	313.23	269.62	239.08	200.84	176.16	102.74
0	11.8	13.2	11/09/2018 20:35	-32.03206253	115.8875676	3	700.00	560.88	431.92	359.66	314.00	269.59	240.36	201.59	183.28	106.63
0	11.8	13.2	11/09/2018 20:35	-32.03206253	115.8875676	4	700.00	540.35	418.22	351.97	305.77	265.09	234.19	196.77	174.06	101.99
0	11.8	13.2	11/09/2018 20:35	-32.03206253	115.8875676	5	700.00	536.87	415.56	348.59	305.35	262.83	233.13	195.15	175.45	102.02
0.005	12.5	13.2	11/09/2018 20:36	-32.03211714	115.8875242	6	700.00	596.66	451.12	355.91	300.05	256.87	225.50	194.38	169.40	105.18
0.005	12.5	13.2	11/09/2018 20:36	-32.03211714	115.8875242	7	700.00	587.71	445.25	352.21	297.04	255.11	224.59	193.57	169.18	104.94
0.005	12.5	13.2	11/09/2018 20:36	-32.03211714	115.8875242	8	700.00	583.99	443.13	351.24	295.58	254.15	223.48	194.05	168.94	104.13
0.005	12.5	13.2	11/09/2018 20:36	-32.03211714	115.8875242	9	700.00	552.16	423.48	339.97	288.34	247.63	217.74	187.96	163.53	98.00
0.005	12.5	13.2	11/09/2018 20:36	-32.03211714	115.8875242	10	700.00	548.28	420.89	338.48	286.95	247.53	217.15	188.95	162.74	100.38
0.01	11.7	13.2	11/09/2018 20:37	-32.03214859	115.887475	11	700.00	643.41	480.16	382.48	322.20	271.63	238.05	202.62	178.63	99.89
0.01	11.7	13.2	11/09/2018 20:37	-32.03214859	115.887475	12	700.00	632.84	473.06	376.84	319.33	267.88	231.89	199.24	179.82	99.93
0.01	11.7	13.2	11/09/2018 20:37	-32.03214859	115.887475	13	700.00	627.65	470.12	373.33	319.51	263.70	225.43	195.80	181.23	99.63
0.01	11.7	13.2	11/09/2018 20:37	-32.03214859	115.887475	14	700.00	597.19	451.71	363.16	309.81	257.46	222.76	190.16	174.00	96.52
0.01	11.7	13.2	11/09/2018 20:37	-32.03214859	115.887475	15	700.00	596.75	450.56	363.48	309.56	257.83	223.18	190.93	175.85	106.75
0.015	11.4	13.1	11/09/2018 20:38	-32.03218652	115.8874331	16	700.00	565.44	438.30	364.96	314.01	279.51	243.64	210.87	185.27	112.42
0.015	11.4	13.1	11/09/2018 20:38	-32.03218652	115.8874331	17	700.00	562.57	435.30	363.95	309.86	279.14	241.21	210.98	186.38	110.63
0.015	11.4	13.1	11/09/2018 20:38	-32.03218652	115.8874331	18	700.00	557.27	433.88	363.26	311.35	278.64	241.96	211.24	186.58	112.12
0.015	11.4	13.1	11/09/2018 20:38	-32.03218652	115.8874331	19	700.00	538.26	422.59	353.49	308.92	271.82	240.91	206.31	178.69	108.39
0.015	11.4	13.1	11/09/2018 20:38	-32.03218652	115.8874331	20	700.00	533.40	419.60	351.90	307.10	270.90	239.80	205.60	178.90	109.70
0.02	11.9	13.1	11/09/2018 20:40	-32.03219828	115.8873947	21	700.00	645.54	458.29	349.38	292.31	253.89	224.17	194.71	171.46	110.28
0.02	11.9	13.1	11/09/2018 20:40	-32.03219828	115.8873947	22	700.00	637.49	452.79	345.21	289.33	252.00	222.77	192.81	170.46	110.16
0.02	11.9	13.1	11/09/2018 20:40	-32.03219828	115.8873947	23	700.00	630.62	447.10	343.04	285.84	249.66	220.32	191.23	169.72	108.05
0.02	11.9	13.1	11/09/2018 20:40	-32.03219828	115.8873947	24	700.00	608.18	441.21	342.12	287.07	250.30	220.81	190.61	168.08	106.67
0.02	11.9	13.1	11/09/2018 20:40	-32.03219828	115.8873947	25	700.00	597.42	439.37	340.72	286.35	249.74	220.79	191.04	168.44	107.12
0.025	11.9	13.1	11/09/2018 20:41	-32.03223035	115.8873514	26	700.00	752.19	559.51	442.76	369.05	302.01	254.03	199.86	171.41	101.66
0.025	11.9	13.1	11/09/2018 20:41	-32.03223035	115.8873514	27	700.00	728.60	546.94	434.42	362.43	298.03	250.41	197.32	169.96	101.33
0.025	11.9	13.1	11/09/2018 20:41	-32.03223035	115.8873514	28	700.00	719.02	542.47	430.07	359.33	296.54	249.79	195.58	171.46	101.95
0.025	11.9	13.1	11/09/2018 20:41	-32.03223035	115.8873514	29	700.00	692.97	529.67	421.10	353.72	293.76	248.26	194.13	170.83	100.53
0.025	11.9	13.1	11/09/2018 20:41	-32.03223035	115.8873514	30	700.00	686.12	522.12	419.01	351.88	290.11	245.10	197.31	167.27	99.94
0.03	11.9	13	11/09/2018 20:42	-32.03225998	115.8873116	31	700.00	517.85	401.02	318.45	273.71	237.85	212.71	184.74	162.80	109.07
0.03	11.9	13	11/09/2018 20:42	-32.03225998	115.8873116	32	700.00	512.21	398.41	317.18	273.01	237.58	212.00	183.42	162.09	106.43
0.03	11.9	13	11/09/2018 20:42	-32.03225998	115.8873116	33	700.00	506.21	395.93	315.25	272.02	236.28	211.47	182.37	162.47	101.81
0.03	11.9	13	11/09/2018 20:42	-32.03225998	115.8873116	34	700.00	495.82	391.08	313.85	272.27	238.42	211.71	183.19	162.60	102.24
0.03	11.9	13	11/09/2018 20:42	-32.03225998	115.8873116	35	700.00	493.11	392.18	312.84	272.77	239.02	211.31	183.49	163.30	98.62
0.035	11.9	13.1	11/09/2018 20:43	-32.03228984	115.8872733	36	700.00	586.93	468.40	387.36	332.38	287.07	248.97	209.38	186.17	108.35
0.035	11.9	13.1	11/09/2018 20:43	-32.03228984	115.8872733	37	700.00	576.49	462.93	382.85	328.35	283.81	247.28	209.02	182.32	107.15
0.035	11.9	13.1	11/09/2018 20:43	-32.03228984	115.8872733	38	700.00	574.80	462.02	382.70	329.36	284.85	246.93	209.50	185.63	109.41
0.035	11.9	13.1	11/09/2018 20:43	-32.03228984	115.8872733	39	700.00	557.21	449.87	376.09	326.30	281.29	245.85	207.21	185.01	107.84
0.035	11.9	13.1	11/09/2018 20:43	-32.03228984	115.8872733	40	700.00	555.41	446.23	374.13	324.17	279.40	244.40	205.61	183.87	106.50
0.04	11.9	13.2	11/09/2018 20:44	-32.03231403	115.8872321	41	700.00	660.92	493.14	376.77	311.42	261.65	228.73	190.14	165.51	92.24
0.04	11.9	13.2	11/09/2018 20:44	-32.03231403	115.8872321	42	700.00	648.61	485.93	372.43	307.98	261.02	226.64	189.05	163.17	91.07
0.04	11.9	13.2	11/09/2018 20:44	-32.03231403	115.8872321	43	700.00	646.67	484.94	371.73	308.89	259.38	226.54	189.01	164.69	91.36
0.04	11.9	13.2	11/09/2018 20:44	-32.03231403	115.8872321	44	700.00	624.96	473.88	368.33	307.40	258.75	225.71	187.44	163.87	90.85
0.04	11.9	13.2	11/09/2018 20:44	-32.03231403	115.8872321	45	700.00	614.42	469.59	365.68	304.45	257.92	223.31	186.63	161.89	91.10
0.045	12.7	13.1	11/09/2018 20:45	-32.03234618	115.887192	46	700.00	604.59	464.21	375.92	317.99	267.55	229.56	193.10	165.66	98.97
0.045	12.7	13.1	11/09/2018 20:45	-32.03234618	115.887192	47	700.00	589.11	454.14	369.40	314.39	264.40	227.19	190.72	164.81	97.51
0.045	12.7	13.1	11/09/2018 20:45	-32.03234618	115.887192	48	700.00	583.87	452.48	367.59	312.48	262.65	225.01	189.58	163.87	96.82
0.045	12.7	13.1	11/09/2018 20:45	-32.03234618	115.887192	49	700.00	564.34	443.20	362.71	310.36	263.05	225.73	190.23	164.41	95.12
0.045	12.7	13.1	11/09/2018 20:45	-32.03234618	115.887192	50	700.00	555.01	438.75	359.77	308.22	260.06	223.06	188.06	162.83	93.73
0.054	12.8	13.3	11/09/2018 20:50	-32.03239387	115.8871217	51	700.00	676.50	494.55	380.02	315.80	262.90	228.33	192.28	168.42	102.72
0.054	12.8	13.3	11/09/2018 20:50	-32.03239387	115.8871217	52	700.00	663.52	487.41	374.52	310.69	260.04	227.01	191.88	168.47	102.66
0.054	12.8	13.3	11/09/2018 20:50	-32.03239387	115.8871217	53	700.00	656.44	483.30	373.71	311.52	258.78	226.01	191.26	167.43	104.63
0.054	12.8	13.3	11/09/2018 20:50	-32.03239387	115.8871217	54	700.00	628.19	471.05	366.65	306.17	257.34	223.94	188.74	164.57	97.98
0.054	12.8	13.3	11/09/2018 20:50	-32.03239387	115.8871217	55	700.00	619.35	466.30	362.35	302.40	254.71	222.25	187.60	164.20	97.88
0.05	12.7	13.3	11/09/2018 20:52	-32.03237537	115.8871471	56	700.00	620.13	482.13	376.88	308.25	257.88	223.00	188.00	166.63	98.50
0.05	12.7	13.3	11/09/2018 20:52	-32.03237537	115.8871471	57	700.00	611.10	476.95	371.22	306.34	257.44	221.83	186.10	169.15	97.20
0.05	12.7	13.3	11/09/2018 20:52	-32.03237537	115.8871471	58	700.00	603.12	472.04	367.47	304.78	256.21	220.90	184.11	169.98	98.50
0.05	12.7	13.3	11/09/2018 20:52	-32.03237537	115.8871471	59	700.00	580.72	462.44	363.38	302.03	255.76	220.26	183.05	167.05	95.14
0.05	12.7	13.3	11/09/2018 20:52	-32.03237537	115.8871471	60	700.00	573.64	459.03	360.65	300.51	254.61	219.96	183.41	167.08	94.69
0.06	12.5	13.4	11/09/2018 20:53	-32.03243213	115.8870698	61	700.00	584.90	442.42	350.99	295.49	246.18	212.48	176.55	148.18	82.51
0.06	12.5	13.4	11/09/2018 20:53	-32.03243213	115.8870698	62	700.00	579.89	433.30	344.53	291.44	242.70	209.88	175.68	147.34	82.31
0.06	12.5	13.4	11/09/2018 20:53	-32.03243213	115.8870698	63	700.00	573.29	430.83	341.88	286.77	240.51	208.65	179.74	147.87	81.44
0.06	12.5	13.4	11/09/2018 20:53	-32.03243213	115.8870698	64	700.00	549.74	419.09	336.93	283.72	237.66	206.88	173.69	145.33	79.55
0.06	12.5	13.4	11/09/2018 20:53	-32.03243213	115.8870698	65	700.00	543.78	415.79	332.78	281.20	233.33	205.09	176.15	144.61	79.31
0.065	12.5	13.4	11/09/2018 20:54	-32.03245657	115.8870268	66	700.00	567.78	417.11	324.53	269.59	223.05	193.06	159.70	136.49	79.16
0.065	12.5	13.4	11/09/2018 20:54	-32.03245657	115.8870268	67	700.00	560.12	406.94	318.05	267.19	221.07	192.72	163.25	132.42	78.21
0.065	12.5	13.4	11/09/2018 20:54	-32.03245657	115.8870268	68	700.00	545.11	408.07	317.64	262.90	218.98	190.44	160.05	133.85	80.95
0.065	12.5	13.4	11/09/2018 20:54	-32.03245657	115.8870268	69	700.00	528.41	395.53	311.29	262.75	217.02	190.24	159.66	131.88	71.60
0.065	12.5	13.4	11/09/2018 20:54	-32.03245657	115.8870268	70	700.00	521.37	390.43	307.48	260.38	215.18	189.79	161.01	129.84	78.07
0.07	12.5	13.4	11/09/2018 20:55	-32.03248795	115.8869866	71	700.00	514.54	371.17	294.45	247.37	207.26	180.60	149.72	128.29	73.74
0.07	12.5	13.4	11/09/2018 20:55	-32.03248795	115.8869866	72	700.00	505.68	367.28	293.33	247.16	206.30	180.37	149.63	128.64	72.10
0.07	12.5	13.4	11/09/2018 20:55	-32.03248795	115.8869866	73	700.00	500.79	361.89	294.22	248.00	200.07	176.16	147.11	129.70	73.56
0.07	12.5	13.4	11/09/2018 20:55	-32.03248795	115.8869866	74	700.00	480.30	356.10	291.40	245.80	201.80	176.70	147.00	128.80	71.50
0.07	12.5	13.4	11/09/2018 20:55	-32.03248795	115.8869866	75	700.00	478.13	353.12	293.18	247.21	197.33	175.20	146.64	132.05	72.21
0.075	12.9	13.4	11/09/2018 20:56	-32.03250821	115.8869443	76	700.00	603.99	451.04	349.62	289.55	243.93	206.98	168.40	147.54	79.68
0.075	12.9	13.4	11/09/2018 20:56	-32.03250821	115.8869443	77	700.00	588.69	441.77	344.31	285.32	240.80	204.68	167.58	146.06	78.53
0.075	12.9	13.4	11/09/2018 20:56	-32.03250821	115.8869443	78	700.00	578.09	434.87	338.35	281.12	240.73	202.81	163.54	146.19	79.29
0.075	12.9	13.4	11/09/2018 20:56	-32.03250821	115.8869443	79	700.00	561.64	429.97	338.28	282.47	239.30	203.42	164.67	144.42	79.56
0.075	12.9	13.4	11/09/2018 20:56	-32.03250821	115.8869443	80	700.00	555.51	425.19	335.72	279.00	238.06	202.01	163.87	143.79	78.09
0.08	13	13.5	11/09/2018 20:56	-32.03253813	115.886904	81	700.00	558.24	424.41	339.05	287.43	241.73	214.15	181.55	164.68	107.27
0.08	13	13.5	11/09/2018 20:56	-32.03253813	115.886904	82	700.00	551.98	418.64	334.81	283.95	240.86	211.23	179.01	159.26	102.72
0.08	13	13.5	11/09/2018 20:56	-32.03253813	115.886904	83	700.00	547.32	416.15	335.58	283.61	238.72	211.62	178.29	164.25	114.01
0.08	13	13.5	11/09/2018 20:56	-32.03253813	115.886904	84	700.00	528.01	405.84	327.38	279.39	237.10	209.29	175.46	160.28	111.37
0.08	13	13.5	11/09/2018 20:56	-32.03253813	115.886904	85	700.00	521.20	403.70	323.40	278.20	236.40	207.30	174.60	156.60	95.40
0.085	13	13.5	11/09/2018 20:57	-32.03257432	115.8868648	86	700.00	536.58	414.05	341.08	293.88	250.64	216.81	185.84	158.34	90.57
0.085	13	13.5	11/09/2018 20:57	-32.03257432	115.8868648	87	700.00	527.67	407.32	337.32	291.69	250.41	218.33	184.88	158.65	90.64
0.085	13	13.5	11/09/2018 20:57	-32.03257432	115.8868648	88	700.00	522.83	404.27	335.26	289.54	248.41	216.07	184.35	158.21	90.19
0.085	13	13.5	11/09/2018 20:57	-32.03257432	115.8868648	89	700.00	502.14	395.22	329.17	284.15	243.77	211.48	181.27	154.51	85.40
0.085	13	13.5	11/09/2018 20:57	-32.03257432	115.8868648	90	700.00	493.30	393.96	327.17	281.50	239.24	207.80	180.66	154.12	94.84
0.09	12.8	13.5	11/09/2018 20:58	-32.03260925	115.8868278	91	700.00	614.26	470.36	376.82	317.01	267.54	227.63	192.00	165.43	98.08
0.09	12.8	13.5	11/09/2018 20:58	-32.03260925	115.8868278	92	700.00	607.00	462.17	376.34	319.58	270.97	223.23	197.14	161.89	100.55
0.09	12.8	13.5	11/09/2018 20:58	-32.03260925	115.8868278	93	700.00	601.73	461.23	375.56	317.16	268.02	226.17	193.21	165.43	97.53
0.09	12.8	13.5	11/09/2018 20:58	-32.03260925	115.8868278	94	700.00	573.18	446.46	364.48	309.26	263.52	221.08	190.33	157.87	95.76
0.09	12.8	13.5	11/09/2018 20:58	-32.03260925	115.8868278	95	700.00	562.99	443.20	361.05	305.69	260.48	219.26	189.19	157.52	104.55
0.095	12.4	13.5	11/09/2018 20:59	-32.03263106	115.8867731	96	700.00	637.45	482.04	370.72	301.48	254.60	214.55	178.54	153.65	91.35
0.095	12.4	13.5	11/09/2018 20:59	-32.03263106	115.8867731	97	700.00	624.02	473.41	364.51	297.07	252.93	212.32	178.17	153.41	89.51
0.095	12.4	13.5	11/09/2018 20:59	-32.03263106	115.8867731	98	700.00	620.18	473.21	362.81	296.54	249.79	211.99	177.67	152.93	91.26
0.095	12.4	13.5	11/09/2018 20:59	-32.03263106	115.8867731	99	700.00	587.70	452.23	352.32	287.76	246.46	206.17	174.35	150.68	87.22
0.095	12.4	13.5	11/09/2018 20:59	-32.03263106	115.8867731	100	700.00	581.45	450.52	350.30	286.35	246.06	204.56	174.35	151.99	86.42
0.1	12.5	13.4	11/09/2018 21:02	-32.03265696	115.8867434	101	700.00	600.96	427.70	323.56	263.24	219.93	191.13	157.62	135.78	79.18
0.1	12.5	13.4	11/09/2018 21:02	-32.03265696	115.8867434	102	700.00	592.16	421.98	321.06	260.95	218.29	190.34	159.79	137.40	81.25
0.1	12.5	13.4	11/09/2018 21:02	-32.03265696	115.8867434	103	700.00	587.78	419.01	318.40	260.25	216.79	188.77	159.88	136.67	80.37
0.1	12.5	13.4	11/09/2018 21:02	-32.03265696	115.8867434	104	700.00	550.00	404.00	311.90	253.90	212.90	186.10	159.90	135.00	78.10
0.1	12.5	13.4	11/09/2018 21:02	-32.03265696	115.8867434	105	700.00	548.35	402.63	309.63	252.88	212.71	185.80	158.58	134.88	79.64

Station	Surface	Air	Time	Latitude	Longitude	DropID	Stress	ND0	ND200	ND300	ND400	ND500	ND600	ND750	ND900	ND1500
0	11	13.9	13/09/2018 20:29	-32.0321	115.8876	1	700.00	513.09	408.93	343.26	303.57	265.57	234.18	201.46	174.64	102.59
0	11	13.9	13/09/2018 20:29	-32.0321	115.8876	2	700.00	502.48	403.11	338.86	299.09	261.28	230.19	198.13	172.43	101.08
0	11	13.9	13/09/2018 20:29	-32.0321	115.8876	3	700.00	500.09	397.86	334.38	295.38	258.22	228.33	196.71	170.88	99.65
0	11	13.9	13/09/2018 20:29	-32.0321	115.8876	4	700.00	483.51	390.94	328.63	292.48	256.83	226.48	195.72	169.86	99.66
0	11	13.9	13/09/2018 20:29	-32.0321	115.8876	5	700.00	482.77	389.37	326.40	290.75	254.29	224.86	194.53	169.33	98.22
0.005	11.4	13.9	13/09/2018 20:29	-32.0321	115.8875	6	700.00	554.91	422.79	350.36	303.86	260.26	229.62	195.83	171.61	104.03
0.005	11.4	13.9	13/09/2018 20:29	-32.0321	115.8875	7	700.00	546.77	417.25	347.63	301.96	259.66	228.22	195.15	171.69	103.07
0.005	11.4	13.9	13/09/2018 20:29	-32.0321	115.8875	8	700.00	538.55	413.50	342.89	297.41	255.73	226.43	193.82	170.16	104.57
0.005	11.4	13.9	13/09/2018 20:29	-32.0321	115.8875	9	700.00	512.54	399.36	333.25	290.17	250.48	221.67	189.76	166.42	100.51
0.005	11.4	13.9	13/09/2018 20:29	-32.0321	115.8875	10	700.00	509.77	398.41	332.15	288.98	249.34	221.20	188.92	166.53	101.27
0.01	11.3	13.8	13/09/2018 20:30	-32.0321	115.8875	11	700.00	649.64	480.43	384.19	328.24	279.01	241.83	207.02	179.79	107.67
0.01	11.3	13.8	13/09/2018 20:30	-32.0321	115.8875	12	700.00	636.24	465.28	374.23	321.98	274.13	234.72	207.55	177.81	111.73
0.01	11.3	13.8	13/09/2018 20:30	-32.0321	115.8875	13	700.00	633.96	457.35	367.69	321.18	273.82	230.78	213.46	179.20	118.23
0.01	11.3	13.8	13/09/2018 20:30	-32.0321	115.8875	14	700.00	601.84	444.66	359.39	311.75	266.22	228.97	203.41	173.95	105.75
0.01	11.3	13.8	13/09/2018 20:30	-32.0321	115.8875	15	700.00	597.84	440.51	354.58	309.17	264.57	228.32	202.83	173.06	105.35
0.015	11.4	13.8	13/09/2018 20:31	-32.0322	115.8874	16	700.00	646.23	520.73	432.76	370.32	320.27	275.79	228.71	198.11	113.86
0.015	11.4	13.8	13/09/2018 20:31	-32.0322	115.8874	17	700.00	629.50	509.70	426.32	363.38	315.43	271.82	225.49	195.88	112.99
0.015	11.4	13.8	13/09/2018 20:31	-32.0322	115.8874	18	700.00	625.11	508.69	423.89	363.42	315.13	271.22	225.30	195.82	114.03
0.015	11.4	13.8	13/09/2018 20:31	-32.0322	115.8874	19	700.00	602.42	495.18	414.92	356.57	310.27	267.85	222.15	191.98	110.83
0.015	11.4	13.8	13/09/2018 20:31	-32.0322	115.8874	20	700.00	602.56	491.59	411.55	354.67	307.74	266.58	221.24	191.80	111.36
0.02	11.2	13.8	13/09/2018 20:32	-32.0322	115.8874	21	700.00	537.85	420.00	345.84	298.11	258.71	228.23	196.91	173.41	111.73
0.02	11.2	13.8	13/09/2018 20:32	-32.0322	115.8874	22	700.00	535.43	416.17	342.47	297.41	256.54	226.17	195.56	174.07	110.86
0.02	11.2	13.8	13/09/2018 20:32	-32.0322	115.8874	23	700.00	526.79	413.21	341.11	295.06	255.68	226.42	194.44	171.73	110.62
0.02	11.2	13.8	13/09/2018 20:32	-32.0322	115.8874	24	700.00	514.54	407.53	336.93	294.48	254.15	224.48	194.01	172.49	108.92
0.02	11.2	13.8	13/09/2018 20:32	-32.0322	115.8874	25	700.00	513.81	406.93	337.24	295.90	253.66	223.98	195.41	175.15	111.53
0.025	11.2	13.8	13/09/2018 20:33	-32.0322	115.8873	26	700.00	705.53	523.40	414.23	340.05	281.11	239.84	198.82	171.56	100.82
0.025	11.2	13.8	13/09/2018 20:33	-32.0322	115.8873	27	700.00	688.00	514.63	408.38	334.50	275.38	236.50	196.13	170.63	101.00
0.025	11.2	13.8	13/09/2018 20:33	-32.0322	115.8873	28	700.00	685.44	514.02	408.47	334.96	276.36	236.93	197.14	170.09	98.75
0.025	11.2	13.8	13/09/2018 20:33	-32.0322	115.8873	29	700.00	653.96	500.20	401.58	330.99	275.05	236.53	196.44	168.02	98.51
0.025	11.2	13.8	13/09/2018 20:33	-32.0322	115.8873	30	700.00	649.01	497.34	399.89	327.37	271.85	234.54	194.11	165.85	106.21
0.03	11.2	13.7	13/09/2018 20:34	-32.0323	115.8873	31	700.00	545.39	421.35	341.28	295.72	252.61	220.56	186.42	162.23	101.07
0.03	11.2	13.7	13/09/2018 20:34	-32.0323	115.8873	32	700.00	533.07	417.02	336.84	293.53	249.84	219.18	186.67	163.71	100.04
0.03	11.2	13.7	13/09/2018 20:34	-32.0323	115.8873	33	700.00	531.70	413.36	336.59	291.56	249.24	218.37	185.76	162.88	101.49
0.03	11.2	13.7	13/09/2018 20:34	-32.0323	115.8873	34	700.00	512.87	407.82	334.12	291.18	249.24	218.89	186.13	164.17	99.86
0.03	11.2	13.7	13/09/2018 20:34	-32.0323	115.8873	35	700.00	513.23	406.82	335.11	289.66	249.32	218.15	185.06	162.13	101.88
0.035	11.3	13.8	13/09/2018 20:35	-32.0323	115.8873	36	700.00	630.98	488.90	394.26	331.12	283.56	243.35	201.79	171.63	102.61
0.035	11.3	13.8	13/09/2018 20:35	-32.0323	115.8873	37	700.00	620.07	482.03	388.25	327.08	279.26	240.28	199.33	169.79	102.24
0.035	11.3	13.8	13/09/2018 20:35	-32.0323	115.8873	38	700.00	612.69	476.77	384.88	323.16	276.91	238.45	199.49	169.43	101.91
0.035	11.3	13.8	13/09/2018 20:35	-32.0323	115.8873	39	700.00	592.22	469.28	382.52	324.82	278.12	241.53	200.18	169.94	100.54
0.035	11.3	13.8	13/09/2018 20:35	-32.0323	115.8873	40	700.00	589.45	467.00	381.47	323.78	278.08	240.76	197.39	168.85	99.86
0.04	11.3	14.1	13/09/2018 20:39	-32.0323	115.8872	41	700.00	664.57	496.77	399.58	334.62	287.63	246.29	200.53	168.54	93.01
0.04	11.3	14.1	13/09/2018 20:39	-32.0323	115.8872	42	700.00	654.41	490.25	395.34	332.31	284.61	246.49	199.16	168.27	92.92
0.04	11.3	14.1	13/09/2018 20:39	-32.0323	115.8872	43	700.00	642.12	480.72	385.62	323.66	277.28	238.20	193.43	162.14	87.19
0.04	11.3	14.1	13/09/2018 20:39	-32.0323	115.8872	44	700.00	624.70	475.30	385.70	326.20	281.50	242.30	197.70	166.20	91.60
0.04	11.3	14.1	13/09/2018 20:39	-32.0323	115.8872	45	700.00	617.12	471.03	382.65	324.64	279.40	240.66	196.82	165.56	92.07
0.045	11.4	14	13/09/2018 20:40	-32.0323	115.8872	46	700.00	579.20	449.49	369.82	309.98	265.01	228.09	186.83	160.07	92.55
0.045	11.4	14	13/09/2018 20:40	-32.0323	115.8872	47	700.00	570.83	442.39	362.43	306.08	258.72	225.01	186.13	159.93	93.01
0.045	11.4	14	13/09/2018 20:40	-32.0323	115.8872	48	700.00	564.34	438.58	359.17	302.92	257.20	221.52	185.22	159.82	94.78
0.045	11.4	14	13/09/2018 20:40	-32.0323	115.8872	49	700.00	544.01	428.84	356.26	301.15	256.57	223.01	185.87	159.26	91.55
0.045	11.4	14	13/09/2018 20:40	-32.0323	115.8872	50	700.00	539.70	426.40	352.50	299.10	254.40	221.20	186.60	161.00	94.10
0.05	11.7	14	13/09/2018 20:41	-32.0324	115.8871	51	700.00	637.26	476.84	369.44	303.25	254.29	220.83	187.24	165.59	96.20
0.05	11.7	14	13/09/2018 20:41	-32.0324	115.8871	52	700.00	621.56	467.54	363.40	299.61	252.45	219.56	186.17	160.98	93.33
0.05	11.7	14	13/09/2018 20:41	-32.0324	115.8871	53	700.00	618.23	467.20	363.01	298.58	252.25	219.79	186.46	162.18	93.79
0.05	11.7	14	13/09/2018 20:41	-32.0324	115.8871	54	700.00	588.08	455.25	357.77	296.63	251.32	217.97	184.51	160.31	91.41
0.05	11.7	14	13/09/2018 20:41	-32.0324	115.8871	55	700.00	587.15	455.05	356.89	296.21	251.13	218.91	185.38	161.07	90.77
0.055	11.4	14	13/09/2018 20:42	-32.0324	115.8871	56	700.00	655.94	470.27	352.73	291.05	241.15	209.88	177.23	155.89	92.84
0.055	11.4	14	13/09/2018 20:42	-32.0324	115.8871	57	700.00	632.47	461.85	346.17	287.41	236.05	206.67	174.20	156.91	91.98
0.055	11.4	14	13/09/2018 20:42	-32.0324	115.8871	58	700.00	637.50	459.49	345.94	285.78	236.94	208.15	176.54	156.49	92.51
0.055	11.4	14	13/09/2018 20:42	-32.0324	115.8871	59	700.00	608.33	446.86	339.22	282.70	234.56	205.31	172.55	153.18	90.17
0.055	11.4	14	13/09/2018 20:42	-32.0324	115.8871	60	700.00	603.75	443.74	337.13	280.91	232.43	203.97	169.27	154.78	89.61
0.06	11.3	14	13/09/2018 20:43	-32.0324	115.8871	61	700.00	593.07	437.84	344.76	292.10	243.57	209.38	170.57	146.86	79.48
0.06	11.3	14	13/09/2018 20:43	-32.0324	115.8871	62	700.00	586.30	430.00	341.36	288.15	241.23	206.17	167.78	148.15	80.49
0.06	11.3	14	13/09/2018 20:43	-32.0324	115.8871	63	700.00	585.44	429.37	340.63	287.79	240.80	207.69	169.58	144.63	76.82
0.06	11.3	14	13/09/2018 20:43	-32.0324	115.8871	64	700.00	557.17	414.04	333.94	281.92	237.68	202.32	165.25	147.17	77.78
0.06	11.3	14	13/09/2018 20:43	-32.0324	115.8871	65	700.00	562.09	423.18	342.84	292.73	248.78	214.77	178.18	156.80	89.59
0.065	11.2	14.1	13/09/2018 20:44	-32.0325	115.887	66	700.00	532.86	392.98	304.32	253.23	208.89	180.53	149.70	130.42	76.14
0.065	11.2	14.1	13/09/2018 20:44	-32.0325	115.887	67	700.00	527.23	387.36	300.35	251.95	206.77	179.47	149.68	132.30	76.21
0.065	11.2	14.1	13/09/2018 20:44	-32.0325	115.887	68	700.00	522.07	385.19	298.97	249.30	207.01	179.68	150.11	129.02	72.62
0.065	11.2	14.1	13/09/2018 20:44	-32.0325	115.887	69	700.00	501.10	376.40	295.10	248.70	204.60	178.30	148.10	130.60	73.20
0.065	11.2	14.1	13/09/2018 20:44	-32.0325	115.887	70	700.00	495.28	376.03	295.26	247.99	206.21	179.39	149.37	130.53	77.08
0.07	11.3	14	13/09/2018 20:45	-32.0325	115.887	71	700.00	489.87	367.69	291.67	247.63	209.50	180.14	149.91	129.84	74.39
0.07	11.3	14	13/09/2018 20:45	-32.0325	115.887	72	700.00	479.77	360.97	287.27	243.40	204.33	175.99	151.58	127.18	74.44
0.07	11.3	14	13/09/2018 20:45	-32.0325	115.887	73	700.00	476.90	359.86	285.74	242.44	204.01	175.94	152.85	127.90	73.99
0.07	11.3	14	13/09/2018 20:45	-32.0325	115.887	74	700.00	461.58	352.73	284.35	240.55	200.90	175.61	153.45	125.94	71.11
0.07	11.3	14	13/09/2018 20:45	-32.0325	115.887	75	700.00	457.56	350.60	282.21	239.53	200.86	174.65	153.76	125.54	70.40
0.075	11.2	13.9	13/09/2018 20:46	-32.0326	115.887	76	700.00	602.45	438.07	342.42	283.54	237.67	201.91	168.81	143.03	80.23
0.075	11.2	13.9	13/09/2018 20:46	-32.0326	115.887	77	700.00	589.98	429.30	337.15	278.41	234.48	200.45	167.66	141.47	78.44
0.075	11.2	13.9	13/09/2018 20:46	-32.0326	115.887	78	700.00	583.70	425.43	334.20	277.41	234.20	200.49	167.90	142.72	80.62
0.075	11.2	13.9	13/09/2018 20:46	-32.0326	115.887	79	700.00	564.55	417.88	331.79	276.97	233.87	200.29	166.50	141.11	77.59
0.075	11.2	13.9	13/09/2018 20:46	-32.0326	115.887	80	700.00	561.00	416.30	331.00	276.30	234.20	200.70	167.60	141.80	78.10
0.08	11.3	13.9	13/09/2018 20:47	-32.0325	115.8869	81	700.00	540.32	403.56	326.09	281.00	238.52	209.50	177.49	156.19	95.04
0.08	11.3	13.9	13/09/2018 20:47	-32.0325	115.8869	82	700.00	530.49	398.02	321.98	276.54	237.53	208.40	177.41	155.93	92.10
0.08	11.3	13.9	13/09/2018 20:47	-32.0325	115.8869	83	700.00	525.75	395.54	320.27	274.48	238.10	207.99	177.38	157.69	93.96
0.08	11.3	13.9	13/09/2018 20:47	-32.0325	115.8869	84	700.00	508.15	387.29	316.89	274.12	236.52	207.61	176.40	155.75	91.54
0.08	11.3	13.9	13/09/2018 20:47	-32.0325	115.8869	85	700.00	508.72	385.35	314.55	271.54	237.08	207.61	175.55	155.23	90.81
0.085	11.3	13.8	13/09/2018 20:48	-32.0326	115.8869	86	700.00	626.61	469.93	359.66	299.32	247.89	209.87	173.87	149.03	88.82
0.085	11.3	13.8	13/09/2018 20:48	-32.0326	115.8869	87	700.00	616.66	464.67	355.63	295.79	246.59	209.76	174.51	151.87	90.80
0.085	11.3	13.8	13/09/2018 20:48	-32.0326	115.8869	88	700.00	610.36	460.53	354.10	295.67	246.43	210.12	174.69	149.57	91.51
0.085	11.3	13.8	13/09/2018 20:48	-32.0326	115.8869	89	700.00	581.44	445.23	345.91	289.97	241.61	206.31	170.01	144.89	84.36
0.085	11.3	13.8	13/09/2018 20:48	-32.0326	115.8869	90	700.00	576.98	441.89	343.72	288.25	241.32	205.88	170.04	145.89	86.10
0.09	11.3	13.9	13/09/2018 20:49	-32.0326	115.8868	91	700.00	603.05	461.05	367.34	308.70	260.53	221.85	187.04	159.84	97.95
0.09	11.3	13.9	13/09/2018 20:49	-32.0326	115.8868	92	700.00	594.51	457.10	363.43	306.87	259.42	221.34	186.58	160.95	97.36
0.09	11.3	13.9	13/09/2018 20:49	-32.0326	115.8868	93	700.00	590.33	453.28	362.40	304.56	258.51	220.56	185.07	159.40	97.88
0.09	11.3	13.9	13/09/2018 20:49	-32.0326	115.8868	94	700.00	561.01	439.41	353.72	299.11	254.25	216.74	182.54	156.49	96.45
0.09	11.3	13.9	13/09/2018 20:49	-32.0326	115.8868	95	700.00	556.13	436.66	352.38	297.15	253.03	216.74	181.74	156.06	95.88
0.095	11.3	13.8	13/09/2018 20:50	-32.0326	115.8868	96	700.00	611.25	458.88	357.25	292.88	242.25	208.13	172.88	147.63	88.25
0.095	11.3	13.8	13/09/2018 20:50	-32.0326	115.8868	97	700.00	602.32	452.39	354.34	291.42	240.90	208.14	172.52	147.70	87.13
0.095	11.3	13.8	13/09/2018 20:50	-32.0326	115.8868	98	700.00	598.23	450.78	353.60	291.42	240.90	207.89	172.39	147.32	88.24
0.095	11.3	13.8	13/09/2018 20:50	-32.0326	115.8868	99	700.00	567.58	435.85	345.91	285.28	239.02	206.41	171.31	146.68	86.45
0.095	11.3	13.8	13/09/2018 20:50	-32.0326	115.8868	100	700.00	563.99	433.56	343.02	283.29	237.12	204.72	170.11	145.48	85.75
0.1	11.3	13.8	13/09/2018 20:50	-32.0327	115.8867	101	700.00	564.26	389.95	292.77	242.18	202.61	176.82	151.40	131.11	81.77
0.1	11.3	13.8	13/09/2018 20:50	-32.0327	115.8867	102	700.00	554.55	384.81	290.41	239.73	201.70	176.05	150.41	130.71	77.06
0.1	11.3	13.8	13/09/2018 20:50	-32.0327	115.8867	103	700.00	549.49	382.77	289.52	239.31	201.71	176.24	150.39	131.10	78.16
0.1	11.3	13.8	13/09/2018 20:50	-32.0327	115.8867	104	700.00	518.54	371.48	283.38	235.95	199.26	174.20	149.15	128.96	74.47
0.1	11.3	13.8	13/09/2018 20:50	-32.0327	115.8867	105	700.00	517.09	370.65	283.53	235.28	199.02	173.94	148.16	129.63	74.53

Comment	Surface	Air	Time	Latitude	Longitude	DropID	Stress	ND0	ND200	ND300	ND400	ND500	ND600	ND750	ND900	ND1500
B	11.1	13.8	13/09/2018 21:30	-32.0324	115.8871	1	700.00	708.31	484.87	374.92	311.88	262.04	229.18	192.53	168.10	112.88
B	11.1	13.8	13/09/2018 21:30	-32.0324	115.8871	2	700.00	693.09	474.94	368.89	306.42	258.40	227.16	191.73	168.40	105.93
B	11.1	13.8	13/09/2018 21:30	-32.0324	115.8871	3	700.00	663.80	461.88	361.77	303.93	257.36	226.75	189.26	167.02	100.21
B	11.1	13.8	13/09/2018 21:30	-32.0324	115.8871	4	700.00	646.78	452.54	355.93	299.10	254.13	223.35	188.03	164.29	102.54
C	10.9	13.9	13/09/2018 21:35	-32.0324	115.8871	5	700.00	646.44	470.94	366.19	302.54	255.71	222.83	188.33	166.90	103.63
C	10.9	13.9	13/09/2018 21:35	-32.0324	115.8871	6	700.00	633.69	463.18	361.20	301.41	253.92	222.06	186.63	168.91	104.69
C	10.9	13.9	13/09/2018 21:35	-32.0324	115.8871	7	700.00	608.70	452.40	357.66	300.03	253.00	221.09	185.95	163.66	98.67
C	10.9	13.9	13/09/2018 21:35	-32.0324	115.8871	8	700.00	593.49	443.06	351.83	294.64	249.44	218.78	184.20	162.33	96.90
D	10.7	13.9	13/09/2018 21:37	-32.0324	115.8871	9	700.00	664.69	472.65	365.61	303.54	254.60	222.39	187.33	165.03	102.21
D	10.7	13.9	13/09/2018 21:37	-32.0324	115.8871	10	700.00	659.95	469.05	363.19	302.55	254.12	222.94	187.57	166.00	101.92
D	10.7	13.9	13/09/2018 21:37	-32.0324	115.8871	11	700.00	626.86	453.28	354.36	297.65	249.67	219.03	183.42	161.61	99.93
D	10.7	13.9	13/09/2018 21:37	-32.0324	115.8871	12	700.00	612.05	444.88	348.86	294.53	247.04	217.79	182.08	160.99	95.74
E	10.7	14	13/09/2018 21:39	-32.0324	115.8871	13	700.00	643.06	459.93	357.02	295.77	249.07	218.38	185.11	162.68	105.99
E	10.7	14	13/09/2018 21:39	-32.0324	115.8871	14	700.00	633.49	455.37	353.99	292.33	247.86	217.47	184.47	161.30	107.86
E	10.7	14	13/09/2018 21:39	-32.0324	115.8871	15	700.00	614.17	450.01	353.39	293.88	249.27	218.12	184.61	161.28	103.30
E	10.7	14	13/09/2018 21:39	-32.0324	115.8871	16	700.00	595.57	440.68	347.44	288.82	245.95	215.22	181.83	157.93	101.68
F	10.9	14	13/09/2018 21:40	-32.0324	115.8871	17	700.00	630.00	463.97	356.98	295.82	245.50	216.60	184.22	162.54	100.14
F	10.9	14	13/09/2018 21:40	-32.0324	115.8871	18	700.00	614.38	454.88	351.25	292.25	243.63	214.88	183.00	161.13	101.50
F	10.9	14	13/09/2018 21:40	-32.0324	115.8871	19	700.00	595.20	446.62	349.10	291.57	244.30	215.28	181.78	159.64	96.52
F	10.9	14	13/09/2018 21:40	-32.0324	115.8871	20	700.00	579.63	437.69	343.43	287.31	241.57	212.87	180.00	157.96	94.72
G	10.9	14.1	13/09/2018 21:44	-32.0324	115.8871	21	700.00	635.20	456.05	347.65	290.04	243.95	213.72	181.38	157.47	88.96
G	10.9	14.1	13/09/2018 21:44	-32.0324	115.8871	22	700.00	626.79	450.49	349.01	288.27	243.33	215.80	182.96	159.01	96.05
G	10.9	14.1	13/09/2018 21:44	-32.0324	115.8871	23	700.00	598.33	437.57	345.04	285.26	241.08	215.86	181.11	154.99	93.63
G	10.9	14.1	13/09/2018 21:44	-32.0324	115.8871	24	700.00	583.33	430.41	339.96	282.79	240.68	213.07	179.51	155.62	89.34
H	10.9	14.1	13/09/2018 21:45	-32.0324	115.8871	25	700.00	623.29	450.96	352.36	290.20	245.19	212.11	182.27	158.77	99.34
H	10.9	14.1	13/09/2018 21:45	-32.0324	115.8871	26	700.00	625.92	451.04	350.25	289.89	246.11	213.22	182.67	160.78	94.24
H	10.9	14.1	13/09/2018 21:45	-32.0324	115.8871	27	700.00	590.24	437.55	345.84	287.14	244.50	211.98	179.86	158.24	87.35
H	10.9	14.1	13/09/2018 21:45	-32.0324	115.8871	28	700.00	579.09	429.83	339.99	283.65	242.75	209.53	179.02	156.28	96.95
H2	10.9	14	13/09/2018 21:48	-32.0324	115.8871	29	700.00	611.64	447.11	342.24	282.22	237.73	210.49	181.04	158.61	90.21
H2	10.9	14	13/09/2018 21:48	-32.0324	115.8871	30	700.00	602.50	440.57	339.47	280.12	235.89	209.01	180.51	157.10	92.42
H2	10.9	14	13/09/2018 21:48	-32.0324	115.8871	31	700.00	582.46	434.14	338.67	282.51	236.28	210.60	180.62	155.54	92.56
H2	10.9	14	13/09/2018 21:48	-32.0324	115.8871	32	700.00	570.81	430.24	336.28	280.94	235.93	209.62	180.59	154.47	94.05
H2	10.9	14	13/09/2018 21:48	-32.0324	115.8871	33	700.00	607.75	439.70	331.01	273.62	226.30	203.48	177.69	153.74	93.95
H2	10.9	14	13/09/2018 21:48	-32.0324	115.8871	34	700.00	607.14	440.86	332.71	273.29	227.29	205.00	180.43	153.57	94.71

ARRB_ID	Chainage(m)	GPS		Date	Time	Temperatures		Drop No	Deflections (µm) Normalised To 700 kPa & Load Distace (mm)									Curvature	Comments
		Latitude	Longitude			Surface C	Air C		0	200	300	400	500	600	750	900	1500		
Run2 Leach on sensors_0.0	0	-32.0324	115.8871	27/10.0/2018	01:08	17.4	19.1	5	548	407	319	268	229	203	173	152	97	148	
Run2 Leach on sensors_0.0	0	-32.0324	115.8871	27/10.0/2018	01:09	17.6	19.1	5	546	406	317	267	229	202	173	152	96	146	
Run2 Leach on sensors_0.0	0	-32.0324	115.8871	27/10.0/2018	01:10	17.5	19.1	5	540	394	312	264	226	200	171	151	95	155	
Run2 Leach on sensors_1.0	1	-32.0324	115.8871	27/10.0/2018	01:12	17.5	19.1	5	522	391	311	263	225	199	172	150	94	140	
Run2 Leach on sensors_1.0	1	-32.0324	115.8871	27/10.0/2018	01:13	17.6	19.1	5	522	392	308	260	223	198	170	148	91	141	
Run2 Leach on sensors_1.0	1	-32.0324	115.8871	27/10.0/2018	01:14	17.5	19	5	518	392	307	257	220	197	171	150	88	136	
Run2 Leach on sensors_1.0	1	-32.0324	115.8871	27/10.0/2018	01:16	17.7	19	5	531	393	308	259	223	197	169	147	89	145	
Run2 Leach sensors complete off_0.0	0	-32.0324	115.8871	27/10.0/2018	01:34	16.8	18.6	5	532	400	313	260	220	194	165	145	92	136	
Run2 Leach sensors complete off_0.0	0	-32.0324	115.8871	27/10.0/2018	01:35	17.3	18.6	5	527	391	307	256	219	195	165	146	92	148	
Run2 Leach sensors complete off_0.0	0	-32.0324	115.8871	27/10.0/2018	01:36	17.2	18.6	5	519	389	303	257	218	192	166	145	94	137	
Run2 Leach sensors complete off_1.0	1	-32.0324	115.8871	27/10.0/2018	01:38	17.4	18.6	5	506	384	300	254	216	190	165	144	91	131	
Run2 Leach sensors complete off_1.0	1	-32.0324	115.8871	27/10.0/2018	01:39	17.1	18.7	5	512	388	303	254	217	194	167	146	90	132	
Run2 Leach sensors complete off_1.0	1	-32.0324	115.8871	27/10.0/2018	01:40	17.5	18.8	5	507	381	301	253	218	196	164	148	90	137	
Run2 Leach sensors complete off_1.0	1	-32.0324	115.8871	27/10.0/2018	01:41	17.4	18.8	5	503	390	306	258	222	194	168	147	89	120	
Run2 Leach sensors offset_0.0	0	-32.0324	115.8871	27/10.0/2018	01:21	17.2	18.8	5	539	401	317	262	223	199	169	147	101	148	
Run2 Leach sensors offset_0.0	0	-32.0324	115.8871	27/10.0/2018	01:22	17.2	18.8	5	536	400	311	263	225	199	171	148	97	144	
Run2 Leach sensors offset_0.0	0	-32.0324	115.8871	27/10.0/2018	01:24	17.3	18.8	5	527	391	310	260	223	196	167	149	94	143	
Run2 Leach sensors offset_1.0	1	-32.0324	115.8871	27/10.0/2018	01:25	17.4	18.9	5	521	389	306	259	221	196	169	149	92	140	
Run2 Leach sensors offset_1.0	1	-32.0324	115.8871	27/10.0/2018	01:26	17.3	19	5	519	386	306	257	218	195	168	149	95	141	
Run2 Leach sensors offset_1.0	1	-32.0324	115.8871	27/10.0/2018	01:27	17.5	18.9	5	513	388	303	257	220	195	168	147	91	133	
Run2 Leach sensors offset_1.0	1	-32.0324	115.8871	27/10.0/2018	01:29	17.4	19	5	514	395	307	257	222	194	168	148	89	125	
Run2 Leach Through site_0.0	0	-32.0323	115.8873	27/10.0/2018	00:50	17.7	19.4	5	458	355	287	248	214	192	166	148	98	102	
Run2 Leach Through site_5.0	5	-32.0323	115.8873	27/10.0/2018	00:51	18.1	19.4	5	561	435	352	306	265	230	198	171	103	125	
Run2 Leach Through site_10.0	10	-32.0323	115.8873	27/10.0/2018	00:52	18.2	19.4	5	485	387	318	286	250	222	182	167	104	100	
Run2 Leach Through site_15.0	15	-32.0323	115.8872	27/10.0/2018	00:53	18.1	19.4	5	557	435	342	280	232	201	168	143	85	122	
Run2 Leach Through site_20.0	20	-32.0324	115.8872	27/10.0/2018	00:54	18.4	19.4	5	585	439	342	291	248	215	182	157	95	147	
Run2 Leach Through site_25.0	25	-32.0324	115.8871	27/10.0/2018	00:57	17.5	19.4	5	591	443	338	281	232	202	171	148	89	149	
Run2 Leach Through site_30.0	30	-32.0324	115.8871	27/10.0/2018	00:58	17.6	19.5	5	539	405	323	267	220	198	164	147	84	136	
Run2 Leach Through site_35.0	35	-32.0324	115.887	27/10.0/2018	00:59	17.4	19.4	5	546	420	335	279	236	205	164	146	79	127	
Run2 Leach Through site_40.0	40	-32.0325	115.887	27/10.0/2018	01:00	17.6	19.4	5	458	340	265	223	189	164	138	121	68	120	
Run2 Leach Through site_45.0	45	-32.0325	115.887	27/10.0/2018	01:01	17.8	19.4	5	479	363	284	243	211	178	148	131	76	115	
Run2 Leach Through site_50.0	50	-32.0325	115.8869	27/10.0/2018	01:01	18.1	19.4	5	668	496	383	312	260	221	181	151	78	171	

APPENDIX C SLR CONSULTING INSTALLATION REPORT

PERMANENT PAVEMENT INSTRUMENTATION

Installation
Leach Highway and Kwinana Freeway

Prepared for:

ARRB
21 McLachlan St,
Fortitude Valley, QLD4006

SLR Ref: 610.17345-R01
Version No: -v0.1
September 2018

PREPARED BY

SLR Consulting Australia Pty Ltd
ABN 29 001 584 612
2 Lincoln Street
Lane Cove NSW 2066 Australia
(PO Box 176 Lane Cove NSW 1595 Australia)
T: +61 2 9427 8100 F: +61 2 9427 8200
E: sydney@slrconsulting.com www.slrconsulting.com

BASIS OF REPORT

This report has been prepared by SLR Consulting Australia Pty Ltd with all reasonable skill, care and diligence, and taking account of the timescale and resources allocated to it by agreement with ARRB (the Client). Information reported herein is based on the interpretation of data collected, which has been accepted in good faith as being accurate and valid.

This report is for the exclusive use of the Client. No warranties or guarantees are expressed or should be inferred by any third parties. This report may not be relied upon by other parties without written consent from SLR

SLR disclaims any responsibility to the Client and others in respect of any matters outside the agreed scope of the work.

DOCUMENT CONTROL

Reference	Date	Prepared	Checked	Authorised
610.17345-R01-v0.1	20 September 2018	Dominik Duschlbauer	Aaron Miller	Dominik Duschlbauer

CONTENTS

DOCUMENT REFERENCES

TABLES

FIGURES

APPENDICES

1 Introduction

SLR Consulting Australia Pty Ltd (SLR) was engaged by The Australian Road Research Board (ARRB) to assist with the permanent installation of sensors arrays in two pavements in the greater Perth area, WA.

This report provides an overview of the two installations and the instrumentation deployed.

2 Leach Highway Array

The sensors were installed in the night of Tuesday 11 September 2018 to Wednesday 12 September 2018. The site is located at SLK 12.35[1] on the westbound outer (slow) lane of the Leach Highway (**Figure 1**).

Figure 1 Approximate Location of the Leach Highway Array

2.1 Numbering, Sensor Types and Sensor Placement

Figure 2 shows the layout of the Leach Highway array. The array was located 1000 mm from the kerb. In **Figure 2**, 'D' refers to the diameter of the hole and 't' refers to the depth of the hole.

Table 1 shows detailed photographs of each sensor installation before the resin was poured. **Appendix A** contains a general description of the sensors and **Appendix B** and **Appendix C** contain detailed information on the accelerometers and geophones, respectively.

[1] From ARRB's installation plan "180627_WARRIP Project - JL - installation plan_Rev01 SN".

All accelerometers and geophones are terminated with BNC leads. The leads are labelled with the serial numbers as well as the name of the hole they are located in.

Figure 2 Leach Highway Array Geometry

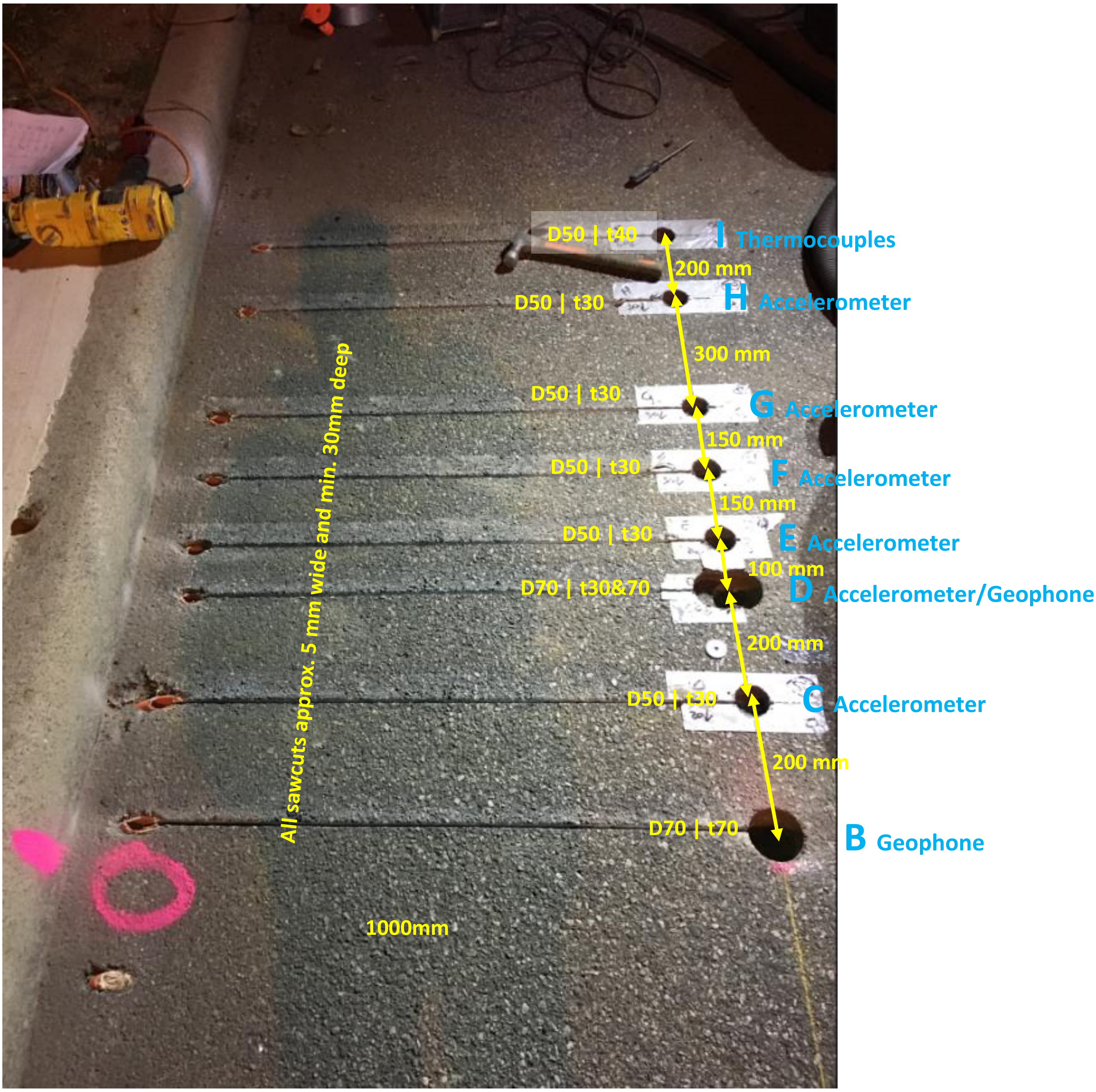

Table 1 Leach Highway Instrumentation

Hole	Photo	Comments
B (D70 mm by t70 mm)		Geophone #5
C (D50 mm by t30 mm)		Accelerometer S/N A10575
D (D70 mm by t30 mm for accelerometer) (D70 mm by t70 mm for geophone)		Geophone #2 Accelerometer S/N A10567

Hole	Photo	Comments
E, F, G, H (D50 mm by t30 mm)	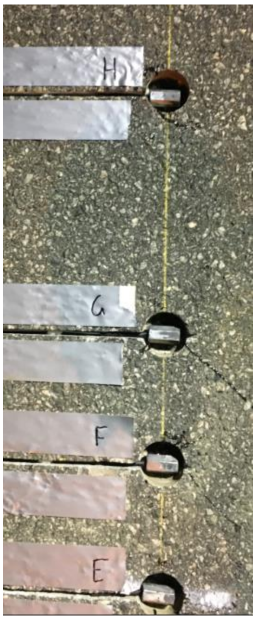 	Accelerometers E: S/N A10570 F: S/N A10637 G: S/N A10568 H: S/N A10260
I (D50 mm by t40 mm)		Two K-type thermocouples. One approximately 10mm from the top. One at the bottom of the 40 mm hole. During the resin pour a lead was observed to rise to the surface and it was pushed back in place. It is not known whether the thermocouple's tip was detached from the concrete in this process.

3 Kwinana Freeway Array

The sensors were installed in the night of Wednesday 12 September 2018 to Thursday 13 September 2018. The site is located at SLK 56.75[2] on the southbound outer (slow) lane of the Kwinana Freeway (**Figure 3**).

Figure 3 Approximate Location of the Leach Highway Array

3.1 Numbering, Sensor Types and Sensor Placement

Figure 4 shows the layout of the Leach Highway array. The array was located 1000 mm from the kerb. In **Figure 4**, ‘D’ refers to the diameter of the hole and ‘t’ refers to the depth of the hole.

Table 2 shows detailed photographs of each sensor installation before the resin was poured. **Appendix A** contains a general description of the sensors and **Appendix B** and **Appendix C** contain detailed information on the accelerometers and geophones, respectively.

All accelerometers and geophones are terminated with BNC leads. The leads are labelled with the serial numbers as well as the name of the hole they are located in.

[2] From ARRB’s installation plan “180627_WARRIP Project - JL - installation plan_Rev01 SN”.

Figure 4 Kwinana Freeway Array Geometry

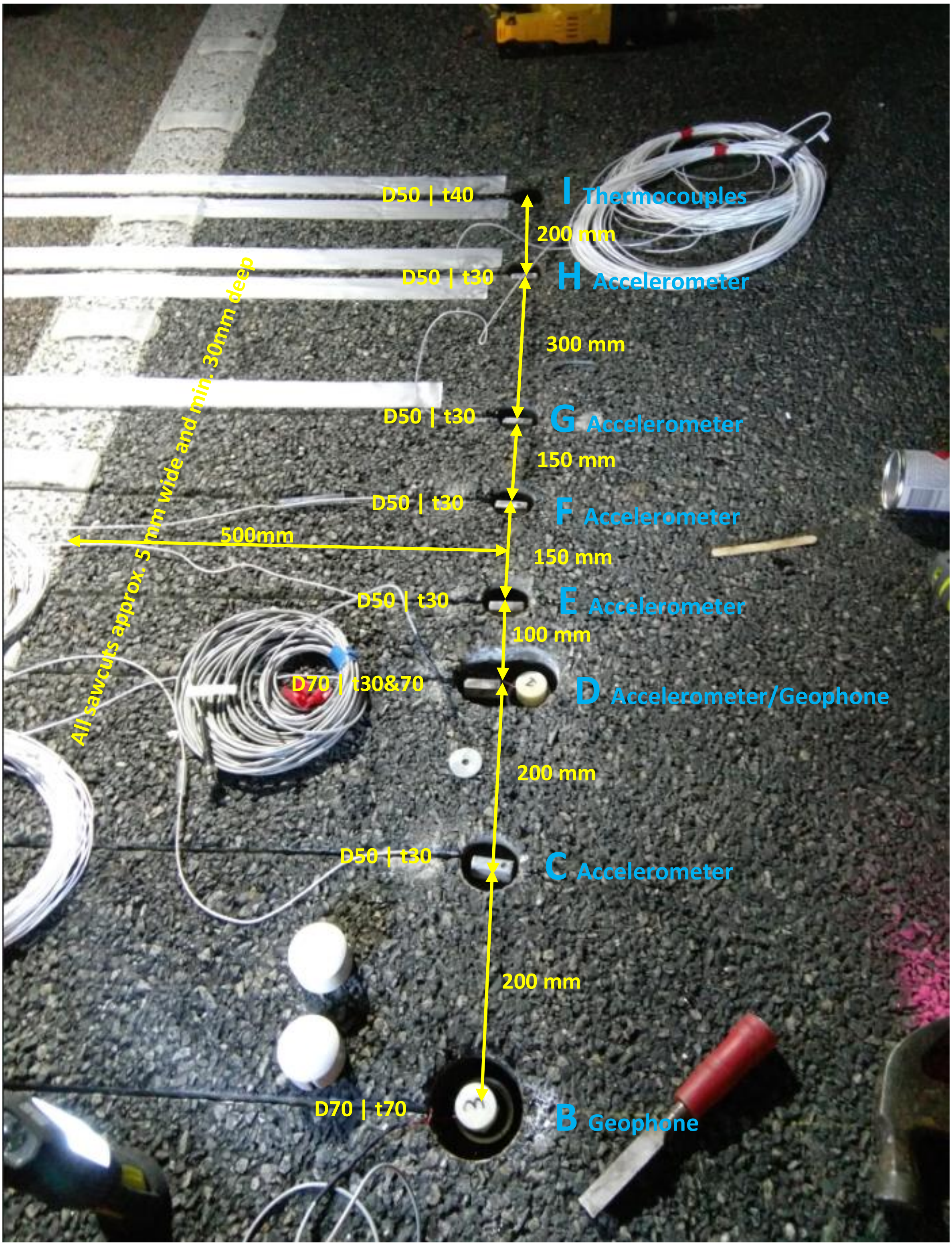

Table 2 Leach Highway Instrumentation

Hole	Photo	Comments
B (D70 mm by t70 mm)		Geophone #3
C (D50 mm by t30 mm)		Accelerometer S/N A10572
D (D70 mm by t30 mm for accelerometer) (D70 mm by t70 mm for geophone)		Geophone #1 Accelerometer S/N A10639
E, F, G, H (D50 mm by t30 mm)		Accelerometers E: S/N A10569 F: S/N A10571 G: S/N A10573 H: S/N A10638

Hole	Photo	Comments
I (D50 mm by t110 mm)		Two K-type thermocouples and two ARRB temperature loggers were used. One pair approximately 40 mm from the top. One pair at the bottom of the 100 mm hole.

4 Conclusions

This report presents the sensor and sensor layout of two permanent installations on the Leach Highway and Kwinana Freeway in the greater Perth area, WA.

APPENDIX A

Sensor Details

Accelerometers

Dytran model 3305A3 accelerometers with a nominal sensitivity of 500 mV/g were used.

The accelerometers were attached to microdot leads and coated in a protective resin.

Subsequently, the lead to accelerometer connection was heat-shrinked. The heat shrink tube extended approx. 50 mm away from the plug but was not shrunk in order to provide some flexibility as additional protection of the lead particularly as it enters the saw cut.

The accelerometers were cold-welded (JB Weld) into steel enclosures. For the purpose the accelerometer was fixed at the correct angle within the enclosure with bolts. Once the cold-weld had cured, the bolts were removed and more cold-weld was injected through the bolt holes.

M8 anchors were bolted into the steel enclosures. The anchors protruded typically 40 mm to 50 mm.

On site, 9 mm pilot holes were drilled into the bottom of each hole. The pilot hole was filled with epoxy glue (5 min Araldite) and the anchor was glued into the hole. Epoxy glue was also used to level the contact zone of the steel enclosure and the bottom of the hole.

The accelerometers had approximately 10 mm of resin cover.

 Moisture protecting resin coat (sticky tape was removed once the resin cured)	 Heat shrink over connector but loose over microdot lead.

Arrangement prior to the accelerometer being cold-welded into the enclosure. The two bolts were removed and the through-holes were used to inject more cold-weld.

Accelerometer prior to installation (above) and installed in hole before being covered with resin (below).

Geophones

Geophones with an internal resistance of 400 Ohm were used. Shaker tests were carried out on all geophones and their natural frequency was nominally 10.5 Hz with nominal sensitivity of 28 V per m/s above the natural frequency.

The terminals of the geophones were coated with resin for moisture protection. Subsequently, a protective cap was glued over the terminals of each geophone.

A M8 anchor was cold-welded (JB Weld) to the underside of each geophone.

On site, 9 mm pilot holes were drilled into the bottom of each hole. The pilot hole was filled with epoxy glue (5 min Araldite) and the anchor was glued into the hole. Epoxy glue was also used to level the contact zone of between the geophone and the bottom of the hole. A protective plastic cup was glued over the geophones to ensure that the resin does not directly touch the geophone due to concerns that stresses imposed on the geophones' bodies may give rise to incorrect readings.

From the top of the protective cup the resin cover was approximately 10 mm.

 Geophone terminals (uncoated)	 Geophone with protective cap in place and anchor cold-welded.

Geophone glued into hole without the protective caps. The protective caps are shown to the left.

Geophone installation with protective cap in place. The slot for the lead was sealed with tape before the resin was poured.

Thermocouples

Welded tip ‘gas and water tight’ PTFE thermocouples Type K with 10 m leads were used. The thermocouples were pushed into holes drilled into the pavement and epoxy glued in place to ensure the thermocouples stay in place as the resin was poured.

A separate, ARRB owned, temperature logger was deployed at the Kwinana site.

ARRB sensor (left) and K-type thermocouple (right).

APPENDIX B

Accelerometer Calibration

Table 3 Accelerometer Summary

S/N	Nominal Sensitivity [mV/g]	Nominal Sensitivity [mV/m/s2]	Lead length	Measured Sensitivity	Location, Hole
10572	500.06	51.0	long	500.1	Kwinana, C
10638	494.34	50.4	long	494.0	Kwinana, H
10637	494.35	50.4	long	494.3	Leach, F
10567	511.58	52.1	long	511.4	Leach, D
10568	494.34	50.4	long	494.2	Leach, G
10570	510.89	52.1	short	510.8	Leach, E
10569	501.53	51.1	short	501.5	Kwinana, E
10573	504.43	51.4	long	504.3	Kwinana, G
10571	503.06	51.3	short	503.1	Kwinana, F
10639	497.1	50.7	short	497.0	Kwinana, D
10260	485.93	49.5	short	485.9	Leach, H
10575	495.1	50.5	short	495.1	Leach, B

APPENDIX C

Geophone Calibration

The geophones have been tested on a shaker and their frequency dependent sensitivity has been determined. The magnitude relationship is shown in **Figure 5** and closely resembles the theoretical relationship which can be described by this equation:

$$H = \frac{a \times \omega^2}{\omega^2 + \frac{\omega \times \omega_n}{Q} + \omega_n^2}$$

Where ω is the complex circular frequency and ω_n is the geophone's resonant circular frequency. Q is the quality factor (the inverse of twice the damping) and *a* is a constant. The installed geophones can be modelled with the following parameters:

- ω_n is $2 \times \pi \times f$ and f is 10.5 Hz
- Q is 1.45
- a is 28.4.

Figure 5 Geophone magnitude characteristics

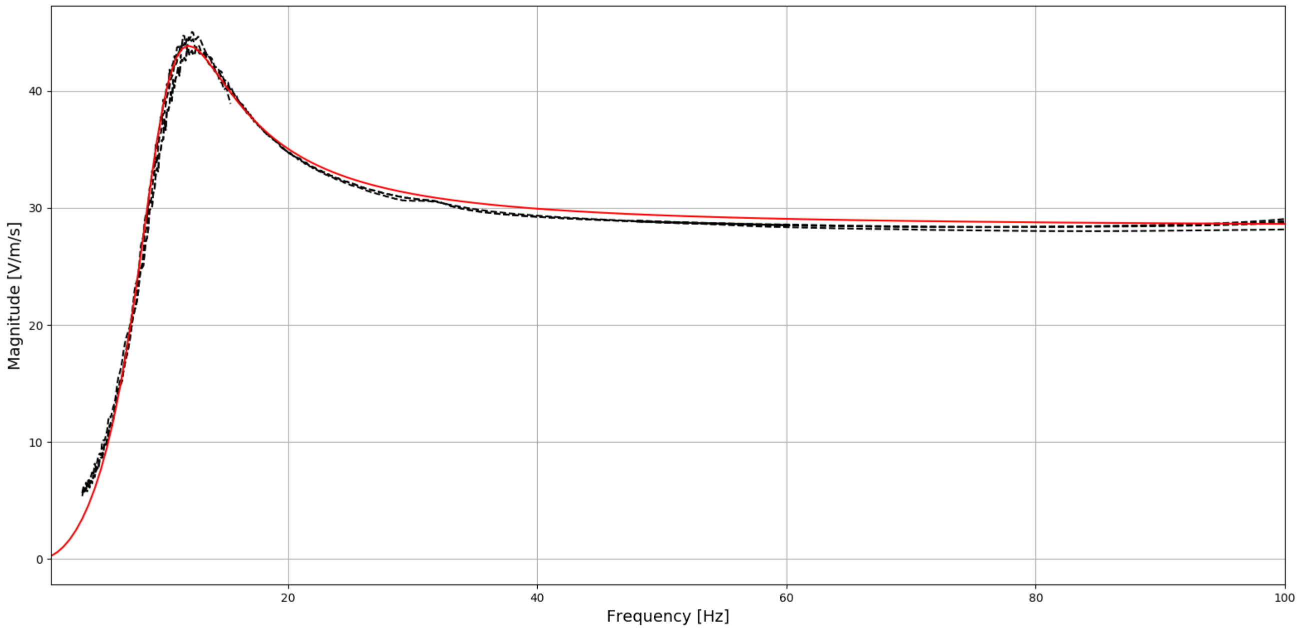

ASIA PACIFIC OFFICES

BRISBANE
Level 2, 15 Astor Terrace
Spring Hill QLD 4000
Australia
T: +61 7 3858 4800
F: +61 7 3858 4801

CANBERRA
GPO 410
Canberra ACT 2600
Australia
T: +61 2 6287 0800
F: +61 2 9427 8200

DARWIN
5 Foelsche Street
Darwin NT 0800
Australia
T: +61 8 8998 0100
F: +61 2 9427 8200

GOLD COAST
Ground Floor, 194 Varsity Parade
Varsity Lakes QLD 4227
Australia
M: +61 438 763 516

MACKAY
21 River Street
Mackay QLD 4740
Australia
T: +61 7 3181 3300

MELBOURNE
Suite 2, 2 Domville Avenue
Hawthorn VIC 3122
Australia
T: +61 3 9249 9400
F: +61 3 9249 9499

NEWCASTLE
10 Kings Road
New Lambton NSW 2305
Australia
T: +61 2 4037 3200
F: +61 2 4037 3201

PERTH
Ground Floor, 503 Murray Street
Perth WA 6000
Australia
T: +61 8 9422 5900
F: +61 8 9422 5901

ROCKHAMPTON
rockhampton@slrconsulting.com
M: +61 407 810 417

SYDNEY
2 Lincoln Street
Lane Cove NSW 2066
Australia
T: +61 2 9427 8100
F: +61 2 9427 8200

TAMWORTH
PO Box 11034
Tamworth NSW 2340
Australia
M: +61 408 474 248
F: +61 2 9427 8200

TOWNSVILLE
Level 1, 514 Sturt Street
Townsville QLD 4810
Australia
T: +61 7 4722 8000
F: +61 7 4722 8001

AUCKLAND
68 Beach Road
Auckland 1010
New Zealand
T: +64 27 441 7849

NELSON
5 Duncan Street
Port Nelson 7010
New Zealand
T: +64 274 898 628

NEW PLYMOUTH
Level 2, 10 Devon Street East
New Plymouth 4310
New Zealand
T: +64 0800 757 695